Department of Mathematics and Statistics
The University of Melbourne

Construction of non-geometric veering triangulations of fibered hyperbolic 3-manifolds

Ahmad Issa

Supervisor: A/Prof. Craig Hodgson

Master's Thesis

February 3, 2014

Acknowledgements

Firstly, I'd like to express my gratitude to Craig; I feel privileged to have had such an excellent supervisor who was generous with his time and ideas, and who helped me grow throughout the course of this project. I'd also like to thank Henry Segerman who contributed substantially to this thesis in various forms, in particular for the many fruitful discussions and for answering my trivial questions. Furthermore, my gratitude goes to Arun Ram for teaching me to write, and for giving me feedback on early drafts of this thesis. Lastly, a heartfelt thanks to my family for their support.

Contents

1 Introduction **1**

1.1 Structure of the thesis . . . 2

1.2 Conventions . . . 3

1.3 Fibered 3-manifolds . . . 3

1.4 Mapping class groups . . . 4

1.5 Automorphisms of a torus . . . 5

1.6 Farey Tessellation . . . 8

1.7 Ideal triangulations of once-punctured torus bundles . . . 11

2 Geometric structures and measured foliations **16**

2.1 Measured foliations . . . 17

2.2 Developing map and holonomy . . . 19

2.3 Classification of surface homeomorphisms . . . 20

3 Train tracks for surface homeomorphisms **22**

3.1 Train tracks . . . 22

3.2 Invariant train tracks . . . 23

3.3 The Bestvina-Handel algorithm . . . 25

3.3.1 Fibered surfaces . . . 26

3.3.2 Irreducibility and Perron-Frobenius theorem . . . 28

3.3.3 Efficiency . . . 28

3.3.4 Algorithm input and output . . . 29

3.3.5 Moves on fibered surfaces . . . 29

3.3.6 Algorithm steps . . . 33

3.3.7 Efficient graph map to invariant train track . . . 34

3.3.8 From train track to foliation . . . 36

3.4 Example — Once-punctured torus . . . 38

3.5 Example — Once-punctured genus 2 surface . . . 40

4 Thurston's picture of surface diffeomorphisms **46**

5 Geodesic laminations **49**

6 Triangulations and gluing equations **53**
6.1 Triangulations . . . 53
6.1.1 Veering triangulations . . . 54
6.1.2 Ideal tetrahedra . . . 55
6.2 Gluing equations . . . 57
6.3 Completeness and Dehn filling equations . . . 60

7 Agol's construction **65**
7.1 Periodic splitting sequences of train tracks . . . 65
7.2 Agol's triangulations . . . 67
7.3 Example — Once-punctured torus . . . 69

8 Implementation **74**
8.1 Outline of steps . . . 74
8.2 Conjugacy testing . . . 78
8.2.1 Algorithm for determining conjugacy in $\mathrm{MCG}(S)$ . . . 80

9 Results **81**
9.1 A non-geometric example . . . 82
9.2 Further work . . . 85

A Tables **87**

B A non-geometric triangulation **92**

Bibliography **95**

Chapter 1

Introduction

The technique of decomposing non-compact finite-volume hyperbolic 3-manifolds into ideal hyperbolic tetrahedra is useful for understanding such 3-manifolds. For example, such triangulations provide an effective means of calculating geometric invariants and for computing deformations of hyperbolic structures. A (topological) ideal triangulation of a 3-manifold M is a decomposition of M into ideal tetrahedra, that is, 3-simplices with their vertices removed, such that their faces are affinely glued in pairs.

A natural question to ask is whether every cusped hyperbolic 3-manifolds admits a geometric ideal triangulation, that is, an ideal triangulation where each tetrahedron can be assigned the shape of a positively-oriented ideal hyperbolic tetrahedron, such that the tetrahedra piece together coherently to define a global hyperbolic structure which agrees with the complete hyperbolic structure on M. To the best of our knowledge, this question remains unanswered.

In [36], it is shown that every cusped hyperbolic manifold has a finite cover admitting a geometric ideal triangulation. In [16], Epstein and Penner show that every hyperbolic 3-manifold admits a canonical geometric cellulation, that is, a decomposition into convex ideal hyperbolic polyhedra. This geometric cellulation often contains only ideal tetrahedra in which case it is, in fact, a geometric ideal triangulation. Moreover, under strong combinatorial conditions, it is shown in [54] that each polyhedron can be decomposed into hyperbolic tetrahedra in such a way that a geometric ideal triangulation is obtained. In practice, the computer program SnapPea [30] by Jeff Weeks always succeeds in finding a geometric triangulation.

In this thesis we focus on ideal triangulations of fibered cusped hyperbolic 3-manifolds, that is, cusped hyperbolic 3-manifolds of the form $M_\varphi = S \times [0,1]/(x,0) \sim (\varphi(x),1)$, where S is a punctured surface and $\varphi : S \to S$ is a pseudo-Anosov homeomorphism. For each such φ, Agol gives a construction of an ideal triangulations of M_{φ°, where φ° is the restriction of φ to a surface obtained by puncturing S at the singularities of the invariant foliations (see [2].) This triangulation is a veering layered triangulation of M_φ° and is canonical, that is, uniquely determined by φ. Agol poses the question:

Question: *Are the veering triangulations coming from this construction geometric?*

The question has been answered in the affirmative in the case of fibered hyperbolic 3-manifolds coming from homeomorphisms of a once-punctured torus (see [23] or [33].) In this case the veering triangulations obtained from Agol's construction coincides with the well-studied monodromy, or Floyd-Hatcher triangulations.

In [27] and [24], it is shown that veering triangulations admit strict angle structures, which is a necessary but insufficient condition for an ideal triangulation to be geometric.

The main goal of this thesis is to

(1) construct examples of veering triangulations coming from Agol's construction, and

(2) investigate whether these ideal triangulations are geometric.

Along the way we also,

(3) describe an algorithm for determining whether or not two pseudo-Anosov mapping classes of a punctured surface are conjugate in the mapping class group, in terms of periodic splitting sequences of train tracks.

To achieve (1), we implement a computer program which, given a pseudo-Anosov homeomorphism, performs Agol's construction. In particular, we construct organised lists of examples in the case of a once-punctured genus 2 surface. With regard to (2), we find a number of examples of veering triangulations where the computer program SnapPea is unable to find a geometric solution to Thurston's gluing and completeness equations, i.e. is unable to find positively-oriented hyperbolic tetrahedra shapes for the complete hyperbolic structure. In particular, for a 13 tetrahedron veering triangulation we outline how we rigorously verified that the triangulation is not geometric. We also implemented the algorithm of (3) as part of our computer program.

Source code for the computer program we implemented, triangulation files produced and spreadsheets of data are available from the author upon request.[1]

1.1 Structure of the thesis

In the remainder of **Chapter 1** we describe the classification of homeomorphisms of the torus, and give an example of the Floyd-Hatcher, or monodromy triangulations of once-punctured torus bundles (see [23].) These triangulations are veering and can be thought of as being generalised by Agol's triangulations to a broader class of surface bundles.

In **Chapter 2**, we introduce measured foliations and state the classification of surface homeomorphisms, which generalises the classification of homeomorphisms of the torus given in Chapter 1. The classification theorem is explored in more detail from various viewpoints in Chapters 3-5. We also briefly define the developing map and holonomy of a hyperbolic manifold.

In **Chapter 3**, we introduce train tracks and in the case of pseudo-Anosov homeomorphisms of surfaces with a single puncture, we give a detailed exposition of the algorithm due to Bestvina and Handel in [5] which produces an invariant train track. We then give a rough description of how the invariant train track can be used to construct the invariant measured foliations. The algorithm is performed for two examples, obtaining invariant train tracks. In one example, starting with a homeomorphism of the once-punctured genus 2 surface, the resulting triangulation from Agol's construction is non-geometric, which is discussed in more detail in Chapter 9.

In **Chapter 4**, we briefly outline Thurston's original proof of the classification of surface homeomorphisms using Thurston's compactification of Teichmüller space by the space of projective measured foliations (see [52].)

[1] Send an email to ahmadissa@gmail.com

In **Chapter 5**, we state an analogous theorem to the classification of surface homeomorphisms, using geodesic laminations. We briefly touch on the relation between measured geodesic laminations and measured foliations.

In **Chapter 6**, we discuss ideal triangulations of 3-manifolds and describe the gluing, completeness and hyperbolic Dehn filling equations for ideal triangulations.

In **Chapter 7**, we present Agol's construction of veering triangulations in terms of periodic splitting sequences of invariant train tracks, following [2]. We use invariant train tracks produced by the algorithm described in Chapter 3 as input to Agol's construction, and perform this construction for an example, continuing the example given in Section 3.4.

In **Chapter 8**, we outline the main steps taken in order to automate Agol's construction and systematically produce lists of examples of veering triangulations. Our approach makes use of the computer program Trains [25], written by Toby Hall, which is an implementation of the Bestvina-Handel algorithm for punctured surfaces. Given an invariant train tracks produced by Trains, a computer program that we implemented carries out the train track splitting procedure and builds Agol's veering triangulation for the bundle, which can then be readily input into the computer program SnapPy [14]. We also explain how periodic splitting sequences can be used to give an effective procedure for determining whether two pseudo-Anosov mapping classes are conjugate.

In **Chapter 9**, we conclude that Agol's veering triangulations are not always geometric. In particular, we focus on a 13 tetrahedron ideal triangulation coming from Agol's construction, for which we outline how we rigorously verified that it is non-geometric. The SnapPy triangulation file for this example is given in **Appendix B**.

Appendix A contains tables of data collected from the veering triangulations constructed, starting with homeomorphisms of the once-punctured genus 2 surface. We have included tables of all examples we have found which SnapPy reports are non-geometric. We have also included tables which are the beginning of longer lists of data that we collected.

1.2 Conventions

All manifolds considered are *orientable*, and all homeomorphisms are *orientation-preserving*, unless stated otherwise. By a hyperbolic manifold we mean a *complete*, *finite-volume* hyperbolic manifold, unless stated otherwise.

1.3 Fibered 3-manifolds

Definition 1. Let $f : S \to S$ be a homeomorphism of a surface S. The *mapping torus* of f is the topological 3-manifold

$$M_f = S \times [0,1]/\sim,$$

where the equivalence relation $\sim$ is given by

$$(x,t) \sim (x,t) \text{ and } (x,0) \sim (f(x),1) \quad \text{for } x \in S, t \in \mathbb{R},$$

and the quotient is endowed with the quotient topology. We call a 3-manifold homeomorphic to a mapping torus a *fibered* 3-manifold.

Fibered 3-manifolds form an important class of 3-manifolds and have been studied intensely. Questions about a mapping torus M_f can often be reduced to a question about

the monodromy f which is often easier to approach. One example of this is the characterisation of when M_f is homeomorphic to a hyperbolic 3-manifold.

Theorem 1. Let $f : S \to S$ be a homeomorphism of a surface S of genus $g \geq 0$ with $n \geq 0$ punctures. Then there exists a complete finite-volume hyperbolic 3-manifold homeomorphic to the mapping torus M_f if and only if f is isotopic to a pseudo-Anosov homeomorphism.

The above theorem is known as the hyperbolization theorem of mapping tori, and is a deep result of Thurston; see [44] for a proof. We will define what it means for a homeomorphism to be pseudo-Anosov in Section 2.3, and isotopy will be defined in the next section.

1.4 Mapping class groups

Definition 2. Let X and Y be topological spaces and let $f, g : X \to Y$ be homeomorphisms. The homeomorphism f is *isotopic* to g if there exists a continuous map $F : X \times [0,1] \to Y$, called an *isotopy* from f to g, such that:

(i) If $t \in [0,1]$ then $F_t = F(\cdot, t) : X \to Y$ is a homeomorphism.

(ii) $F_0 = f$ and $F_1 = g$.

Furthermore, if $A \subseteq X$ then f and g are *isotopic rel* A if there is an isotopy F from f to g such that if $t \in [0,1]$ and $a \in A$, then $F(t,a) = f(a) = g(a)$.

Briefly, an isotopy is a homotopy which is a homeomorphism at each stage, and two homeomorphisms are isotopic rel A if there's an isotopy between them which is constant at each point of A throughout the isotopy.

Definition 3. Let S be a surface and let $P \subseteq S$. The *mapping class group* $\mathrm{MCG}(S,P)$ of S relative to P is the group

$$\{f : S \to S \mid f \text{ is a homeomorphism and } f(P) = P\}/\sim,$$

where $f \sim g$ if f and g are isotopic rel P, and the group operation is given by composition, that is, $[f][g] = [f \circ g]$.

We will mostly be interested in surfaces with punctures. A surface S of genus $g \in \mathbb{Z}_{\geq 0}$ with $k \in \mathbb{Z}_{\geq 0}$ punctures can be thought of either as a closed surface of genus g with k points removed, or as a closed surface of genus g with a set P of k distinguished points. In the case that we deal with distinguished points, the mapping class group we will be interested in is relative to P, otherwise P is considered to be the empty set.

Definition 4. Let $A = \{z \in \mathbb{C} : 1 \leq |z| \leq 2\}$ be an annulus with orientation induced from the orientation of $\mathbb{C}$. The homeomorphism

$$\begin{aligned} D : A &\to A \\ z &\mapsto e^{2\pi i |z|} z, \end{aligned}$$

is a *positive Dehn twist* of A.

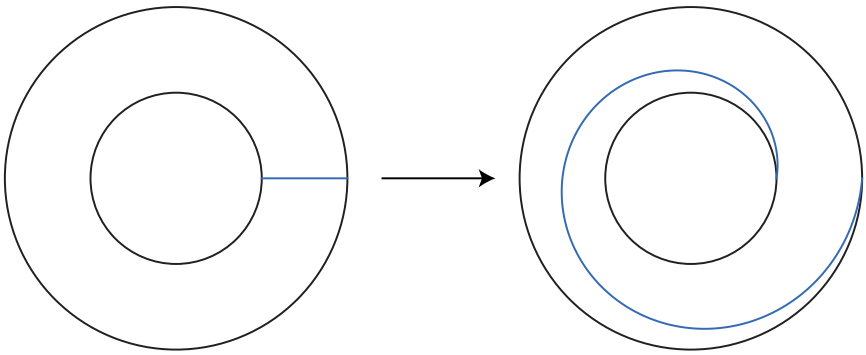

Figure 1.1: Dehn twist.

Let S be an orientable surface and let $C \subseteq S$ be a simple closed curve in S. Let $N \subseteq S$ be a closed regular neighbourhood of C, and let $\iota : A \to N$ be an orientation-preserving homeomorphism.

The homeomorphism $D_C : S \to S$ defined by

$$D_C(x) = \begin{cases} \iota \circ D \circ \iota^{-1}(x) & \text{if } x \in N \\ x & \text{if } x \in S \backslash N, \end{cases}$$

is a left *Dehn twist* in C.

Note that the Dehn twist D_C is only defined up to isotopy. Furthermore, if γ and γ' are isotopic curves then D_γ and $D_{\gamma'}$ are equal up to isotopy.

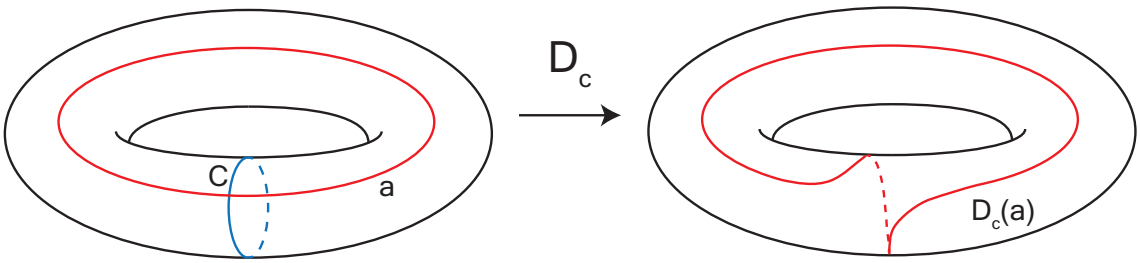

Figure 1.2: Dehn twist in C.

1.5 Automorphisms of a torus

In this section we give a classification of the elements of the mapping class group of the torus, following §0 of [12]. Throughout this section let $T = \mathbb{R}^2/\mathbb{Z}^2$ be the torus.

Let $A = \left(\begin{smallmatrix} a & b \\ c & d \end{smallmatrix}\right)$ be an element of the group $\mathrm{SL}_2(\mathbb{Z})$, of 2×2 integer matrices with determinant 1. The matrix A can be thought of as a linear transformation $A : \mathbb{R}^2 \to \mathbb{R}^2$ given by matrix multiplication, which maps the lattice $\mathbb{Z}^2$ to itself and therefore descends to a continuous function $\phi_A : T \to T$ defined by

$$\begin{aligned} \phi_A : T &\to T \\ [x, y] &\mapsto A\left(\begin{smallmatrix} x \\ y \end{smallmatrix}\right) = [ax + by, cx + dy]. \end{aligned}$$

Since $\phi_A^{-1} = \phi_{A^{-1}}$ is continuous, the map ϕ_A is a homeomorphism of the torus. In fact, every orientation preserving homeomorphism of the torus is equal, up to isotopy, to a homeomorphism ϕ_A arising from a matrix A in precisely this way.

Proposition 1 (Ch. 2, §D of [47])**.** Let

$$\begin{aligned} \Phi : \mathrm{SL}_2(\mathbb{Z}) &\to \mathrm{MCG}(T) \\ A &\mapsto [\phi_A]. \end{aligned}$$

Then Φ is a group isomorphism.

We use the isomorphism Φ in Prop. 1 to identify $\mathrm{SL}_2(\mathbb{Z}) \cong \mathrm{MCG}(T)$, and we think of an element $A \in \mathrm{SL}_2(\mathbb{Z})$ as both a matrix, and a homeomorphism of T.

Let $A = \left(\begin{smallmatrix} a & b \\ c & d \end{smallmatrix}\right) \in \mathrm{SL}_2(\mathbb{Z})$. The characteristic polynomial $p(x)$ of A is given by $x^2 - \mathrm{tr}(A)x + 1$, and A has eigenvalues

$$\lambda_\pm = \frac{1}{2}\left(\mathrm{tr}(A) \pm \sqrt{(\mathrm{tr}A)^2 - 4}\right).$$

We consider three cases:

(1) $|\mathrm{tr}(A)| < 2$: In this case A has finite order, which can be seen as follows. By the Cayley-Hamilton theorem we know that $p(A) = A^2 - \mathrm{tr}(A)A + I = 0$.

- If $\mathrm{tr}(A) = -1$, then $A^2 = -A - I$, therefore $A^3 = -A^2 - A = I$.
- If $\mathrm{tr}(A) = 0$, then $A^2 = -I$, so $A^4 = I$.
- If $\mathrm{tr}(A) = 1$, then $A^2 = A - I$, so $A^3 = A^2 - A = -I$. Hence $A^6 = I$.

(2) $|\mathrm{tr}(A)| = 2$: In this case A preserves a simple closed curve in T. To see this, notice that A has a single real eigenvalue $\lambda = \frac{1}{2}\mathrm{tr}(A) = \pm 1$. Since $A - \lambda I$ has integer entries we can find an eigenvector $(p, q) \in \mathbb{Z}^2$ where p and q are coprime. The straight line connecting the origin to (p, q) descends to a simple closed curve on T which is setwise preserved by A.

(3) $|\mathrm{tr}(A)| > 2$: This is the most interesting case. A has two distinct real eigenvalues λ, λ^{-1} with $|\lambda| > 1$, and corresponding eigenvectors v_+, v_- respectively. We partition or 'foliate' $\mathbb{R}^2$ by leaves, that is, by lines parallel to v_+. The linear map A preserves the foliation, that is, it sends leaves of the foliation to leaves of the foliation, but squashes them closer together, (see Figure 1.3.)

More precisely, we can define a 'transverse measure' μ on the foliation which assigns to each arc $\alpha : [0, 1] \to \mathbb{R}^2$ transverse to the leaves, a real number given by the distance between the leaves containing the endpoints. Intuitively, $\mu(\alpha)$ is a measure of the quantity of leaves crossed by α. The linear map A squashes the arc α by a factor of $|\lambda|$, that is $\mu(A(\alpha)) = |\lambda|^{-1}\mu(\alpha)$. Similarly, there is a foliation of $\mathbb{R}^2$ by lines parallel to v_- with a transverse measure defined in the same way. In this case the leaves are spread apart, or stretched in the transverse direction by a factor of $|\lambda|$.

Since A preserves these foliations, each foliation projects to a foliation of T. As the lines in $\mathbb{R}^2$ have irrational slope each leaf in T is infinite and dense. The transverse measures also project to transverse measures on the foliations of T. If α is a curve on T transverse to a foliation on T, then we can lift α to $\mathbb{R}^2$ and use the corresponding measure on $\mathbb{R}^2$ to assign a measure to α.

In the three cases we call the homeomorphism A *periodic*, *reducible* and *Anosov*, respectively. We will see that pseudo-Anosov homeomorphisms are generalisations of Anosov homeomorphisms for surfaces with negative Euler characteristic.

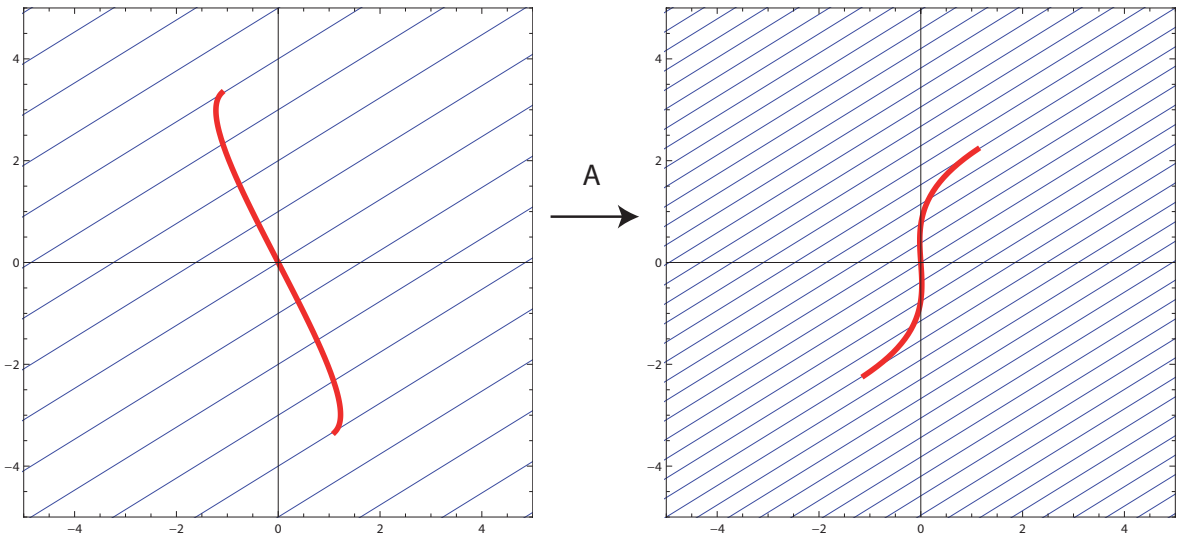

Figure 1.3: A few of the leaves parallel to v_+, and a transverse arc α shown left. The image under $A = \left(\begin{smallmatrix} 2 & 1 \\ 1 & 1 \end{smallmatrix}\right)$ is shown right.

1.6 Farey Tessellation

Theorem 2. Let A be a matrix in $\mathrm{SL}_2(\mathbb{Z})$ with $\mathrm{tr}(A) > 2$. Then there exist $B \in \mathrm{SL}_2(\mathbb{Z})$, $n \in \mathbb{Z}$, and non-negative integers $a_1, \ldots, a_n, b_1, \ldots, b_n$ such that

$$BAB^{-1} = L^{a_1} R^{b_1} L^{a_2} R^{b_2} \cdots L^{a_n} R^{b_n},$$

where

$$L = \begin{pmatrix} 1 & 1 \\ 0 & 1 \end{pmatrix} \text{ and } R = \begin{pmatrix} 1 & 0 \\ 1 & 1 \end{pmatrix}.$$

We prove this using properties of the Farey tessellation of the hyperbolic-upper half plane. Relevant sources for this section include [8, Chapter 9], [49] and [50].

Definition 5. The *upper-half plane model of the hyperbolic plane* is the metric space

$$\mathbb{H}^2 = \{(x, y) \in \mathbb{R}^2 = \mathbb{C} \mid y > 0\}$$

with distance function

$$d(a, b) = \inf\{\ell(\gamma) \mid \gamma : [0, 1] \to \mathbb{H}^2 \text{ smooth}, \gamma(0) = a, \gamma(1) = b\}$$

where

$$\ell(\gamma) = \int_0^1 \frac{\sqrt{x'(t)^2 + y'(t)^2}}{y(t)} dt$$

is the *hyperbolic length* of the curve $\gamma(t) = (x(t), y(t))$.

The *geodesics* of $\mathbb{H}^2$ are vertical lines and semicircles centred on a point in $\mathbb{R} \subseteq \mathbb{C}$. An *ideal hyperbolic triangle* is the region of $\mathbb{H}^2$ bounded by the geodesics pairwise joining three distinct points in $\mathbb{Q} \cup \{\infty\}$ which is homeomorphic to a triangle with its vertices removed.

Convention 1. When considering an element $\frac{p}{q} \in \mathbb{Q} \cup \{\infty\}$ we assume that p and q are coprime and $q > 0$, with the exception of ∞ which we consider to be $\infty = \frac{1}{0} = \frac{-1}{0}$.

Definition 6. The elements $\frac{p}{q}, \frac{p'}{q'} \in \mathbb{Q} \cup \{\infty\}$ form a *Farey pair* if $pq' - p'q = \pm 1$.

Definition 7. The *Farey tessellation* is the set of hyperbolic ideal triangles which are bounded by the geodesics whose endpoints in $\mathbb{Q} \cup \{\infty\}$ form Farey pairs.

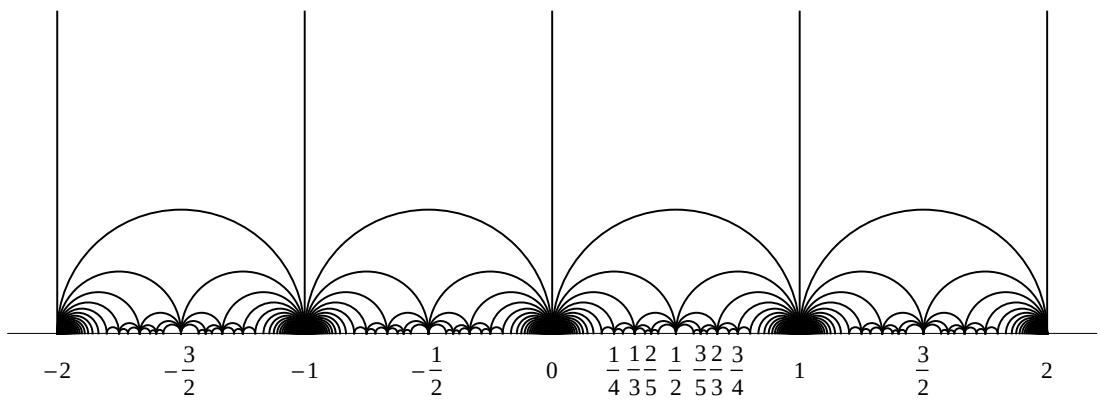

Figure 1.4: Part of the Farey tessellation

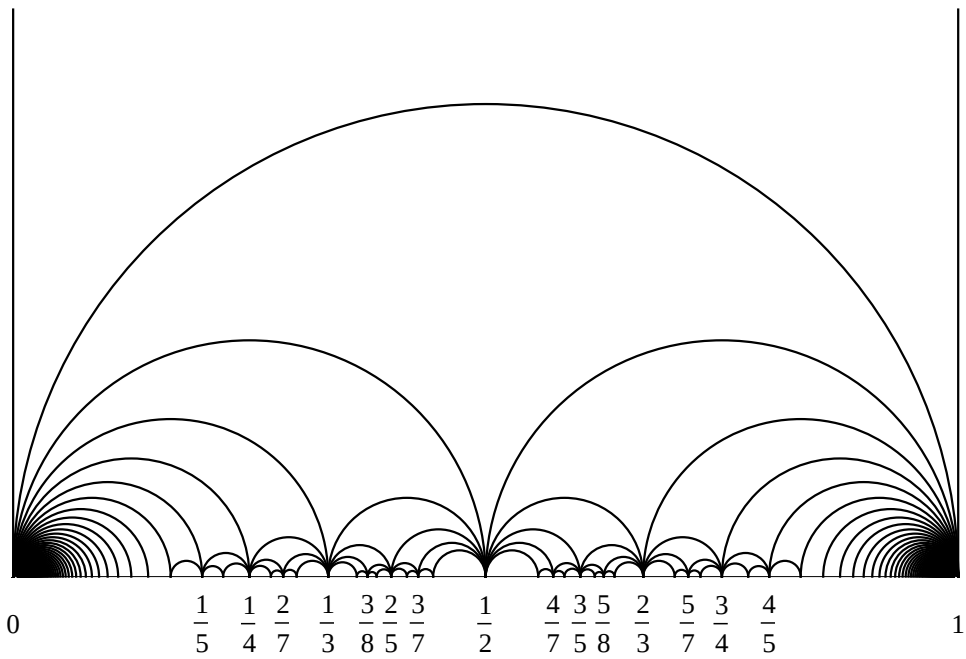

Figure 1.5: $[0,1]$ region of the Farey tessellation

Lemma 1. If T is a Farey triangle, then the set of vertices of T is $\{\frac{a}{b}, \frac{c}{d}, \frac{a+c}{b+d}\}$, for some $\frac{a}{b}, \frac{c}{d} \in \mathbb{Q} \cup \{\infty\}$.

Proof. Let $\frac{a}{b} > \frac{e}{f} > \frac{c}{d}$ be the three vertices of T. Then $af - be = 1$, $ed - fc = 1$ and $ad - bc = 1$. Solving for e and f in the first two equations, then using the third equation to simplify the result, we obtain $e = a + c$ and $f = b + d$ as required. □

Lemma 2. If $\varphi(z) = \frac{az+b}{cz+d}$, where $ad - bc = 1$, is in $\mathrm{PSL}(2, \mathbb{Z})$ then A preserves the Farey tessellation, that is, if $\frac{u}{v}, \frac{s}{t} \in \mathbb{Q} \cup \{\infty\}$ are a Farey pair then $\varphi(\frac{u}{v}), \varphi(\frac{s}{t})$ form a Farey pair.

Proof. Since $\varphi(\frac{u}{v}) = \frac{au+bv}{cu+dv}$ and $\varphi(\frac{s}{t}) = \frac{as+bt}{cs+dt}$, we have

$$(au + bv)(cs + dt) - (cu + dv)(as + bt) = (ad - bc)(ut - vs) = \pm 1,$$

as required. □

Proof of Theorem 2.

Step 1. Given a matrix $M \in \mathrm{SL}_2(\mathbb{Z})$ let φ_M denote the induced isometry of the upper half plane given by

$$A = \left(\begin{smallmatrix} a & b \\ c & d \end{smallmatrix}\right) \mapsto \varphi_A(z) = \frac{az + b}{cz + d}.$$

Since $\mathrm{tr}(A) > 2$, the isometry φ_A is hyperbolic and fixes a geodesic axis G with repelling fixed point α_- and attracting fixed point α_+. Furthermore, α_- and α_+ are irrational real numbers, so G does not coincide with any edge of the Farey tessellation. We give G an orientation from repelling to attracting fixed point. As we traverse the oriented geodesic G there is a bi-infinite sequence of triangles of the Farey tessellation which are crossed by G.

Claim. There exists an isometry $h \in \mathrm{PSL}_2(\mathbb{Z})$ such that the oriented geodesic axis G' of $h \circ \varphi_A \circ h^{-1}$ crosses the vertical geodesic joining 0 to ∞ from left to right, i.e. so that the attracting fixed point of G' is a positive real number.

Proof of claim. Pick a Farey triangle T crossed by G and let the vertices be given by $\frac{p}{q}, \frac{r}{s}, \frac{p+r}{q+s}$ in clockwise order. The isometry $f(z) = \frac{qz-p}{-sz+r}$, which is in $\mathrm{PSL}_2(\mathbb{Z})$, maps T to the triangle Δ with vertices $0, \infty, 1$. Furthermore, the isometry $\theta(z) = \frac{1}{1-z}$ which is in $\mathrm{PSL}_2(\mathbb{Z})$ acts on the Farey tessellation by rotating Δ by $2\pi/3$ counter-clockwise, that is, cyclically permuting its vertices counter-clockwise. Hence, the isometry $\theta^i \circ f$, where $i \in \{0, 1, 2\}$ is appropriately chosen, sends the oriented geodesic G to an oriented geodesic which crosses the vertical geodesic from 0 to ∞ from left to right. Therefore, the isometry $h = \theta^i \circ f$ has the property stated in the claim.

Step 2. Let $\varphi' = h \circ \varphi_A \circ h^{-1}$, where h is the isometry from Step 1. Let

$$(\ldots, \Delta_{-1}, \Delta_0, \Delta_1, \Delta_2, \ldots)$$

be the bi-infinite sequence of Farey triangles crossed by the oriented geodesic axis G' of φ', where $\Delta_0 = \Delta$ is the triangle with vertices $0, \infty, 1$. For each triangle Δ_j we distinguish the edge in which G' enters Δ_j. For $f \in \mathrm{PSL}_2(\mathbb{Z})$, we will use the notation $f(\Delta_j) = \Delta_k$ to mean that f sends Δ_j to Δ_k as a set, and preserves the distinguished edge. Observe that f is completely specified by the equation $f(\Delta_j) = \Delta_k$, as this determines f on the vertices of Δ_j.

When the oriented geodesic G' enters a triangle Δ_i there are exactly two possible edges for which it can exit Δ_i and enter Δ_{i+1}, either through the edge to the left or to the right of where it enters. In this way we associate a matrix A_i to Δ_i which is L (resp. R) if G' exits Δ_i to the left (resp. right) of where it enters.

Since φ' acts as a translation along its geodesic axis, and sends Farey triangles to Farey triangles, there exists $m \in \mathbb{Z}$ such that $\varphi'(\Delta_0) = \Delta_m$.

Claim. Let $k \in \mathbb{Z}_{\geq 0}$ and let ψ_k be the isometry induced by $A_0 A_1 A_2 \cdots A_k$. Then $\psi(\Delta_0) = \Delta_k$.

Assume the claim. Then $\psi_m(\Delta_0) = \varphi'(\Delta_0) = \Delta_m$, and so $\varphi' = \psi_m$. Therefore A and $M := A_0 A_1 A_2 \cdots A_m$ are conjugate in $\mathrm{PSL}_2(\mathbb{Z})$, i.e. there exists $P \in \mathrm{PSL}_2(\mathbb{Z})$ such that $PAP^{-1} = \pm M$ as matrices in $\mathrm{SL}_2(\mathbb{Z})$. We know that $\mathrm{tr}(M) > 0$, and by assumption $\mathrm{tr}(A) > 2$, therefore $PAP^{-1} = M$, which completes the proof.

Proof of claim by induction on $k \in \mathbb{Z}_{\geq 0}$.

Base case $k = 0$.

(a) If $A_0 = L$ then $\psi_0(z) = z + 1$, hence $(0, \infty, 1) \mapsto (1, \infty, 2)$ as required.

(b) If $A_0 = R$ then $\psi_0(z) = \frac{z}{z+1}$, therefore $(0, \infty, 1) \mapsto (0, 1, \frac{1}{2})$ as required.

Assume the claim is true for $k \in \mathbb{Z}_{\geq 0}$. Assume first that $A_{k+1} = L$. We know that $\psi_k(\Delta_0) = \Delta_k$, so by continuity ψ_k maps the triangle to the left of Δ_0 to the triangle to the left of Δ_k, preserving the distinguished edge. Hence

$$(\psi_k \circ \varphi_L)(\Delta_0) = \psi_k(\varphi_L(\Delta_0)) = \Delta_{k+1}.$$

Since $\psi_k \circ \varphi_L$ is induced by $(A_0 \cdots A_k)L = A_0 \cdots A_{k+1}$, so $\psi_{k+1} = \psi_k \circ \varphi_L$. Therefore $\psi_{k+1}(\Delta_0) = \Delta_{k+1}$, as required. The case $A_{k+1} = R$ is analogous.

Example 1. Let

$$A = \begin{pmatrix} -4 & 11 \\ -3 & 8 \end{pmatrix} \in \mathrm{SL}_2(\mathbb{Z}).$$

The oriented geodesic axis G of the isometry given by A is shown in Figure 1.6. It cuts through the Farey triangle with vertices $2, 3, \infty$. By translating left two units G is sent to G', which cuts the Farey triangle $0, 1, \infty$. Conjugating A by this translation we obtain,

$$A' = \begin{pmatrix} 1 & -2 \\ 0 & 1 \end{pmatrix} \begin{pmatrix} -4 & 11 \\ -3 & 8 \end{pmatrix} \begin{pmatrix} 1 & -2 \\ 0 & 1 \end{pmatrix}^{-1} = \begin{pmatrix} 2 & -1 \\ -3 & 2 \end{pmatrix}.$$

We see that G' is oriented from right to left, hence we cyclically rotate the Farey triangle $0, 1, \infty$ twice sending G' to G''. Conjugating the matrix A' by this rotation we obtain,

$$A'' = \begin{pmatrix} 0 & 1 \\ -1 & 1 \end{pmatrix}^2 \begin{pmatrix} 2 & -1 \\ -3 & 2 \end{pmatrix} \begin{pmatrix} 0 & 1 \\ -1 & 1 \end{pmatrix}^{-2} = \begin{pmatrix} 3 & 2 \\ 1 & 1 \end{pmatrix}.$$

Finally, the isometry given by A'' sends the Farey triangle $0, 1, \infty$ to $2, 3, \frac{5}{2}$, so we may read off from Figure 1.6 the cutting sequence of A'' as LLR. Hence, $A'' = LLR$. Combining these steps, we can check that,

$$\begin{pmatrix} -1 & 3 \\ -1 & 2 \end{pmatrix} A \begin{pmatrix} -1 & 3 \\ -1 & 2 \end{pmatrix}^{-1} = LLR,$$

where L and R are as given in Theorem 2.

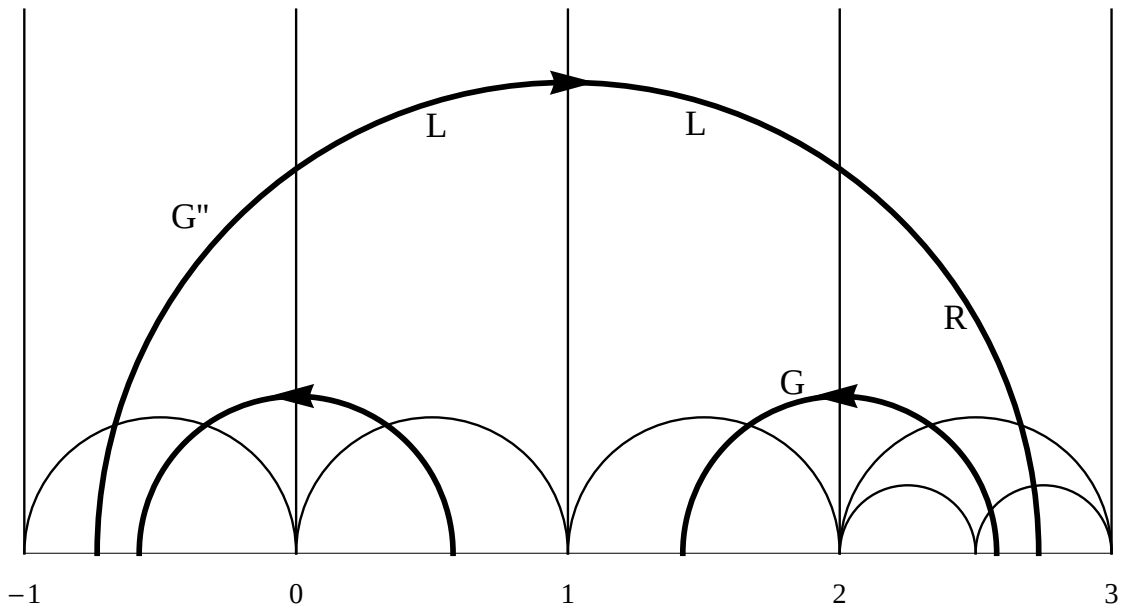

Figure 1.6: Geodesic axes and cutting sequence

1.7 Ideal triangulations of once-punctured torus bundles

Let $A \in \mathrm{SL}_2(Z)$ be a linear transformation of $\mathbb{R}^2$. We saw that A descends to a homeomorphism of the torus T. In fact, since A preserves the lattice $\mathbb{Z}^2$ which projects to a single point p in the torus, the homeomorphism A restricts to a homeomorphism of the punctured torus $T^\circ = T \backslash \{p\} = (\mathbb{R}^2 \backslash \mathbb{Z}^2)/\mathbb{Z}^2$.

Let $A = LR = \left(\begin{smallmatrix} 2 & 1 \\ 1 & 1 \end{smallmatrix}\right)$, where $L = \left(\begin{smallmatrix} 1 & 1 \\ 0 & 1 \end{smallmatrix}\right)$ and $R = \left(\begin{smallmatrix} 1 & 0 \\ 1 & 1 \end{smallmatrix}\right)$. We will show how to obtain an ideal triangulation of the once-punctured torus bundle with monodromy A. From Theorem 2 an element $B \in \mathrm{SL}_2(\mathbb{Z})$ with $\mathrm{tr}(B) > 2$ is conjugate to a product of matrices which are equal

to either L or R, which can be used to obtain an ideal triangulation of the once-punctured toruswith monodromy B; see [23] for details.

Step 1. Ideally triangulate the surface T°.

An *ideal triangle* is a topological space homeomorphic to a triangle with its vertices removed. An *ideal triangulation* of $T^\circ = T\backslash\{p\}$ is a decomposition of T° along ideal arcs into ideal triangles, where an ideal arc is the image $\alpha((0,1)) \subseteq T^\circ$ of a simple closed curve $\alpha : [0,1] \to T$ based at p.

A matrix $M \in \mathrm{SL}_2(\mathbb{Z})$ defines an ideal triangulation of T° described as follows. The columns of the matrix define two vectors u, v in $\mathbb{R}^2$. The vectors u, v form a parallelogram with diagonal $u + v$. The parallelogram, excluding its vertices, defines a fundamental domain for T°.

Furthermore, the edges of the parallelogram (excluding the vertices), together with the diagonal $u + v$ project to curves in T° which bound two ideal triangles, where an ideal triangle is a topological triangle with its vertices removed.

Taking M to be the identity matrix we obtain a triangulation of T° as shown in Figure 1.7.

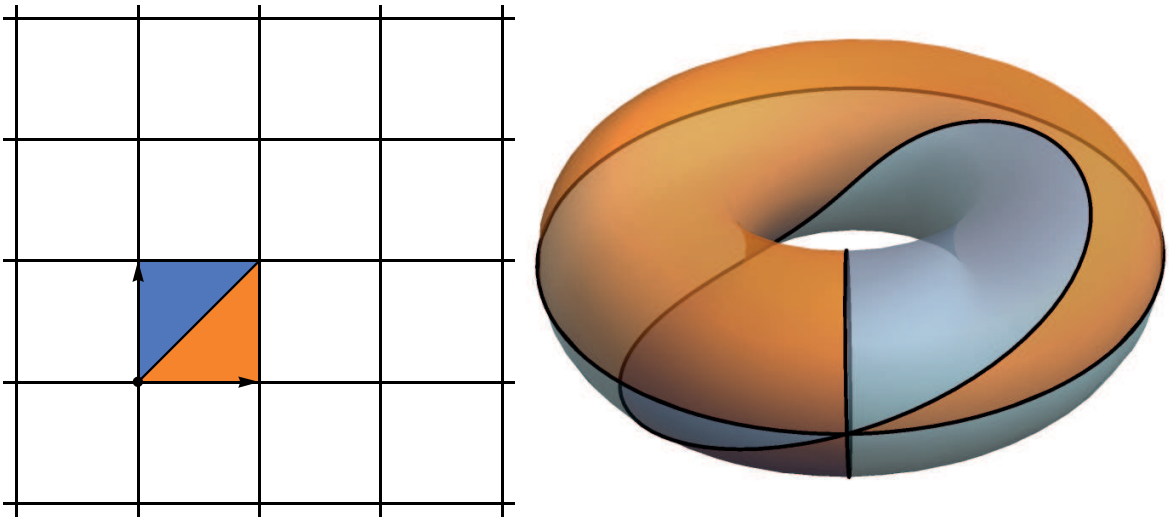

Figure 1.7: Layer 0 triangulation of T°. Note that in the image on the right, the vertex where the triangles meet in the torus is a puncture point, although this is not shown.

Step 2. Interpolate between $\mathcal{T}_0$ and $A(\mathcal{T}_0)$ by diagonal exchanges.

We obtain two more triangulations, one for each letter in the word representation of A, i.e. LR. Let M_0 denote the identity matrix, which induces triangulation $\mathcal{T}_0$. Define $M_1 = M_0 L$ and $M_2 = M_1 R$, and denote their induced triangulations on T° by $\mathcal{T}_1$ and $\mathcal{T}_2$ respectively, see Figures 1.8 and 1.9. (More generally, if $A = A_0 A_1 \cdots A_k$ where each A_i is either L or R, then we would define $M_{n+1} = M_n A_n$ for $n \in \{0, 1, \ldots, k\}$.)

What is the effect of each multiplication on the right by L or R on the induced triangulation? Suppose that we start with a parallelogram defined by the vectors (x_1, y_1) and (x_2, y_2), with diagonal $(x_1 + x_2, y_1 + y_2)$. Multiplying on the right by R we obtain

$$\begin{pmatrix} x_1 & x_2 \\ y_1 & y_2 \end{pmatrix} \begin{pmatrix} 1 & 0 \\ 1 & 1 \end{pmatrix} = \begin{pmatrix} x_1 + x_2 & x_2 \\ y_1 + y_2 & y_2 \end{pmatrix},$$

which gives a parallelogram defined by the vectors $(x_1 + x_2, y_1 + y_2)$ and (x_2, y_2), with diagonal $(x_1 + 2x_2, y_1 + 2y_2)$. Hence, the effect on the level of triangulations is that the

edge joining the origin to (x_1, y_1) is removed and replaced by the edge joining the origin to $(x_1, y_1) + 2(x_2, y_2)$.

The effect of multiplication on the right by L is similar, in this case (x_2, y_2) is replaced by $2(x_1, y_1) + (x_2, y_2)$.

Notice that the columns $x, y \in \mathbb{R}^2$ of $M_2 = LR = A$ are precisely the image of the vectors $(1, 0)$ and $(0, 1)$ under the linear transformation A. Therefore, the triangulation induced by M_2 is equal to the image of $\mathcal{T}_0$ under the homeomorphism A.

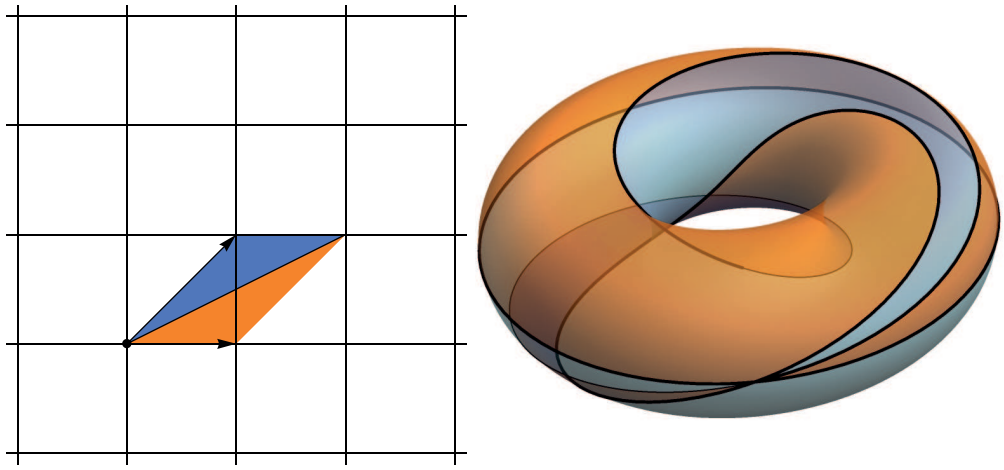

Figure 1.8: Layer 1 triangulation $\mathcal{T}_1$.

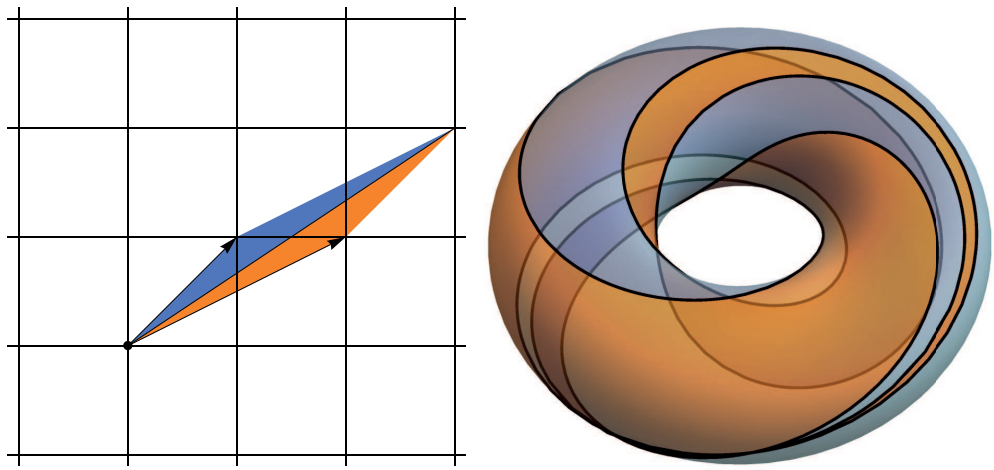

Figure 1.9: Layer 2 triangulation $\mathcal{T}_2$.

Step 3. Insert ideal tetrahedra between layers of surface triangulations.

The removal of an edge adjacent with two triangles in a triangulation of T°, followed by the addition of the other edge which forms a diagonal with the two triangles is known as a diagonal exchange or Whitehead move, see Figure 1.10. In Step 2 we saw that each successive triangulation obtained by multiplication by R or L corresponds to such a diagonal exchange.

For each diagonal exchange we attach an ideal tetrahedron to the two triangles which are removed, see Figure 1.10. Roughly speaking, the tetrahedron is thought of as being very close to flat so that the dihedral angle at the exchanged edges are close to π and the

remaining dihedral angles are close to 0. It has two bottom faces attached to the triangles of $\mathcal{T}_0$ and two top faces attached to the triangles of $\mathcal{T}_1$.

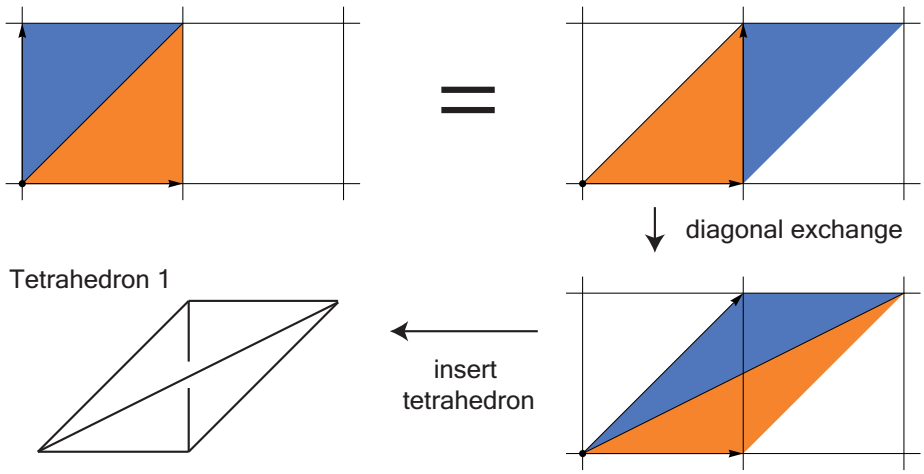

Figure 1.10: $\mathcal{T}_1$ is obtained by a diagonal exchange of an edge of $\mathcal{T}_0$, induced by multiplication on the right by L.

Similarly we insert a tetrahedron between the triangulations $\mathcal{T}_1$ and $\mathcal{T}_2$, as shown in Figure 1.11.

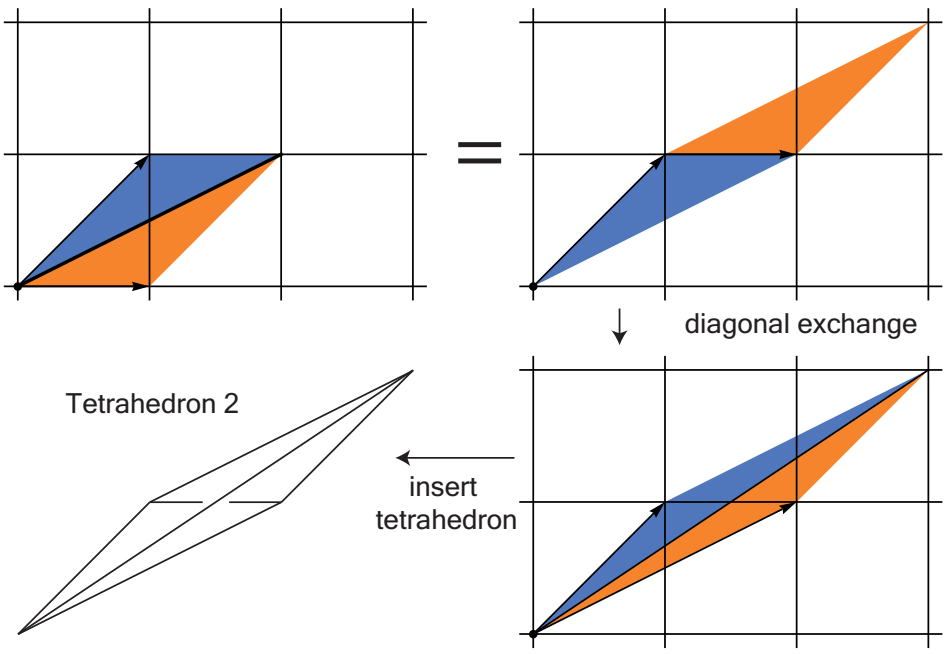

Figure 1.11: $\mathcal{T}_2$ is obtained by a diagonal exchange of an edge of $\mathcal{T}_1$, induced by multiplication on the right by R.

Step 4. Determine the face pairings between tetrahedra.

The front two faces, i.e. faces which are facing the reader in Figure 1.10, of tetrahedron 1 are paired to the back faces of tetrahedron 2 via $\mathcal{T}_1$. Since $A(\mathcal{T}_0) = \mathcal{T}_2$ and the back faces of tetrahedron 1 are paired with the front faces of tetrahedron 2 via the monodromy. The result is a topological ideal triangulation of the mapping torus with monodromy A.

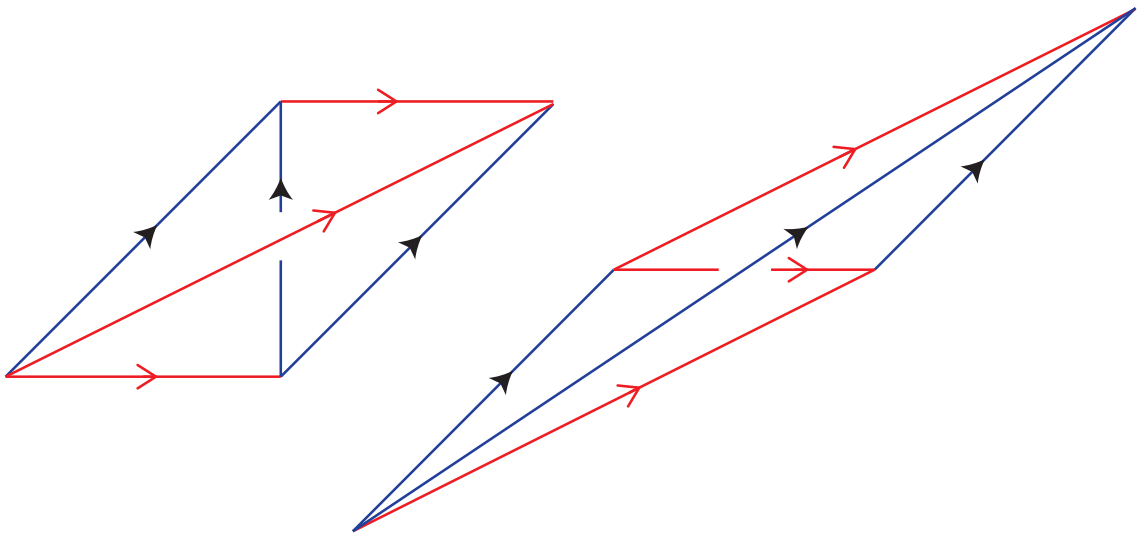

Figure 1.12: Faces with the same arrow pattern are glued, or paired, in such a way that the edge patterns are respected.

Remark 1. The mapping torus with monodromy A, which we triangulated, is homeomorphic to the figure eight knot complement in the three sphere $S^3 = \mathbb{R}^3 \cup \{\infty\}$ (compare with the triangulations in [53, Example 1.4.8] or [20, Chapter 8].)

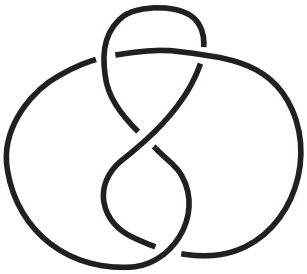

Figure 1.13: The figure eight knot.

Chapter 2

Geometric structures and measured foliations

Definition 8. The *Poincaré disk model of the hyperbolic plane* is the metric space

$$\mathbb{H}^2 = \{(x, y) \in \mathbb{R}^2 \mid x^2 + y^2 < 1\}$$

with distance function

$$d(a, b) = \inf\{\ell(\gamma) \mid \gamma : [0, 1] \to \mathbb{H}^2 \text{ smooth}, \gamma(0) = a, \gamma(1) = b\}$$

where

$$\ell(\gamma) = \int_0^1 \frac{2\sqrt{x'(t)^2 + y'(t)^2}}{1 - x(t)^2 - y(t)^2} dt$$

is the *hyperbolic length* of the curve $\gamma(t) = (x(t), y(t))$.

Definition 9 (3.1.1 of [53])**.** A *pseudogroup* on a topological space X is a set $\mathcal{G}$ of homeomorphisms between open sets of X satisfying the following:

(i) The domains of elements of $\mathcal{G}$ cover X.

(ii) The restriction of an element of $\mathcal{G}$ to an open set contained in its domain is also in $\mathcal{G}$.

(iii) The composition $g_1 \circ g_2$ of elements of $\mathcal{G}$, when defined, is in $\mathcal{G}$.

(iv) The inverse of an element of $\mathcal{G}$ is in $\mathcal{G}$.

(v) The property of being in $\mathcal{G}$ is *local*, that is, if $g : U \to V$ is a homeomorphism between open subsets of X, and U is covered by open sets U_α such that each restriction $g|_{U_\alpha}$ is in $\mathcal{G}$, then $g \in \mathcal{G}$.

Definition 10 (3.1.2 of [53])**.** Let $\mathcal{G}$ be a pseudogroup on a topological space X. A $\mathcal{G}$-*manifold* is a topological space M with a $\mathcal{G}$-*atlas*, which is a collection of pairs (U_α, ϕ_α), called *charts*, where $U_\alpha \subseteq M$ is open and $\phi_\alpha : U_\alpha \to X$ is continuous, which satisfies the following:

(i) The charts cover M, that is, $\cup_\alpha U_\alpha = S$.

(ii) If (U_α, ϕ_α) is a chart then $\phi_\alpha(U_\alpha)$ is open in X and ϕ_α is a homeomorphism onto its image.

(iii) If (U_α, ϕ_α) and (U_β, ϕ_β) are charts and $U_\alpha \cap U_\beta \neq \emptyset$, then they are $\mathcal{G}$-compatible, that is, the *transition map*

$$\phi_\beta \circ \phi_\alpha^{-1} : \phi_\alpha(U_\alpha \cap U_\beta) \to \phi_\beta(U_\alpha \cap U_\beta)$$

is an element of $\mathcal{G}$.

We also call $\{(U_\alpha, \phi_\alpha)\}$ a *$\mathcal{G}$-structure* on M.

Convention 2. We assume that all manifolds are Hausdorff and have a countable basis as a topological space.

Definition 11. Let $\mathcal{G}_0$ be a set of homeomorphisms of a topological space X. The pseudogroup $\mathcal{G}$ *generated by* $\mathcal{G}_0$ is the unique minimal pseudogroup on X that contains $\mathcal{G}_0$.

Definition 12. Let $n \in \mathbb{Z}_{>1}$. The *upper-half space model of n-dimensional hyperbolic space* is the metric space

$$\mathbb{H}^n = \{(x_1, x_2, \ldots, x_n) \in \mathbb{R}^n \mid x_n > 0\}$$

with distance function

$$d(a, b) = \inf\{\ell(\gamma) \mid \gamma : [0, 1] \to \mathbb{H}^n \text{ smooth}, \gamma(0) = a, \gamma(1) = b\}$$

where

$$\ell(\gamma) = \int_0^1 \frac{\sqrt{x_1'(t)^2 + \cdots + x_n'(t)^2}}{x_n(t)} dt$$

is the *hyperbolic length* of the curve $\gamma(t) = (x_1(t), \ldots, x_n(t))$.

Definition 13. Let $n \in \mathbb{Z}_{>1}$. Let $\mathcal{G}$ be the pseudogroup generated by the set of isometries of $\mathbb{H}^n$. A *hyperbolic n-manifold* is a $\mathcal{G}$-manifold.

Convention 3. We reserve hyperbolic manifold to mean a *complete* hyperbolic manifold. We will mention explicitly when dealing with an incomplete hyperbolic manifold.

2.1 Measured foliations

Definition 14 (cf. 11.2.2 of [17])**.** A *measured singular foliation*, or *measured foliation* $\mathcal{F}$ on a surface S is a decomposition of the surface into subsets of S called *leaves*, and a finite set of points $\{p_i\}$, called *singularities* or *singular points*, such that:

(i) Let $\mathcal{G}$ be the pseudogroup generated by diffeomorphisms ϕ between open subsets of $\mathbb{R}^2$ which take horizontal lines to horizontal lines and preserve distance in the y direction, that is, diffeomorphisms of the form

$$\phi(x, y) = (\phi_1(x, y), c \pm y),$$

where $c \in \mathbb{R}$ is a constant depending on ϕ. We require that from the atlas of $S \backslash \{p_i\}$ as a differentiable manifold there exists a subcollection of charts $\{(U_\alpha, \phi_\alpha)\}$, called charts for the foliation, which form a $\mathcal{G}$-structure for $S \backslash \{p_i\}$, such that each chart $\phi_\alpha : U_\alpha \to \mathbb{R}^2$ maps leaves to horizontal line segments of $\mathbb{R}^2$.

(ii) For each singular point p, there is a chart of S from a neighbourhood of p to $\mathbb{R}^2$ which takes leaves to the level sets of a k-pronged saddle, and which takes p to the origin, shown in red, see Figure 2.1. If p is at a puncture (distinguished point) of S, then we allow $k \geq 1$, otherwise we require that $k \geq 3$.

(iii) Each puncture of S is a singular point of $\mathcal{F}$.

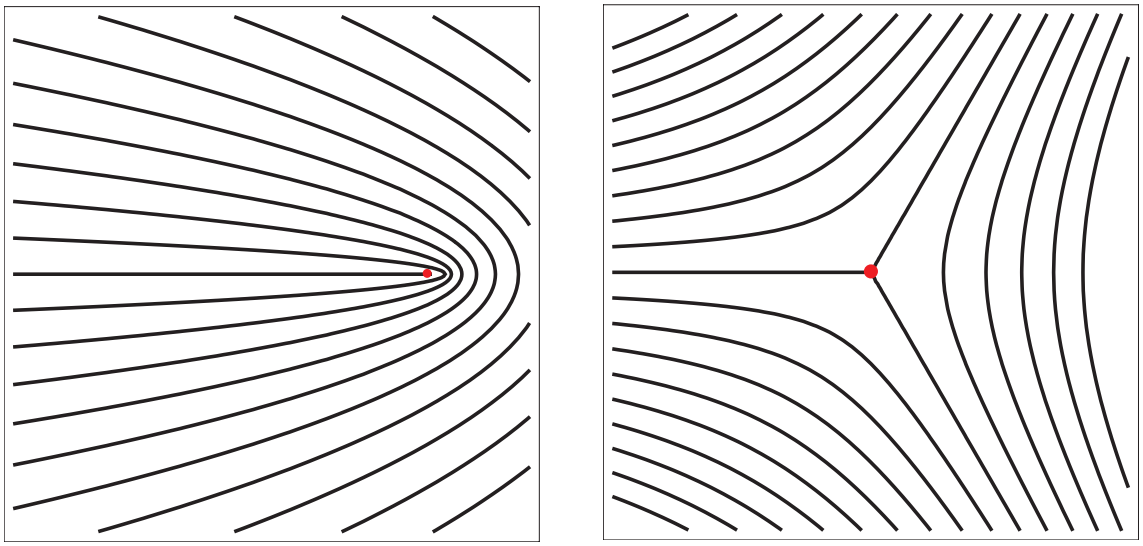

Figure 2.1: Model for k-prong, for $k = 1, 3$. These are the level sets of $f(z) = \mathrm{Re}(z^{k/2})$ in $\mathbb{C}$. The singular point p is mapped to the origin shown in red.

Definition 15. Let $\mathcal{F}$ be a measured singular foliation on a surface S. Then $\mathcal{F}$ induces a *transverse measure* on $\mathcal{F}$, which is a function $\mu : \mathcal{C} \to \mathbb{R}_{\geq 0}$, where $\mathcal{C}$ is the set of simple (possibly closed) curves on S which do not pass through any singular points, defined as follows. For $\alpha : [0, 1] \to S$, a curve in $\mathcal{C}$, $\mu(\alpha)$ is the total-variation in the direction transverse to $\mathcal{F}$, that is,

$$\mu(\alpha) = \sum_{i=1}^{k} |\phi_i^y \circ \alpha(t_i) - \phi_i^y \circ \alpha(t_{i-1})|,$$

where

- $k \in \mathbb{Z}_{>0}$ and
$$0 = t_0 < t_1 < t_2 < \cdots < t_k = 1$$
is a subdivision such that for $i = 1, 2, \ldots, k$, the segment of α from $\alpha(t_{i-1})$ to $\alpha(t_i)$ is contained in a single chart ϕ_i of the measured foliation, and
- the notation $\phi^y(x)$ denotes the projection of $\phi(x)$ onto the y-axis in $\mathbb{R}^2$.

Remark 2. We will often think of a measured foliation as a pair $(\mathcal{F}, \mu)$ where $\mathcal{F}$ is a measured foliation and μ the induced measure.

Definition 16. Let $\mathcal{F}$ be a measured foliation on a surface S, with $K \subseteq S$ the set of singular points, charts for the foliation $\{(U_\alpha, \phi_\alpha)\}$ and transverse measure μ.

(i) Let $\lambda \in \mathbb{R}_{>0}$. We denote by $\lambda\mathcal{F}$ the foliation with the same set of singular points as $\mathcal{F}$ and with charts $\{(U_\alpha, \lambda\phi_\alpha)\}$. Then the decomposition of the surface into leaves is the same as that of $\mathcal{F}$, but the induced measure on $\lambda\mathcal{F}$ is equal to $\lambda\mu$.

(ii) Let $f : S \to S$ be a homeomorphism which is a diffeomorphism away from the singular points, i.e. the restriction

$$f : S \backslash K \to S \backslash K$$

is a diffeomorphism. Define $f(\mathcal{F})$ to be the measured foliation with singular points $K' = \{f(p) : p \in K\}$ and charts for the foliation $\{(f(U_\alpha), f^{-1} \circ \phi_\alpha)\}$. Observe that with these charts if ℓ is a leaf of $\mathcal{F}$ then $f(\ell)$ is a leaf of $f(\mathcal{F})$.

2.2 Developing map and holonomy

We give succinct definitions of the developing map and holonomy, see Section 3.4 of [53] for motivation and more detailed discussion.

Definition 17. Let M be a connected hyperbolic n-manifold, where $n > 1$. Let $x_0 \in M$ be a basepoint and let (U_0, ϕ_0) be a chart containing the basepoint. Let $\pi : \widetilde{M} \to M$ be the universal cover of M, where the elements of $\widetilde{M}$ are equivalence classes of paths in M starting at x_0 (as in e.g. [34, Theorem 12.8].) The *developing map* is the continuous function

$$D : \widetilde{M} \to \mathbb{H}^n$$

defined as follows.
Let $[\alpha] \in \widetilde{M}$, where $\alpha : [0,1] \to M$ is a path in M starting at x_0. Subdivide the path α at points

$$x_0 = \alpha(t_0), x_1 = \alpha(t_1), \ldots, x_k = \alpha(t_k),$$

where $t_0 = 0$ and $t_k = 1$, such that each subpath $\alpha([t_i, t_{i+1}])$ is contained in a coordinate chart (U_i, ϕ_i). We define,

$$D([\alpha]) = \gamma_{01}(x_1) \circ \gamma_{12}(x_2) \circ \cdots \circ \gamma_{k-1,k}(x_k) \circ \phi_k(x_k)$$

where $\gamma_{i,i+1}(x_i) \in \mathrm{Isom}(\mathbb{H}^n)$ is the unique isometry of $\mathbb{H}^n$ which agrees with $\phi_i \circ \phi_{i+1}^{-1}$ in an open neighbourhood of x_i, for $0 \leq i < k$.

Definition 18. Let M be a connected hyperbolic n-manifold, where $n > 1$. Fix a basepoint $x_0 \in M$ and a chart (U_0, ϕ_0) containing the basepoint. The *holonomy* of M is the group homomorphism

$$H : \pi_1(M, x_0) \to \mathrm{Isom}(\mathbb{H}^n)$$

defined as follows. Let $\alpha : [0,1] \to M$ be a loop based at x_0. Subdivide the path α at points

$$x_0 = \alpha(t_0), x_1 = \alpha(t_1), \ldots, x_k = \alpha(t_k)$$

where $t_0 = 0$ and $t_1 = 1$, such that:

(i) For $0 \leq i < k$, each subpath $\alpha([t_i, t_{i+1}])$ is contained in a coordinate chart (U_i, ϕ_i).

(ii) The initial and final coordinate charts are equal, that is, $(U_0, \phi_0) = (U_{k-1}, \phi_{k-1})$.

Define

$$H([\alpha]) = \gamma_{01}(x_1) \circ \gamma_{12}(x_2) \circ \cdots \circ \gamma_{k-1,k}(x_k),$$

where $\gamma_{i,i+1}(x_i) \in \mathrm{Isom}(\mathbb{H}^n)$ is the unique isometry of $\mathbb{H}^n$ which agrees with $\phi_i \circ \phi_{i+1}^{-1}$ in an open neighbourhood of x_i, for $0 \leq i < k$.

The *holonomy group* is the image $H(\pi_1(M, x_0))$.

Remark 3. The definition of both the developing map and holonomy depends on a choice of basepoint and chart. If we make the same choice for both the developing map and holonomy H, then we say that H is the holonomy *corresponding to* the developing map.

Proposition 2. Let M be a connected hyperbolic n-manifold, where $n > 1$. Let $D : \widetilde{M} \to \mathbb{H}^n$ be a developing map with corresponding holonomy $H : \pi_1(M, x_0) \to \mathrm{Isom}(\mathbb{H}^n)$. Then

$$D \circ T_\alpha = H(\alpha) \circ D,$$

where $T_\alpha : \widetilde{M} \to \widetilde{M}$ is the deck transformation associated with $\alpha \in \pi_1(M, x_0)$, that is, $T_\alpha(x_0) = \widetilde{\alpha}(1)$ where $\widetilde{\alpha} : [0,1] \to \widetilde{M}$ is the lift of α such that $\widetilde{\alpha}(0) = x_0$.

$$\begin{tikzcd}
\widetilde{M} \arrow[r, "T_\alpha"] \arrow[d, "D"'] & \widetilde{M} \arrow[d, "D"] \\
\mathbb{H}^n \arrow[r, "H(\alpha)"'] & \mathbb{H}^n
\end{tikzcd}$$

Proposition 3. [53, Proposition 3.4.15] Let M be a hyperbolic 3-manifold and let $D : \widetilde{M} \to \mathbb{H}^3$ be a developing map of M. Then, the developing map $D : \widetilde{M} \to \mathbb{H}^3$ is a homeomorphism if and only if M is complete as a metric space.

2.3 Classification of surface homeomorphisms

Definition 19. Let $S = S_{g,n}$ be a closed surface of genus $g \in \mathbb{Z}_{\geq 0}$ with $n \in \mathbb{Z}_{\geq 0}$ punctures, which we consider to be distinguished points on S. Let $S_0 = S \backslash \{\text{punctures}\}$ be the corresponding punctured surface which we assume has negative Euler characteristic. Let $\varphi : S \to S$ be a homeomorphism which permutes the punctures.

The homeomorphism φ is *pseudo-Anosov* if there exists a pair of measured foliations $(\mathcal{F}^\pm, \mu_\pm)$, such that

1. The set of singularities of the two foliations coincide. Let C be the set of singularities.
2. φ is a diffeomorphism away from the singularities, that is, the restriction $\varphi : S \backslash C \to S \backslash C$ is a diffeomorphism.
3. The foliations are transverse, that is, their leaves intersect *transversely*, i.e. intersecting leaves define distinct tangent lines at each of their points of intersection.
4. There exists $\lambda \in \mathbb{R}_{>1}$, called the *dilatation* of φ, such that

$$\varphi(\mathcal{F}^+) = \lambda \mathcal{F}^+ \quad \text{and} \quad \varphi(\mathcal{F}^-) = \lambda^{-1} \mathcal{F}^-.$$

The foliations $(\mathcal{F}^+, \mu_+)$ and $(\mathcal{F}^-, \mu_-)$ are called the (invariant) *stable* and *unstable* measured foliations of φ. Intuitively, each leaf of the unstable foliation is stretched by φ by a factor of λ.

The following theorem is known as Thurston's classification of surface homeomorphisms.

Theorem 3. Let $S = S_{g,n}$ be a closed surface of genus $g \in \mathbb{Z}_{\geq 0}$ with $n \in \mathbb{Z}_{\geq 0}$ punctures, which we consider to be distinguished points on S. Let $S_0 = S \backslash \{\text{punctures}\}$ be the corresponding punctured surface which we assume has negative Euler characteristic. Let $\varphi' : S \to S$ be a homeomorphism which permutes the punctures.

Then φ' is isotopic rel punctures to a homeomorphism φ such that at least one of the following holds:

(i) φ is *periodic*, that is, φ^k is the identity map for some $k \in \mathbb{Z}_{>0}$.

(ii) φ is *reducible*, that is, there exists $J \subseteq S_0$ which is the union of a finite collection of disjoint closed curves in S_0, satisfying:

  (a) Each connected component of $S_0 \backslash J$ has negative Euler characteristic.

  (b) J is φ-invariant, that is, $\varphi(J) = J$.

(iii) φ is a *pseudo-Anosov* homeomorphism.

We say that the mapping class $[\varphi'] \in \mathrm{MCG}(S_0)$ is periodic, reducible and pseudo-Anosov in the three respective cases above. In the reducible case the set J is called a *reducing set of curves.*

Remark 4.

- The only overlap in the cases above are (i) and (ii), i.e. φ' is pseudo-Anosov if and only if it is not isotopic to a reducible or periodic homeomorphism. A hyperelliptic involution of a genus 2 surface is an example of a homeomorphism which is both periodic and reducible.

- There are various approaches to proving Theorem 3:

  (1) Significant closely related work was done by Nielsen prior to Thurston, see [43]. In fact, Theorem 3 is sometimes called the Nielsen-Thurston classification.

  (2) Thurston's original proof via the compactification of Teichmüller space which we outline in Chapter 4, see also [18] and [52].

  (3) Using geodesic laminations. The analogous theorem in this approach is stated as Theorem 10 of Chapter 5, see also [12] and [11].

  (4) There is an algorithmic proof due to Bestvina and Handel in [5] using train tracks. We give an exposition of this approach in Chapter 3. This is the approach we will be most interested in.

  (5) There is an approach due to Bers in [4] which uses Teichmüller theory.

Chapter 3

Train tracks for surface homeomorphisms

3.1 Train tracks

Definition 20 (cf. §1.1 of [45])**.** Let S be a surface with set of punctures P, which we consider to be distinguished points on S, such that $S^\circ = S \backslash P$ is a hyperbolic surface. A *train track* $\tau \subseteq S^\circ$ is a connected graph embedded in S such that:

(i) The interior of each edge e of τ is C^1, that is, there is a continuously differentiable curve $\alpha : [0,1] \to S$ parametrizing e.

(ii) If v is a vertex of τ, then there is a well-defined one-dimensional tangent space $T_v(\tau) \subseteq T_v(S)$ of τ at v such that, if $\alpha : [0,1] \to S$ is a C^1 curve parametrizing an edge of τ and $\alpha(1) = v$ then $\alpha'(1^-) \in T_v(\tau)$.

(iii) If v is a vertex of τ, then there are edges incident to v on both sides of the tangent space to v, that is, there exists a curve $\alpha : (0,1) \to \tau$ which is C^1 into S such that $\alpha(\frac{1}{2}) = v$.

(iv) Let Σ be the metric completion of a connected component of $S^\circ \backslash \tau$. Then Σ has a piecewise C^1 boundary with $k \in \mathbb{Z}_{\geq 0}$ cusps, i.e. non-smooth points. We require that $\chi(\Sigma) - \frac{1}{2}k < 0$, where $\chi(\Sigma)$ is the Euler characteristic of Σ.

See Figure 3.1 for an example of a train track. Parenthetically, condition (iv) ensures that closed curves carried by the train track are essential in the surface. We allow τ to have self-loops and multiple edges between vertices. We also call the edges of τ *branches* and the vertices *switches*.

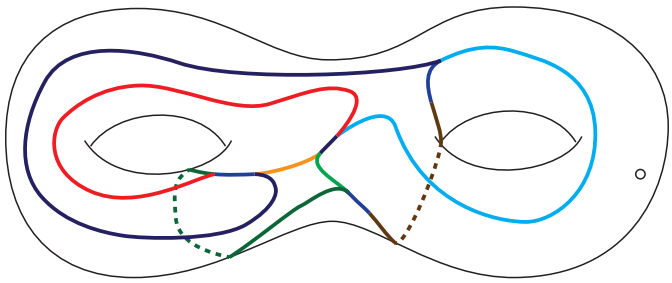

Figure 3.1: An example of a train track on a genus 2 surface with one puncture.

Definition 21. A *measured train track* τ is a train track on a surface S with a *transverse measure*, which is a function $\mu : E(\tau) \to \mathbb{R}_{>0}$ assigning positive *weights* to the edges $E(\tau)$ of τ such that the following switch condition holds (see Figure 3.2):

- If v is a vertex and $e_1, e_2, \ldots, e_k \in E(\tau)$ are the edges which come into v from one side, and $e'_1, e'_2, \ldots, e'_m \in E(\tau)$ are the edges which come into v from the opposite side, then
$$\sum_{i=1}^{k} \mu(e_i) = \sum_{i=1}^{m} \mu(e'_i).$$

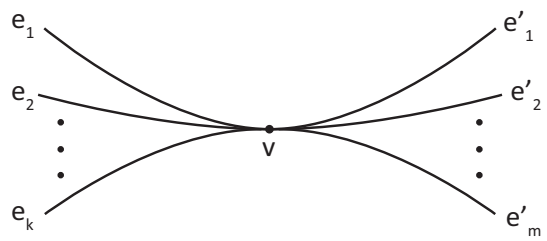

Figure 3.2: Switch condition: the sum of the weights of edges to the left and to the right of v are equal.

3.2 Invariant train tracks

Definition 22. Let $f : S \to S$ be a homeomorphism of a surface S and let $\tau, \tau' \subseteq S$ be train tracks.

(i) τ *carries* τ' if there exists a *carrying map*, that is, a C^1 map $\varphi : S \to S$ homotopic to the identity satisfying the following:

  (a) $\varphi(\tau') \subseteq \tau$.

  (b) If s is a vertex of τ' then $\varphi(s)$ is a vertex of τ.

  (c) If v is a non-zero tangent vector of τ' then $d\varphi(v)$ is non-zero.

(ii) τ is *invariant* with respect to f if f is isotopic to a diffeomorphism ϕ such that τ carries $\phi(\tau)$.

(iii) Assume that f is isotopic to a diffeomorphism ϕ such that τ carries $\phi(\tau)$.

Let $e_1, e_2, \ldots, e_k : [0, 1] \to S$ be the edges of τ and let φ be a carrying map. The *incidence* or *transition matrix* is the matrix $M = M(\tau, f)$ where $M_{i,j}$ is the number of times the curve $\varphi \circ \phi(e_j)$ crosses e_i as it is traversed, that is,

$$M_{i,j} = |e_j \cap (\varphi \circ \phi)^{-1}(e_i)| \quad 1 \leq i, j \leq k,$$

where $|A|$ indicates the number of connected components of A, and the edges do not include their endpoints (see Example 2.)

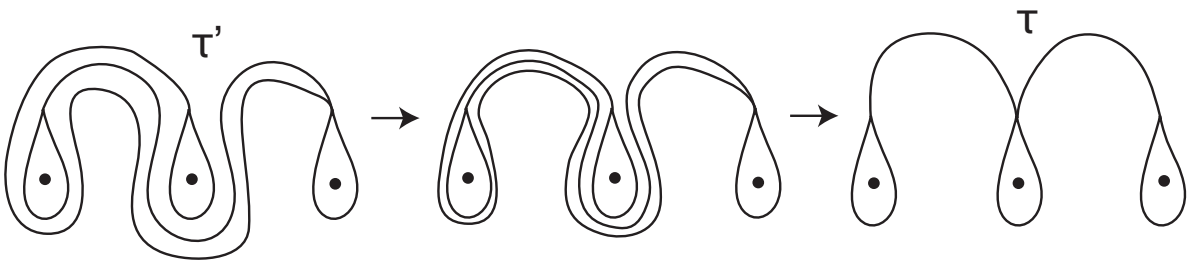

Figure 3.3: Intuitively, we can collapse strands of τ' to obtain τ, hence we say that τ carries τ'.

The following theorem provides a useful test to show that a homeomorphism is pseudo-Anosov.

Theorem 4 (Theorem 3.4 of [35])**.** Let $f : S \to S$ be an orientation-preserving homeomorphism of a surface S such that there exists an invariant train track $\tau \subseteq S$ satisfying the following conditions:

(i) The train track τ is connected, and fills the surface S, that is, each connected component of $S \backslash \tau$ is topologically homeomorphic to a disk or a once-punctured disk.

(ii) The incidence matrix M with respect to the edges $e_1, e_2, \ldots, e_k$ of τ has a real eigenvalue $\lambda > 1$, such that if $\lambda' \in \mathbb{C}$ is an eigenvalue of M then $\lambda \geq |\lambda'|$.

(iii) The eigenvalue λ has multiplicity 1, and its corresponding eigenspace is spanned by an eigenvector v with strictly positive entries.

(iv) Assigning the weights $v_1, v_2, \ldots, v_k$ to the branches $e_1, e_2, \ldots, e_k$ respectively, turns τ into a measured train track, that is, the assigned weights satisfy the switch condition.

Then f is isotopic to a pseudo-Anosov homeomorphism with dilatation λ.

Given a pseudo-Anosov homeomorphism, the Bestvina-Handel algorithm of [5], which we describe in Section 3.3, constructs a train track satisfying the properties of Theorem 4. Moreover, in Chapter 9 of [39] a procedure is described which decides whether a mapping class $[f]$ is pseudo-Anosov, given an invariant train track.

Example 2. Let S be the thrice punctured plane. Let $f : S \to S$, $f = \sigma_1^{-1} \circ \sigma_2$ be a homeomorphism, where for $i = 1, 2$, σ_i is the homeomorphism which is a counter-clockwise *half-twist* which exchanges punctures i and $i + 1$. More precisely, if puncture i is placed at $(-1, 0)$, puncture $i+1$ is placed at $(1, 0)$ and no other puncture is contained in the disk of radius 2 about the origin, then in polar coordinates σ_i is given by

$$\sigma_i(r, \theta) = \begin{cases} (r, \theta + \pi(2 - r)), & \text{if } r \leq 2 \\ (r, \theta), & \text{if } r > 2. \end{cases}$$

We assume for convenience, by an isotopy if necessary, that f is a diffeomorphism.

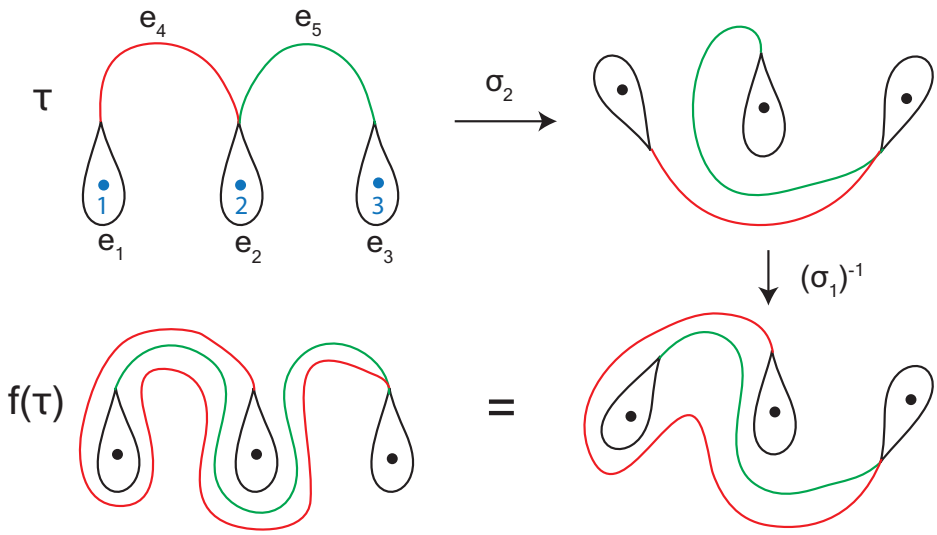

Figure 3.4: An invariant train track τ. Note that there exists a carrying map which collapses 'parallel' strands of the train track $f(\tau)$ shown in the bottom left.

Let φ be the carrying map. We compute the transition matrix

$$M = \begin{array}{c} \\ e_1 \\ e_2 \\ e_3 \\ e_4 \\ e_5 \end{array} \begin{array}{c} \begin{array}{ccccc} e_1 & e_2 & e_3 & e_4 & e_5 \end{array} \\ \begin{pmatrix} 0 & 0 & 1 & 1 & 0 \\ 1 & 0 & 0 & 1 & 1 \\ 0 & 1 & 0 & 0 & 0 \\ 0 & 0 & 0 & 2 & 1 \\ 0 & 0 & 0 & 1 & 1 \end{pmatrix} \end{array}.$$

For example, the 2nd entry of the 4th column is the number of times e_2 appears in the list e_1, e_2, e_4, e_4, e_5, of edges crossed by the curve $\varphi \circ f(e_4)$. We check that the transition matrix has a largest eigenvalue of multiplicity one, given by $\lambda = \frac{1}{2}(3+\sqrt{5}) = 2.618..$, with an associated eigenvector which assigns weights to the train track as shown below.

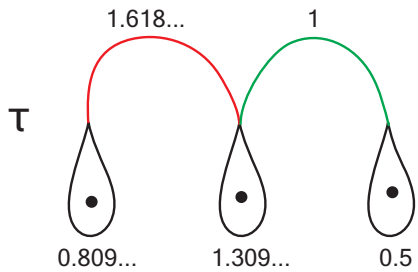

Figure 3.5: We may compute the weights exactly, but for clarity only decimal approximations are shown.

We can check that the switch conditions are satisfied. By Theorem 4, we conclude that f is isotopic to a pseudo-Anosov homeomorphism with dilatation $\lambda = \frac{1}{2}(3+\sqrt{5}) = 2.618...$

3.3 The Bestvina-Handel algorithm

In this section we give an exposition of the algorithm which is used in [5] to prove Thurston's classification of surface automorphisms. Other useful related references in-

clude [26], [9] and [6]. We remind the reader that all homeomorphisms considered are orientation-preserving.

3.3.1 Fibered surfaces

Definition 23. A *fibered surface* is a compact topological surface F with boundary, which is partitioned into arcs and into polygons such that:

(i) Each path component of the union of the arcs is a *strip*, fibered by the arcs (Figure 3.6.)

(ii) Each polygon is a *k-junction*, for some $k \in \mathbb{Z}_{>0}$ (Figure 3.6.)

An arc or junction is called a *decomposition element*.

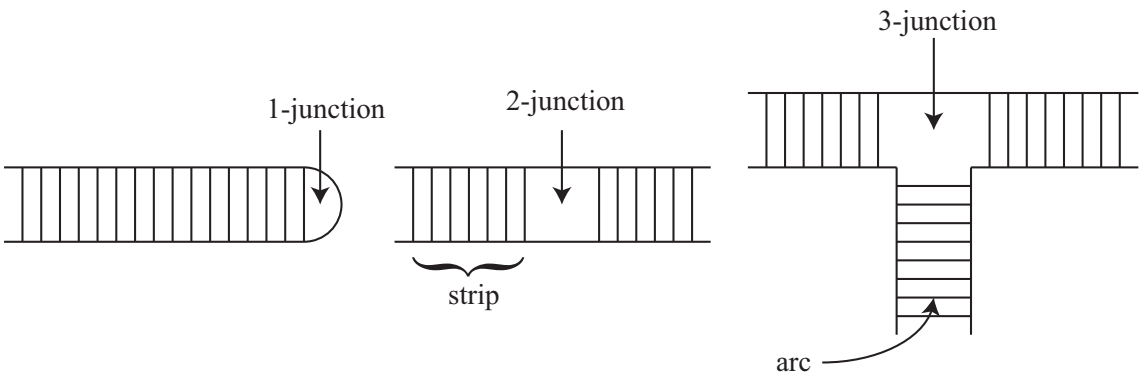

Figure 3.6: Model for k-junctions, for $k = 1, 2, 3$. Only a few of the arcs which fiber the strips are shown.

Definition 24. Let S be a surface and let $F \subseteq S$ be a fibered surface in S. Let $G = G(F)$ denote the topological space obtained by identifying each decomposition element to a point. We will denote the quotient map by $\pi : F \to G$.

Observe that G is a topological graph. Each k-junction is identified to a vertex of G with degree k, and each strip is mapped by π to the interior of an edge of G (see Figure 3.7.)

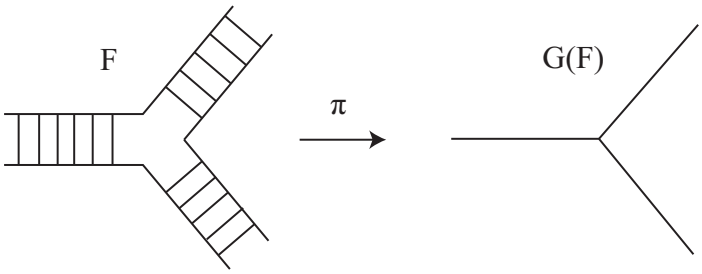

Figure 3.7: The quotient map $\pi : F \to G(F)$ near a 3-junction of the fibered surface F.

Notation 1. If S is a surface possibly with punctures (distinguished points), then we will denote the surface $S - \{\text{punctures}\}$ by S_0.

Definition 25. A *spine* of a surface S is an embedded graph $G \subseteq S_0$ such that S_0 deformation retracts onto G.

If F is a fibered surface then we can think of $G(F)$ as being embedded in F as a spine.

Definition 26. Let S be a surface and let $F \subseteq S_0$ be a fibered surface in S_0 and let $f : S_0 \to S_0$ be a homeomorphism. The fibered surface F *carries* f if

(i) S_0 deformation retracts onto F,

(ii) f restricts to a map $f : F \to F$,

(iii) f maps each decomposition element of F into a decomposition element, and each junction into a junction.

Notation 2. If G is a graph, then we use the notation $\mathcal{E}_{dir}(G)$ and $\mathcal{E}_{und}(G)$ to denote the set of directed edges of G and the set of undirected edges of G, respectively. If $e \in \mathcal{E}_{dir}(G)$ then we use $\overline{e}$ to denote the edge e with its orientation reversed.

Definition 27. Let S be a fibered surface, let $F \subseteq S$ be a fibered surface which carries a homeomorphism $\phi : S_0 \to S_0$. Let $G = G(F)$ and let $\pi : F \to G$ be the quotient map.

(i) A *graph map* on G is a continuous map $\mathfrak{g} : G \to G$, which maps vertices to vertices and an oriented edge $e \in \mathcal{E}_{dir}(G)$ to an *edge-path*, which is an oriented path $e_1 e_2 \cdots e_k$, where $e_1, \ldots, e_k \in \mathcal{E}_{dir}(G)$ and the terminal vertex of e_i is equal to the initial vertex of e_{i+1}, for $i = 1, 2, \ldots, k-1$.

(ii) The homeomorphism ϕ *induces* a graph map

$$\mathfrak{g} : G \to G$$

given as follows.

Let $e \in \mathcal{E}_{dir}(G)$. The oriented strip $\pi^{-1}(e)$ is mapped by ϕ to a sequence of strips, which are collapsed by π to a sequence of edges $e_1, e_2, \ldots, e_k \in \mathcal{E}_{dir}(G)$ respectively, where $k \in \mathbb{Z}_{\geq 0}$. Define $g(e)$ to be the edge-path $g(e) = e_1 e_2 \cdots e_k$.

(iii) Let $e_1, e_2, \ldots, e_n \in \mathcal{E}_{dir}(G)$ be oriented representatives of the edges in $\mathcal{E}_{und}(G)$. The *transition matrix* of a graph map $\mathfrak{g} : G \to G$ is the $n \times n$ matrix M such that M_{ij} is equal to the number of times either of e_i or $\overline{e_i}$ occurs in the edge-path $\mathfrak{g}(e_j)$. The *growth rate* of $\mathfrak{g}$ is the largest real eigenvalue of M, provided that it exists.

(iv) Let $\mathfrak{g} : G \to G$ be a graph map which does not map any edge to an empty edge-path. The *derivative* of $\mathfrak{g}$ is

$$\begin{aligned} D\mathfrak{g} : \mathcal{E}_{dir} &\to \mathcal{E}_{dir} \\ e &\mapsto D\mathfrak{g}(e) \end{aligned}$$

where $D\mathfrak{g}(e)$ is the first edge in the edge-path $\mathfrak{g}(e)$.

(v) The *link* $Lk(v, G) \subseteq \mathcal{E}_{dir}(G)$ of a vertex v is the set of oriented edges emanating from v. Let $e_1, e_2, \ldots, e_m$ be the elements of $Lk(v, G)$ ordered in cyclic order of edges encountered as one traverses a small loop around v. A set $K \subseteq L(v, G)$ is *connected* provided that if $i < j$ and $e_i, e_j \in K$ then either $e_i, e_{i+1}, \ldots, e_j \in K$ or $e_j, e_{j+1}, \ldots, e_m, e_1, \ldots, e_i \in K$.

(vi) Define an equivalence relation $\sim$ on $Lk(v, G)$ by,

$$e_1 \sim e_2 \quad \text{if there exists } k \in \mathbb{Z}_{>0} \text{ such that } (D\mathfrak{g})^k(e_1) = (D\mathfrak{g})^k(e_2).$$

The equivalence classes are called *gates* (with respect to $\mathfrak{g}$.)

3.3.2 Irreducibility and Perron-Frobenius theorem

Definition 28. Let $M \in \mathrm{M}_n(\mathbb{Z}_{\geq 0})$ be a $n \times n$ matrix with non-negative integer entries. The matrix M is *irreducible* if any of the following equivalent conditions hold:

(i) If $1 \leq i, j \leq n$, then there exists $k \in \mathbb{Z}_{>0}$ such that $M_{ij}^k > 0$.

(ii) There does not exist a permutation matrix P such that

$$PMP^{-1} = \begin{pmatrix} A & B \\ 0 & C \end{pmatrix}$$

where A and C are square matrices.

(iii) If G is a directed graph with adjacency matrix that equals M, then there is a directed path from u to v for each pair (u, v) of vertices of G.

Theorem 5 (Perron-Frobenius Theorem)**.** Let M be an irreducible matrix. Then M has a unique eigenvalue $\lambda \in \mathbb{R}_{\geq 1}$ such that

(i) If $\lambda' \in \mathbb{C}$ is an eigenvalue of M then $\lambda \geq |\lambda'|$.

(ii) The eigenspace associated with λ is 1-dimensional and is spanned by an eigenvector with strictly positive real entries. Such an eigenvector is called a *Perron eigenvector* of M.

Furthermore, if $\lambda = 1$, then M is a permutation matrix.

For a proof of the Perron-Frobenius Theorem see [9, Theorem 3.1.1], or [21, XIII §2 Theorem 2].

3.3.3 Efficiency

Let S be a surface with a single puncture. Let $\varphi : S \to S$ be an orientation-preserving homeomorphism fixing the puncture, which is carried by a fibered surface $F \subseteq S_0$. Let $\mathfrak{g} : G \to G$ be the induced graph map on the graph $G = G(F)$ and let M be the transition matrix.

Definition 29. The graph map $\mathfrak{g}$ and homeomorphism φ are *irreducible* if M is irreducible and G has no valence 1 or 2 vertices.

Definition 30. Suppose that $\mathfrak{g}$ is irreducible, and that the transition matrix M is written with respect to the edges $e_1, e_2, \ldots, e_n \in \mathcal{E}_{und}(G)$. Since M is irreducible it has a Perron eigenvector $v \in \mathbb{R}^n$. For $i \in \{1, 2, \ldots, n\}$, the *weight assigned* to e_i is $w(e) = v_i \in \mathbb{R}$, the ith coordinate of v. Note that the weights are only defined up to scalar multiplication.

Definition 31. The graph map $\mathfrak{g}$ and fibered surface F are *efficient* if $\mathfrak{g}$ is irreducible and the following conditions are satisfied:

1. If $k \in \mathbb{Z}_{>0}$ then the graph map $\mathfrak{g}^k$ maps each edge to an edge-path which does not *backtrack*, i.e. does not contain an edge $e \in \mathcal{E}_{dir}$ followed by $\overline{e}$.

2. If $e \in \mathcal{E}_{dir}(G)$ then the edge-path $\mathfrak{g}(e) = e_1 e_2 \cdots e_k$ does not backtrack, and $D\mathfrak{g}(\overline{e_i})$ and $D\mathfrak{g}(e_{i+1})$ are in distinct gates, for $1 \leq i < k$.

If $\mathfrak{g}$ is irreducible then conditions (i) and (ii) are equivalent, see Lemma 3.1.2 of [5].

3.3.4 Algorithm input and output

We describe the Bestvina-Handel algorithm in the case where the surface has a single puncture, which is the case where the algorithm is most transparent. In [5], modifications to the algorithm are described which deal with surfaces with multiple punctures as well as closed surfaces.

Let S be a surface with one puncture which we consider to be a distinguished point on our surface. Let $S_0 = S - \{\text{puncture}\}$ be the surface with the distinguished point removed.

Input

1. An orientation-preserving homeomorphism $f : S \to S$ which fixes the puncture.
2. A fibered surface $F \subseteq S$ carrying f.

Output
The algorithm either determines that f is isotopic rel punctures to a homeomorphism which is either reducible, otherwise the algorithm outputs the following:

1. A homeomorphism $f' : S \to S$, isotopic rel puncture to f.
2. An efficient, irreducible fibered surface $F' \subseteq S$ carrying f'.

3.3.5 Moves on fibered surfaces

Let S be a surface with a single puncture and let $F \subseteq S$ be a fibered surface carrying a homeomorphism $f : S \to S$ fixing the puncture. Before describing the steps of the algorithm we describe moves we can use to modify F to obtain another fibered surface F' carrying a homeomorphism f' isotopic to f. Each move will generally modify F and isotope f rel puncture. Let $\mathfrak{g} : G \to G$ be the graph map induced by (F, f). We will denote the new graph and graph map obtained from the modification by G' and $\mathfrak{g}'$, respectively.

Collapsing an invariant forest

Suppose that $\mathfrak{g}$ has an *invariant forest*, that is, a subgraph H such that each connected component of H is contractible and $\mathfrak{g}(H) \subseteq H$.

- The homeomorphism is unchanged, $f' = f$.
- The fibered surface F' is obtained from F by declaring each subsurface of F corresponding to a connected component of H to be a junction.
- The new graph G' can be thought of as being obtained from G by collapsing each component of H to a point. Thus, $\mathfrak{g}'(e)$ is obtained from $\mathfrak{g}(e)$ by removing all occurrences of edges in the invariant forest.

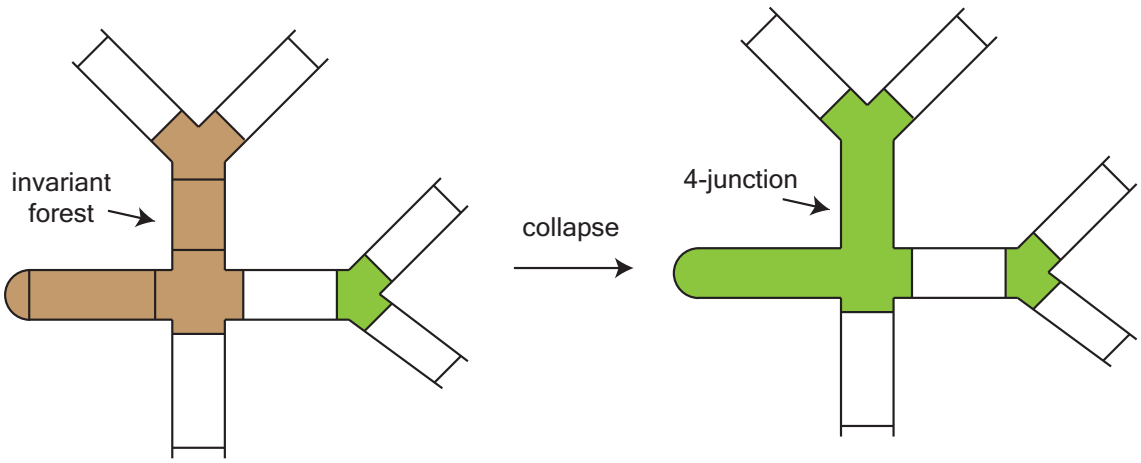

Figure 3.8: Collapsing an invariant forest.

Valence 1 isotopy

Suppose that G has a valence 1 vertex. Let J be the union of the strip E incident to the 1-junction and the two adjacent junctions. Let $h : S \to S$ be a homeomorphism isotopic to the identity which is equal to the identity map outside of J, such that $h \circ f(F)$ misses the strip E.

- The new homeomorphism is $f' = h \circ f$.
- F' is obtained from F by removing E and the 1-junction.
- G' can be thought of as obtained from G by removing the valence 1 vertex and incident edge.
- If e is an edge in G' then $\mathfrak{g}'(e)$ can be thought of as obtained from $\mathfrak{g}(e)$ by removing all occurrence of the removed edge.

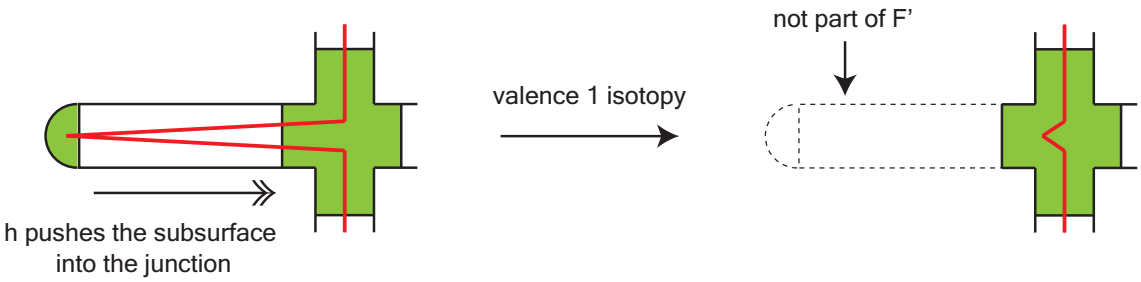

Figure 3.9: Valence 1 isotopy. The red lines schematically indicate the image of the fibered surface under the homeomorphism.

Valence 2 isotopy

Suppose that G has a valence 2 vertex v with adjacent edges e_i and e_j oriented away from v. We describe a valence 2 isotopy *across* e_i. Let J be the union of the two strips corresponding to e_i, e_j and adjacent junctions (generally, there are 3 junctions.) Let $h : S \to S$ be a homeomorphism isotopic to the identity which, intuitively, pushes the 2-junction across the strip corresponding to e_i and into the adjacent junction, and is the identity map outside of J.

- The new homeomorphism is $f' = h \circ f$. Note that no junction is mapped into the 2-junction by f'.
- F' is obtained from F by foliating the 2-junction with arcs so that the two adjacent strips now form one strip.
- G' can be thought of as obtained from G by removing the valence 2-vertex and amalgamating the incident edges to form a single edge e'_j.
- If e is an edge of G' other than e'_j then $\mathfrak{g}'(e)$ can be thought of as obtained from $\mathfrak{g}(e)$ by removing all occurrences of e_i and replacing occurrences of e_j by e'_j. If e'_j is oriented in the same direction as e_j then $\mathfrak{g}'(e'_j)$ can be thought of as obtained from $\mathfrak{g}(\overline{e_i}e_j) = \mathfrak{g}(\overline{e_i})\mathfrak{g}(e_j)$ by removing occurrences of e_i and replacing e_j by e'_j.

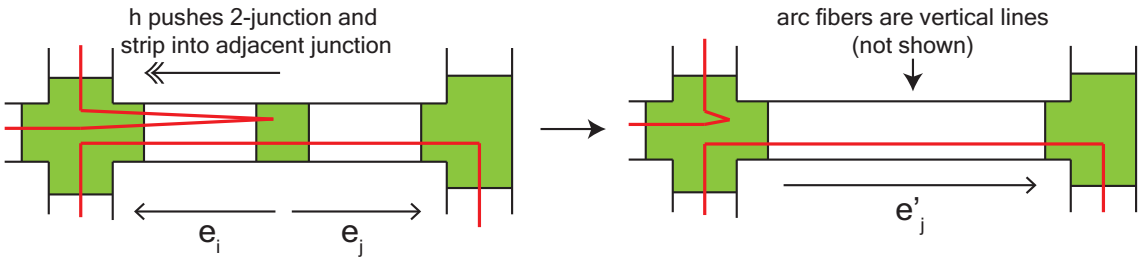

Figure 3.10: Valence 2 isotopy. The red lines schematically indicate the image of the fibered surface under the homeomorphism.

Pulling tight

There are two ways to pull tight. The fibered surface F and graph G do not change in both cases.

Pull tight type 1

Suppose v is a vertex of G and $D\mathfrak{g}(e_i)$ is independent of the edge e_i emanating from v. Let $h : S \to S$ be a homeomorphism isotopic to the identity which equals the identity map outside of the strip corresponding to $D\mathfrak{g}(e_i)$ and two adjacent junctions, such that the new homeomorphism $f' = h \circ f$ induces a graph map which removes the first edge in each edge path $\mathfrak{g}(e_i)$ (see Figure 3.11.)

After performing this a finite number of times, starting with "innermost" vertices first we may assume that $D\mathfrak{g}'$ is not constant at any vertex.

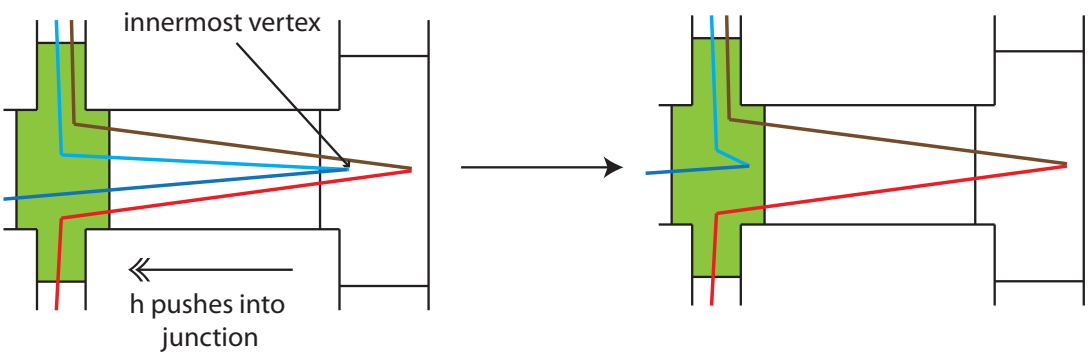

Figure 3.11: Pull tight type 1. Colours schematically represent the image of the fibered surface under the homeomorphism, with different colours indicating different strips. We work on the innermost vertex first.

Pull tight type 2

Suppose that e is an edge such that $\mathfrak{g}(e)$ backtracks, i.e. contains a subpath $e_i\,\overline{e_i}$ where $e_i \in \mathcal{E}_{dir}(G)$. Let $h : S \to S$ be isotopic to the identity, which is the identity outside of the union of the strip corresponding to e_i and the two adjacent junctions, and such that the graph map $\mathfrak{g}'$ induced by $f' = h \circ f$ no longer has the occurrence of $e_i\,\overline{e_i}$ in $\mathfrak{g}'(e)$ (see Figure 3.12.)

After performing this a finite number of times, starting with "innermost" edges first, we may assume that for $e' \in \mathcal{E}_{dir}(G)$, $\mathfrak{g}'(e')$ does not backtrack. The resulting graph map is independent of the order in which the tightening operations occur, and we can ignore consideration of which edges and vertices are "innermost."

We have $G' = G$ and $\mathfrak{g}'$ can be thought of as obtained from $\mathfrak{g}$ by removing the occurrences of backtracking in the image of each edge.

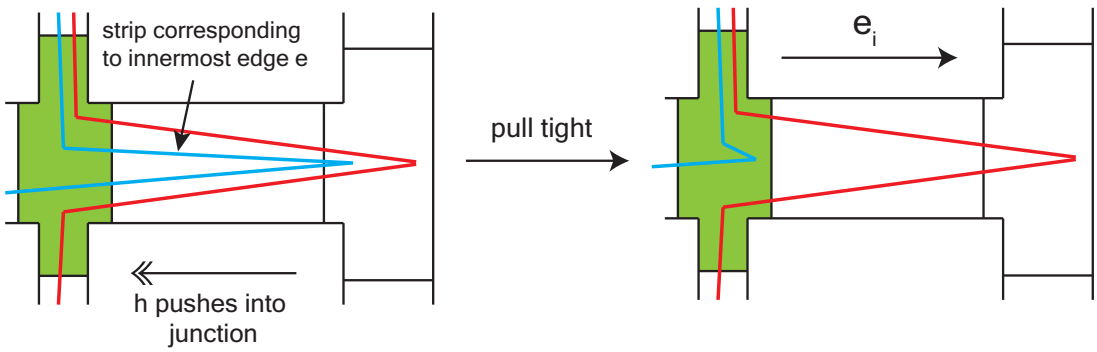

Figure 3.12: Pull tight type 2. The blue lines represent the image of a single strip.

Folding

Suppose that K is a connected collection of edges in the link of a vertex in G such that all the edges in K map to the same edge-path which does not backtrack. Then f sends the corresponding strips to "parallel" bands. Assume that $f(F)$ does not come between the bands, this can always be arranged by isotoping f.

- The homeomorphism is unchanged, $f' = f$.
- The strips corresponding to the edges in K, and their adjacent junctions are enlarged into a single strip and two junctions to obtain F' (see Figure 3.13.)
- G' can be thought of as obtained from G by identifying all the edges in K into a single edge e^*.
- If $e \in \mathcal{E}_{dir}(G')$ then $\mathfrak{g}'(e)$ can be thought of as obtained from $\mathfrak{g}(e)$ by replacing each occurrence of an edge in K with e^*.

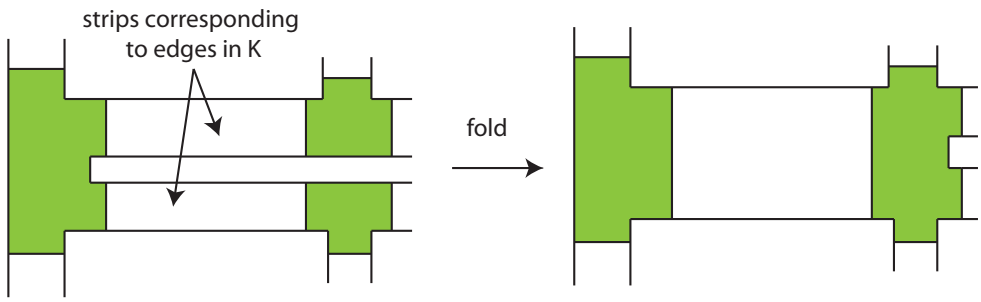

Figure 3.13: Folding two strips adjacent to a junction.

Subdivision

Suppose that v is a point in the interior of $e \in \mathcal{E}_{dir}(G)$ such that $\mathfrak{g}(e)$ is a vertex. We can declare v to be a vertex by introducing a 2-junction in the strip corresponding to e to obtain F'.

- The homeomorphism is unchanged, $f' = f$.
- The graph G' can be thought of as obtained from G by replacing e by a pair of edges e' and e'' with v as a common vertex.
- If E is an edge of G' other than e' or e'' then $\mathfrak{g}'(E)$ can be thought of as obtained from $\mathfrak{g}(E)$ by replacing every occurrence of e with the concatenation $e'e''$. Replacing each occurrence of e with $e'e''$ in $\mathfrak{g}(e)$ gives the concatenation $\mathfrak{g}'(e') \cdot \mathfrak{g}'(e'')$.

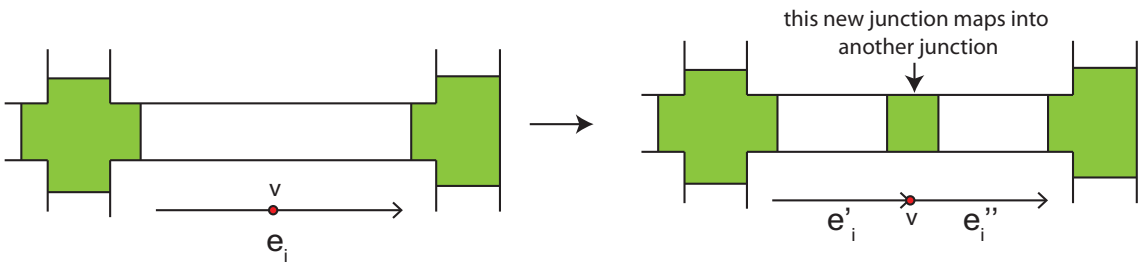

Figure 3.14: Subdivision.

3.3.6 Algorithm steps

Let S be a surface with one puncture which we consider to be a distinguished point on our surface and let $S_0 = S - \{\text{puncture}\}$ be the surface with the distinguished point removed. Let $f : S \to S$ be an orientation preserving homeomorphism fixing the puncture.

Choose a graph $G \subseteq S_0$ which forms a spine of S_0. For example, if S_0 is thought of topologically as a polygon punctured at its center, with its sides identified, then the sides of the polygon form edges of a spine $G \subseteq S_0$. The fibered surface F be can taken to be a regular neighbourhood of the graph G, with a junction for each vertex in G and fibering arcs transverse to G. In the polygon example this is a closed annulus 'border,' i.e. a closed regular neighbourhood of the boundary of the polygon.

By an isotopy of f we can arrange that G maps into F so that the vertices of G map into junctions, and the edges of G map into F transversely to the fibering arcs. By a further isotopy we can arrange that decomposition elements map into decomposition elements so that F carries f. Let $\mathfrak{g} : G \to G$ be the induced graph map.

(1) Pull-tight $\mathfrak{g}$ until $\mathfrak{g}$ is tight, that is, no further pull-tight moves are possible.

(2) While $\mathfrak{g}$ has an invariant, non-trivial forest, collapse it. If the new map is not tight, then go back to (1).

(3) If G has valence 1 vertices, remove them all by performing valence 1 isotopies. If the new map is not tight, or has an invariant non-trivial forest then go back to (1) or (2), respectively.

(4) If G contains a non-trivial invariant subgraph, then f is isotopic to a reducible homeomorphism and the algorithm stops.

(5) Note that at this stage $\mathfrak{g}$ is irreducible. Suppose that G has a valence 2 vertex v. Perform a valence 2 isotopy at v across the incident edge which gets assigned a larger weight by $\mathfrak{g}$ (if the assigned weights are equal, pick either one.)

If $\mathfrak{g}$ is not tight, go back to (1). If $\mathfrak{g}$ has a non-trivial invariant subgraph go back to (4).

(6) If the fibered surface F is efficient, then the algorithm stops. Otherwise F is not efficient. Hence, there exists $k \in \mathbb{Z}_{>0}$ and a point p in the interior of an edge $e \in \mathcal{E}_{dir}(G)$ in which $\mathfrak{g}^k$ is not locally injective, that is,

$$\mathfrak{g}^k(e) = e_1 e_2 \cdots e_{q-1}\ e_q \overline{e_q}\ e_{q+2} \cdots e_{m-1} e_m, \qquad \text{for some } q \in \mathbb{Z}_{>0}.$$

Backtracking occurs due to the appearance of $e_q \overline{e_q}$ in $\mathfrak{g}^k(e)$.

We choose k to be minimal above. Then $v_1 = \mathfrak{g}(p)$ is a vertex (otherwise, $\mathfrak{g}^{k-1}$ is not locally injective at v_1 and we could have chosen $k-1$ instead of k.)

Let $v_i = \mathfrak{g}^i(p)$ for $i = 1, 2, \ldots, k$. The point p divides the edge e into two 'half' edges a, b, oriented away from p. Let a_1, b_1 be the first edge in the edge-paths $\mathfrak{g}(a), \mathfrak{g}(b)$, respectively, and let

$$a_i = D\mathfrak{g}^{i-1}(a_1), \quad b_i = D\mathfrak{g}^{i-1}(b_1) \qquad \text{for } i = 2, 3, \ldots, k-1.$$

Let $c = D\mathfrak{g}(a_{k-1}) = D\mathfrak{g}(b_{k-1})$.

At this point the idea is that we would like to fold edges at v_{k-1}, so that $\mathfrak{g}^{k-1}$ backtracks. We continue folding at v_{k-2}, v_{k-3} etc., until finally $\mathfrak{g}$ backtracks, and we can pull-tight.

Let $d_1, d_2, \ldots, d_n$ be the edges in the link of v_{k-1} which map to c under $D\mathfrak{g}$. Then $\{d_1, \ldots, d_n\}$ is a connected set of edges in the link. Subdivide these edges if necessary, so that each edge maps to c under $\mathfrak{g}$.

(a) If p is not an endpoint of any of them, then fold the edges.

(b) Otherwise, if p is an endpoint of an edge, then folding would turn p into a vertex of valence greater than 2 and we would not be able to eventually pull-tight.

To avoid this, iterate c until it maps to an edge-path of length greater than 1, then subdivide c and its iterates. More precisely, consider c, $\mathfrak{g}(c)$, $\mathfrak{g}^2(c)$, $\ldots$, $\mathfrak{g}^r(c)$ where $r \in \mathbb{Z}_{>0}$ is minimal such that $\mathfrak{g}^r(c)$ has length greater than 1. Subdivide $\mathfrak{g}^{r-1}(c)$ at any interior point which maps to a vertex, then subdivide $\mathfrak{g}^{r-2}(c)$ in the same way, and so on until we subdivide c. Finally, subdivide then fold the edges in the link of v_{k-1} which map to c' (the edge incident to v_k resulting from a subdivision of c.)

Repeat the above procedure $k-2$ more times, folding at v_{k-2} and so on until we fold at v_1. After folding, the graph map $\mathfrak{g}$ is not tight, go back to (1).

When the algorithm terminates the graph map $\mathfrak{g}$ will be irreducible and efficient, and we will have an efficient fibered surface F which carries (a map isotopic to) f.

3.3.7 Efficient graph map to invariant train track

Let S be a surface with a single puncture and let $F \subseteq S_0$ be an efficient fibered surface carrying a homeomorphism $f : S_0 \to S_0$, e.g. as in the algorithm given above. If the growth rate $\lambda \in \mathbb{R}_{\geq 1}$ of the induced graph map $\mathfrak{g} : G \to G$ is equal to 1, then by the

Perron-Frobenius theorem (Theorem 5), the transition matrix is a permutation. Thus, a positive power of $\mathfrak{g}$ is the identity map, and f is isotopic to a periodic homeomorphism. Hence, we assume that $\lambda > 1$.

By definition of G there is a quotient map $\pi : F \to G$. Recall that the graph G can be thought of as embedded in F with vertices of G inside junctions of F, and edges of G which intersect fibering arcs transversely. We will construct an invariant train track τ by *graph smoothing* G.

For each vertex v of G. Draw a smooth closed curve C_v in the junction $\pi^{-1}(v)$. For each gate $\gamma \subseteq Lk(v, G)$ assign a point $p(\gamma)$ on C_v, such that the assigned points respect the cyclic order of edges around v.

There are two types of edges of τ:

- For each $e \in \mathcal{E}_{und}(G)$, there is a *real* edge of τ lying outside C_v, "parallel" to e, with endpoints on the assigned points of the C_v's corresponding to the appropriate gates.
- Let γ_1, γ_2 be gates at a vertex v. Then there is an *infinitesimal* edge of τ inside C_v joining $p(\gamma_1)$ to $p(\gamma_2)$ if a positive power of $\mathfrak{g}$ maps an edge to an edge-path which enters then exits the gates, that is, there exists $m \in \mathbb{Z}_{>0}$ and $e \in G$ such that $\mathfrak{g}^m(e)$ contains a subpath $e_i e_{i+1}$ where $\overline{e_i} \in \gamma_1$ and $e_{i+1} \in \gamma_2$. The resulting train track τ is C^1 at the assigned points on C_v, see Figure 3.15.

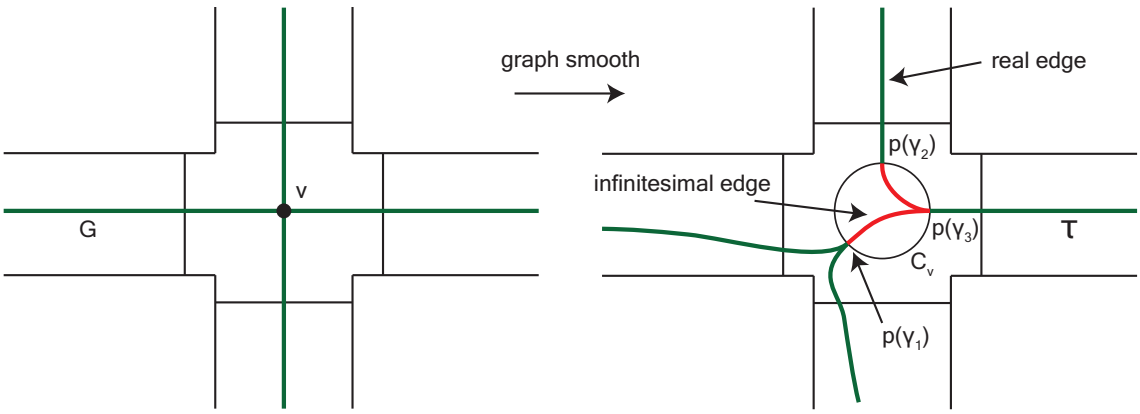

Figure 3.15: Example of graph smoothing at a junction.

If τ does not fill the surface, i.e. there is a connected component of $S \backslash \tau$ which is not homeomorphic to a disk or punctured disk, then f is isotopic to a reducible homeomorphism; the idea being that a regular neighbourhood of τ will have at least one essential boundary component, and the essential boundary components form a reducing set of curves (see Proposition 3.3.2 in [5].)

Assume that τ fills S_0. If v is a vertex with $k \in \mathbb{Z}_{>1}$ gates then one of the following cases occurs (see Figure 3.16, and Proposition 3.3.4 in [5] for a proof):

(i) $k = 2$ and there is one infinitesimal edge.

(ii) $k > 2$ and each pair of adjacent gates are connected, forming a k-gon.

(iii) $k > 2$ and all but one pair of adjacent gates are connected, forming a k-gon with a side missing.

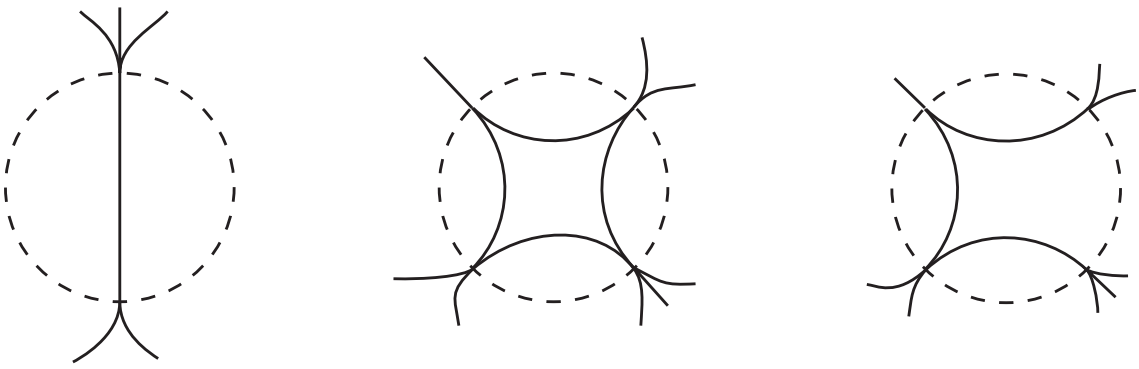

Figure 3.16: Three possible cases (i), (ii), (iii) respectively.

Definition 32. Let τ be a train track on a surface. A *train track map* $\mathfrak{h} : \tau \to \tau$ is a C^1 graph map such that for $i \in \mathbb{Z}_{>0}$, $\mathfrak{h}^i$ is an immersion, i.e. if v is a non-zero tangent to τ then $d\mathfrak{h}(v)$ is non-zero.

The graph map $\mathfrak{g}$ induces a train track map $\mathfrak{h} : \tau \to \tau$ as follows.

- Each real edge e of τ is sent to $\mathfrak{g}(e)$ where between every two consecutive edges in the edge path the infinitesimal edge joining the edges is inserted.
- Each infinitesimal edge e is sent to another infinitesimal edge, determined by the two gates to which $\mathfrak{g}$ sends the two gates of e.

The train track τ is invariant with respect to f. Note that the efficiency of $\mathfrak{g}$ ensures that the train track map does not backtrack on real edges and hence if u is a non-zero tangent vector to τ then $d\mathfrak{h}(u)$ is non-zero, i.e. $\mathfrak{h}$ is an immersion.

3.3.8 From train track to foliation

We continue from the previous section and show how to construct the invariant measured foliations for a homeomorphism isotopic to f using τ and $\mathfrak{h} : \tau \to \tau$. We only give a rough treatment, refer to Section 3.4 of [5] for more details.

(1) Recall that $\lambda > 1$ is the eigenvalue of the graph map $\mathfrak{g}$. Let M be the transition matrix of $\mathfrak{h}$ with respect to the ordered set of edges $e_1, e_2, \ldots, e_m \in \mathcal{E}_{und}(\tau)$, which includes both real and infinitesimal edges. It is shown in Section 3.4 of [5] that λ is an eigenvalue of M with eigenspace spanned by an eigenvector $W \in \mathbb{R}^m$ with positive entries (the graph map $\mathfrak{h}$ is not irreducible so this is not just the Perron-Frobenius theorem.) For $1 \leq i \leq m$, assign the ith entry of W as the weight $w(e_i)$ of e_i. The weights satisfy the switch condition, and hence τ becomes a measured train track with measure w.

(2) Similarly, $\lambda > 1$ is an eigenvector of M^t (transpose of M) with eigenspace spanned by an eigenvector $L \in \mathbb{R}^m$ with non-negative entries. For $1 \leq i \leq m$, assign the ith entry of L as the *length* $l(e_i) \in \mathbb{R}_{\geq 0}$ of e_i. Infinitesimal edges are assigned lengths of 0 and real edges are assigned positive lengths.

(3) For each edge e, place a euclidean rectangle $R_e = S_e \times U_e$ of width $w(e)$ and length $l(e)$ on the surface. Each such rectangle has two foliations: by horizontal lines of length $l(e)$, and by vertical lines of length $w(e)$. The horizontal lines are "parallel" to

the edge e. Each foliation has a transverse measure given by the euclidean distance in the transverse direction. We will identify the boundaries of the rectangles so that the horizontal lines will form the leaves of the unstable foliation and the vertical lines will form the leaves of the stable foliation, with transverse measures induced by the transverse measures on the rectangles.

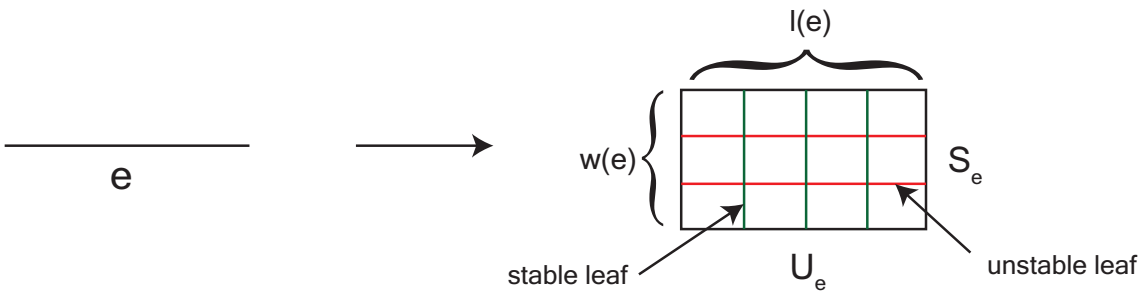

The infinitesimal edges have rectangles of length 0 which are thought of as just line segments. Identify the edges of the form $S_e \times \partial U_e$ using τ as shown below, to obtain a subset $\mathcal{R} \subseteq S_0$.

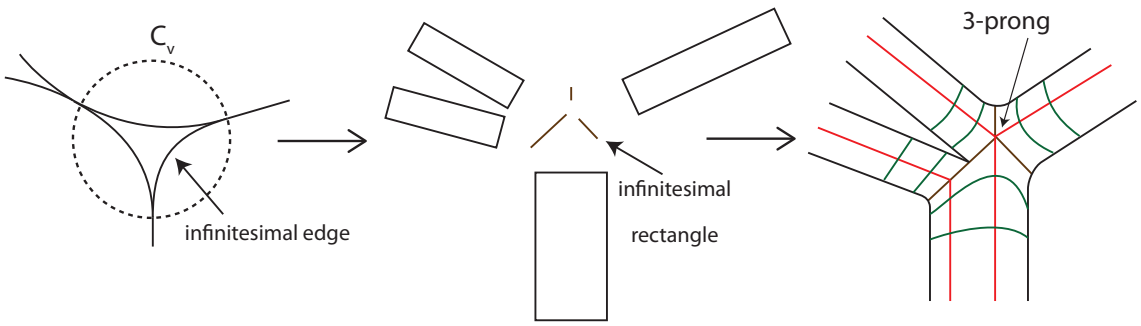

Figure 3.17: The region $\mathcal{R} \subseteq S_0$ is shown on the right. Note that a k-gon complementary region gives rise to a singularity of the foliations, but a k-gon with a missing side does not.

(4) Finally, $S_0 \backslash \mathcal{R}$ consists of one component homeomorphic to a punctured disk bounded by $\partial\mathcal{R}$. The boundary $\partial\mathcal{R}$ consists of $k \in \mathbb{Z}_{>0}$ cusps, i.e. non-smooth points. Adjacent sides of $\partial\mathcal{R}$ can be identified inside S, so that the puncture is the point in common to all sides, and the identification respects the euclidean measure of the rectangles. The stable and unstable foliations of the rectangles piece together to form the transverse measured foliations, invariant under a pseudo-Anosov homeomorphism isotopic to f.

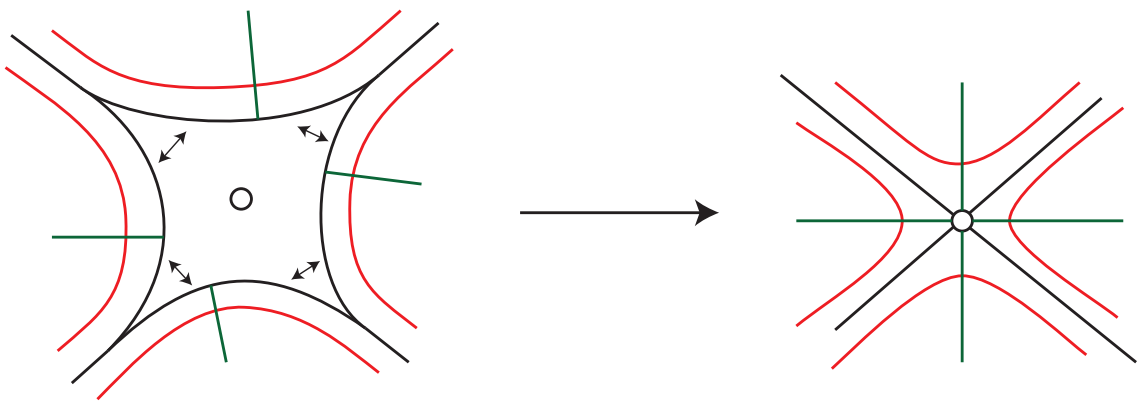

Figure 3.18: Identify adjacent sides of the boundary $\partial\mathcal{R}$.

3.4 Example — Once-punctured torus

We choose a spine G for the once-punctured torus T with an associated fibered surface F consisting of two strips and a single 4-junction as shown in Figure 3.19. The homeomorphism $f : T \to T$ is given by a left Dehn twist in b followed by a right Dehn twist in a.

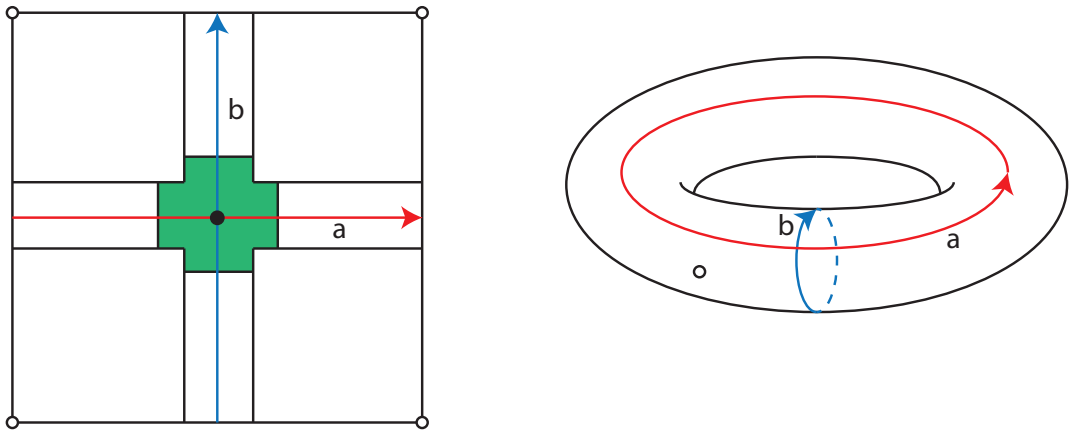

Figure 3.19: A spine of the punctured torus with two edges and one vertex. Opposite sides of the square are identified, and the puncture is placed at the corners. The arcs which fiber the strips of F are not shown.

We compute the image $f(G)$ of G as shown in Figures 3.20 and 3.21.

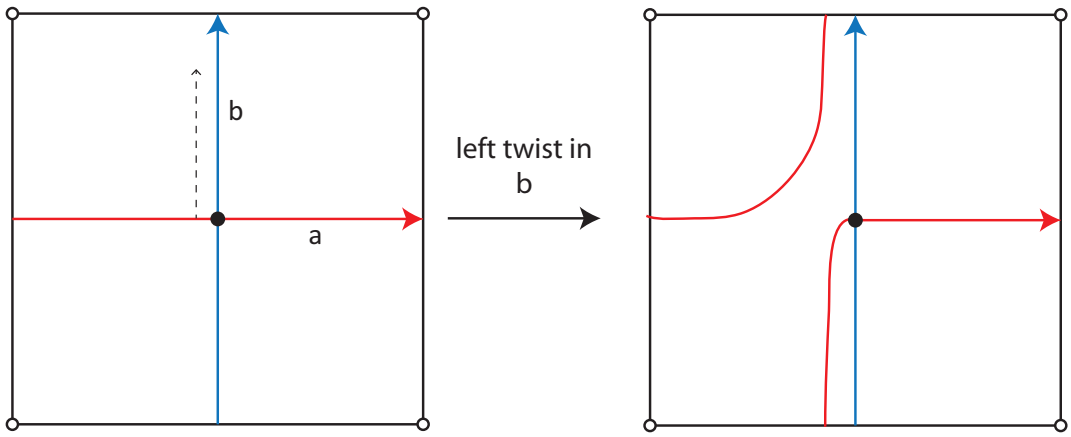

Figure 3.20: Left Dehn twist in b

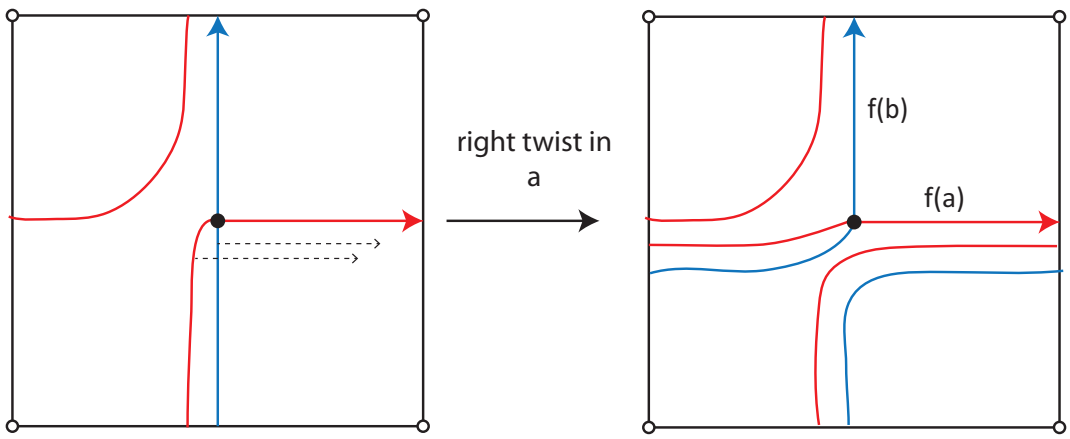

Figure 3.21: Right Dehn twist in a

To obtain a graph map representing f, we draw the image of G in the fibered surface F associated to G so that the image of each edge is transverse to the arcs which fiber the strips. Recall that by an isotopy if necessary we may assume that F carries f.

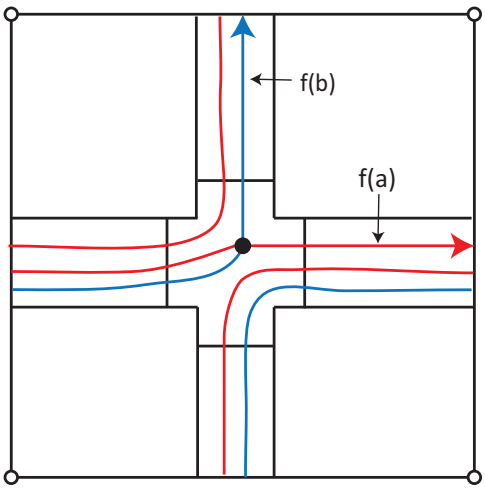

Figure 3.22: F carries f.

We can now read off the graph map $\mathfrak{g} : G \to G$ from Figure 3.22. The edge a maps to the edge-path $\mathfrak{g}(a) = aba$ and the edge b maps to the edge-path $\mathfrak{g}(b) = ba$.

Graph map:

$$\begin{array}{rcl} \mathfrak{g} : G & \to & G \\ a & \mapsto & aba \\ b & \mapsto & ba. \end{array}$$

Transition matrix of $\mathfrak{g}$:

$$M = \begin{array}{c} \\ a \\ b \end{array} \begin{array}{c} \begin{array}{cc} a & b \end{array} \\ \begin{pmatrix} 2 & 1 \\ 1 & 1 \end{pmatrix} \end{array}$$

The growth rate of $\mathfrak{g}$ is $\lambda = 1 + \phi \approx 2.618$ where $\phi = \frac{1}{2}(1 + \sqrt{5})$ is the golden ratio.

Nothing needs to be done for Steps 1-5 of the Bestvina-Handel algorithm, hence g is irreducible. We compute the gates at the single vertex v of G. The set of links at v is $Lk(v, G) = \{a, b, \bar{a}, \bar{b}\}$. We iterate $(a, b, \bar{a}, \bar{b})$ by $D\mathfrak{g}$ until it becomes periodic, i.e. we get a repeat:

$$(a, b, \bar{a}, \bar{b}) \mapsto (a, b, \bar{a}, \bar{a}) \mapsto (a, b, \bar{a}, \bar{a}).$$

The edges which are mapped by a power of $D\mathfrak{g}$ to the same edge belong to the same gate, hence the gates are: $\{a\}, \{b\}, \{\bar{a}, \bar{b}\}$.

To check that g is efficient, it suffices to check that as we traverse each edge-path in the image of $\mathfrak{g}$, each time we enter and then exit a vertex, we exit the vertex through a different gate to the one we entered. In the edge-path $\mathfrak{g}(a) = aba$, as we traverse ab we enter v through the gate $[\bar{a}]$ and exit through $[b]$, and as we traverse ba we enter v through the gate $[\bar{b}]$ and exit through $[a]$. Similarly, for the edge-path $g(a) = ba$, we enter v through $[\bar{b}]$ and exit through $[a]$, which are distinct gates. Hence $\mathfrak{g}$ is efficient.

We smooth the graph G at the vertices to obtain a train track. We draw a small circle C at the vertex v, and select three points on C corresponding to the three gates. Deform each edge of G so that:

1. each endpoint is at the selected point on C corresponding to the gate the endpoint determines,

2. the edge is disjoint from the interior of the circle, and

3. all the edges with endpoints at a point p of C are tangent at p.

This is shown in the left of Figure 3.23.

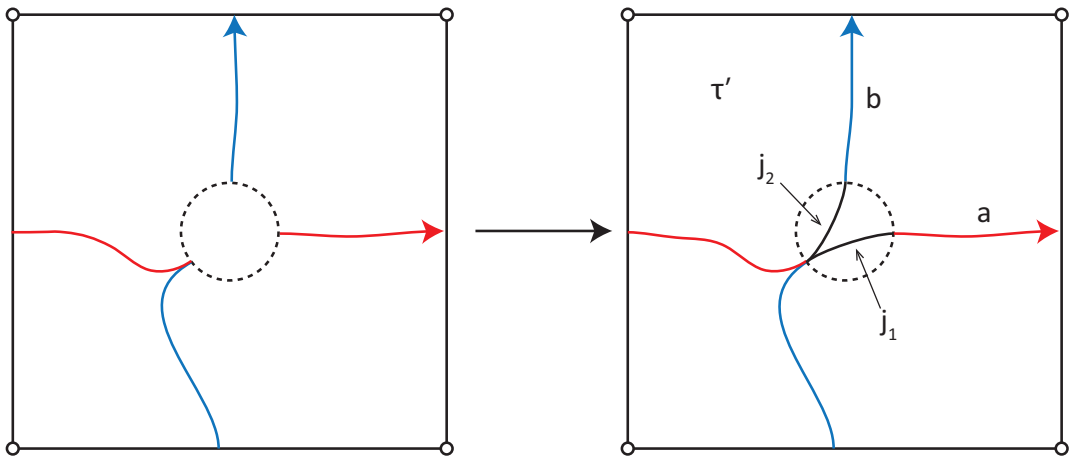

Figure 3.23: Smoothing the graph to a train track.

We compute the infinitesimal edges to obtain the train track τ'. For each pair of consecutive edges $e_i e_{i+1}$ in an edge-path in the image of $\mathfrak{g}$, calculate

$$(\overline{e_i}, e_{i+1}) \mapsto (D\mathfrak{g}(\overline{e_i}), D\mathfrak{g}(e_{i+1})) \mapsto (D\mathfrak{g}^2(\overline{e_i}), D\mathfrak{g}^2(e_{i+1})) \mapsto \cdots,$$

until the sequence becomes periodic. Connect gates corresponding to each pair of edges computed. In our example, $(\overline{a}, b) \mapsto (\overline{a}, b)$ and $(\overline{b}, a) \mapsto (\overline{a}, a) \mapsto (\overline{a}, a)$. We insert infinitesimal edges as shown above.

The transition matrix of g is given by

$$M = \begin{array}{c} \\ j_1 \\ j_2 \\ a \\ b \end{array} \begin{array}{c} \begin{array}{cccc} j_1 & j_2 & a & b \end{array} \\ \begin{pmatrix} 1 & 0 & 1 & 1 \\ 0 & 1 & 1 & 0 \\ 0 & 0 & 2 & 1 \\ 0 & 0 & 1 & 1 \end{pmatrix} \end{array}.$$

The dilatation is the largest positive eigenvalue of M, which is $\lambda = 1 + \varphi$ and with a corresponding eigenvector

$$\begin{array}{c} j_1 \\ j_2 \\ a \\ b \end{array} \begin{pmatrix} \varphi \\ 1 \\ \varphi \\ 1 \end{pmatrix},$$

which assigns weights to the branches of τ'.

3.5 Example — Once-punctured genus 2 surface

Let S be the genus two surface with a single puncture. Let $\varphi : S \to S$ be the homeomorphism given by left Dehn twists in the curves $C_5, C_4, C_5, C_5, C_5, C_2, C_3$, in that order, where the curves are as shown in Figure 3.24. We will see in Chapter 9 that this example gives a hyperbolic mapping torus with non-geometric veering triangulation.

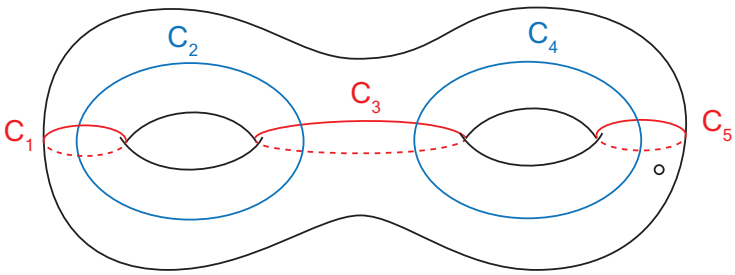

Figure 3.24: Humphries generators for MCG(S).

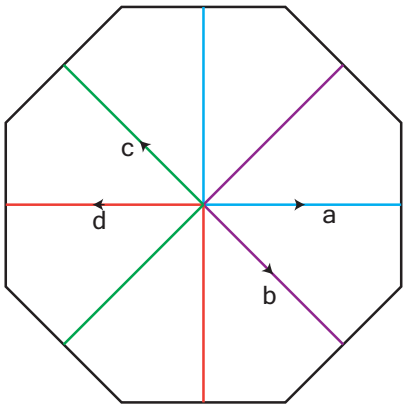

Figure 3.25: Spine G of a once-punctured genus 2 surface. The puncture is at the corners (vertices) of the octagon, and sides are identified via the colouring of edges.

Let F be the fibered surface naturally associated with the graph G, i.e. a regular neighbourhood of G with one 8-junction. We may isotope φ if necessary so that it carries F, and induces the graph map:

$$\begin{aligned} \mathfrak{g} : G &\to G \\ a &\mapsto db\overline{a}\overline{b}a\overline{b}\,\overline{d} \\ b &\mapsto \overline{b}\,\overline{b}a\overline{b}\,\overline{d} \\ c &\mapsto dbc \\ d &\mapsto \overline{c}\overline{b}. \end{aligned}$$

The graph map $\mathfrak{g}$ is calculated by our computer program, in a way similar to the previous example in Section 3.4. We will simply use $\mathfrak{g}$ as our starting point in performing the Bestvina-Handel algorithm to obtain an efficient graph map. Following [5, §6.1], we illustrate moves on the fibered surface by its effect on the graph G.

Move 1

Nothing needs to be done for Steps 1-5 of the Bestvina-Handel algorithm. By computing $\mathfrak{g}^2$, we see that

$$a \mapsto \ldots b\overline{a} \ldots \mapsto \ldots \overline{b}a\overline{b}\,\overline{d}\; db\overline{a}ba\overline{b} \ldots,$$

so $\mathfrak{g}^2$ backtracks in the interior of edge a. Hence we fold the start of $\overline{b}$ and $\overline{a}$ which map to $db\overline{a}b$. Let $a = a'x$ and $b = b'x$ where $x \mapsto \overline{b}a\overline{b}\,\overline{d}$. The new graph and graph map are shown

below. By abuse of notation we continue to use $\mathfrak{g} : G \to G$ to denote the new graph map. Notice that $x\overline{x}$ occurs in $\mathfrak{g}(a')$, so we pull-tight by cancelling.

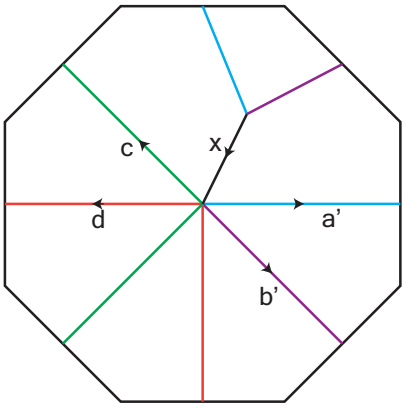

$$\begin{aligned}
\mathfrak{g} : G &\to G \\
a' &\mapsto db\overline{a} = db'x\overline{x}\overline{a'} = db'\overline{a'} \\
b' &\mapsto \overline{b} = \overline{x}\overline{b'} \\
c &\mapsto dbc = db'xc \\
d &\mapsto \overline{c}\overline{b} = \overline{c}\overline{x}b' \\
x &\mapsto \overline{b}a\overline{b}\,\overline{d} = \overline{x}\overline{b'}a'x\overline{x}\overline{b'}\,\overline{d} = \overline{x}\overline{b'}a'\overline{b'}\,\overline{d}
\end{aligned}$$

We drop the primes, i.e. in our notation we replace a', b' by a, b respectively.

Move 2

Since

$$c \mapsto \ldots xc \mapsto \ldots \overline{b}\,\overline{d}db \ldots,$$

we see that $\mathfrak{g}^2$ backtracks in the interior of edge c. We fold the start of $\overline{x}$ and c which maps to db. Let $c = yc'$ and $x = x'\overline{y}$, where $y \mapsto db$.

Remark 5. Let p be the point of c at which $\mathfrak{g}^2$ backtracks. Since this folding move involves c, which is the edge in which $\mathfrak{g}^2$ backtracks, we must check that folding does not turn p into a vertex in the new graph, i.e. p is not the intersection of the new edges y and c'.

In this case, this does not happen. We see that $\mathfrak{g}(c) = dbxc$ and p maps to the point of c between x and c in the image of c. Since $y \mapsto db, c' \mapsto xc$, so p does not turn into a vertex.

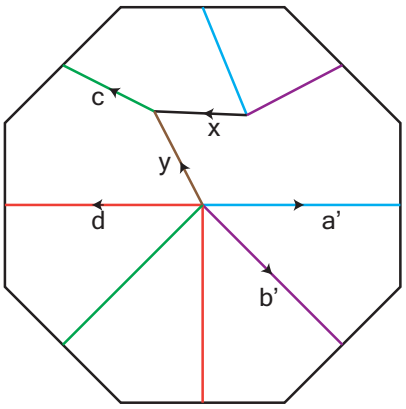

$$\begin{aligned}
\mathfrak{g} : G &\to G \\
a &\mapsto db\overline{a} \\
b &\mapsto \overline{x}\overline{b} = y\overline{x'}\,\overline{b} \\
c' &\mapsto xc = x'\overline{y}yc' = x'c' \\
d &\mapsto \overline{c}\,\overline{x}b = \overline{c'}\overline{y}y\overline{x'b} = \overline{c'}\,\overline{x'}\,\overline{b} \\
x' &\mapsto \overline{x}\overline{b}a = y\overline{x'b}a \\
y &\mapsto db
\end{aligned}$$

Move 3

Since

$$x \mapsto \ldots \overline{b}a \ldots \mapsto \ldots \overline{y}d \ldots \mapsto \ldots \overline{d}\overline{c} \ldots \mapsto \ldots xc\overline{c}\,\overline{x} \ldots,$$

so $\mathfrak{g}^4$ backtracks in the interior of edge x. We perform a sequence of 3 folding moves before we pull-tight.

Fold 1. We fold the start of d and $\overline{c}$ which maps to $\overline{c}\,\overline{x}$. We have $\mathfrak{g}(\overline{c}) = \overline{c}\,\overline{x}$ so we are folding the entire edge $\overline{c}$ with the start of d.

To see this most clearly we first isotope the graph so that c becomes a "short" edge.

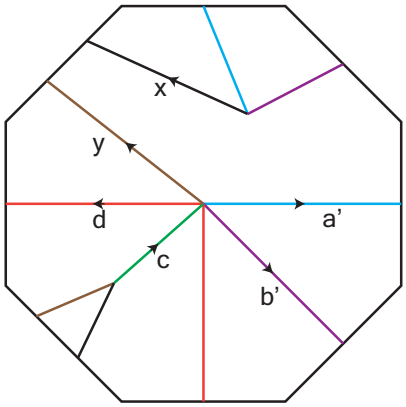

Let $c = c'$ and $d = \overline{c'}d'$ where $c' \mapsto xc$ and $d' \mapsto \overline{b}$.

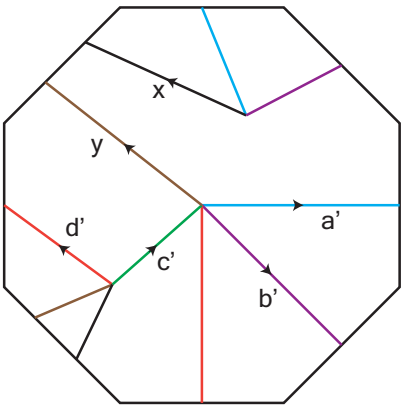

$$\begin{array}{rcl} \mathfrak{g} : G & \to & G \\ a & \mapsto & db\overline{a} = \overline{c'}d'b\overline{a} \\ b & \mapsto & y\overline{x}\overline{b} \\ c' & \mapsto & xc = xc' \\ d' & \mapsto & \overline{b} \\ x & \mapsto & y\overline{x}\overline{b}a \\ y & \mapsto & db = \overline{c'}d'b \end{array}$$

Fold 2. We drop the primes. Observe that we now have

$$x \mapsto \ldots \overline{b}a \ldots \mapsto \ldots \overline{yc} \ldots \mapsto \ldots c\overline{c} \ldots .$$

We would like to fold the start of y and $\overline{c}$ which maps to $\overline{c}$. However, we see that we also have $a \mapsto \overline{c} \ldots$ so we fold the start of y, $\overline{c}$ and a. Let $c = c'z$, $y = zy'$ and $a = za'$, where $z \mapsto \overline{c}$.

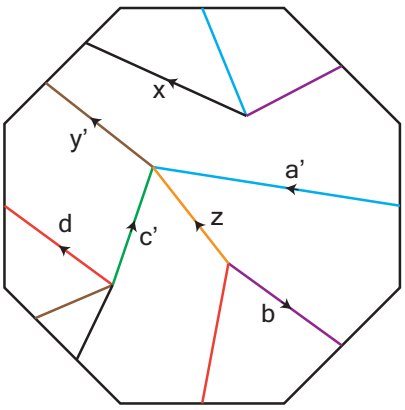

$$\begin{array}{rcl} \mathfrak{g} : G & \to & G \\ a' & \mapsto & db\overline{a} = db\overline{a'}\overline{z} \\ b & \mapsto & y\overline{x}\overline{b} = zy'\overline{x}\overline{b} \\ c' & \mapsto & x \\ d & \mapsto & \overline{b} \\ x & \mapsto & y\overline{x}\overline{b}a = zy'\overline{x}\overline{b}za' \\ y' & \mapsto & db \\ z & \mapsto & \overline{c} = z\overline{c'} \end{array}$$

Fold 3. We drop the primes. We now have

$$x \mapsto \ldots \overline{b}z \ldots \mapsto \ldots \overline{z}z \ldots .$$

Fold the start of b and z which maps to z. Then pull-tight.
Let $b = wb'$ and $z = wz'$, where $w \mapsto z$.

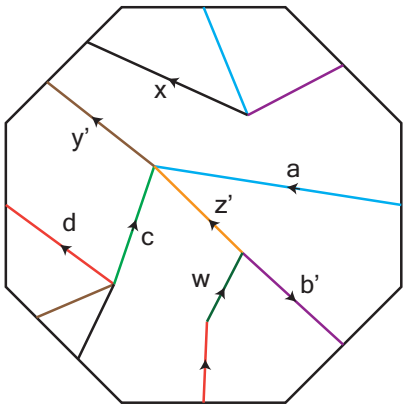

$$\begin{array}{rcl} \mathfrak{g} : G & \to & G \\ a & \mapsto & db\overline{a}\,\overline{z} = dwb'\overline{a}\overline{z'}\overline{w} \\ b' & \mapsto & y\overline{x}\overline{b} = y\overline{x}\overline{b'}\overline{w} \\ c & \mapsto & x \\ d & \mapsto & \overline{b} = \overline{b'}\overline{w} \\ x & \mapsto & zy\overline{x}\overline{b}za = wz'y\overline{x}\overline{b'}\overline{w}wz'a = wz'y\overline{x}\overline{b'}z'a \\ y & \mapsto & db = dwb' \\ z' & \mapsto & \overline{c} \\ w & \mapsto & z = wz' \end{array}$$

Move 4

We drop primes. There is a degree 2 vertex incident with edges w and $\overline{d}$, so we perform a valence 2-isotopy. The transition matrix of $\mathfrak{g}$ is

$$M = \begin{array}{c} \\ a \\ b \\ c \\ d \\ x \\ y \\ z \\ w \end{array} \begin{array}{c} \begin{array}{cccccccc} a & b & c & d & x & y & z & w \end{array} \\ \begin{pmatrix} 1 & 0 & 0 & 0 & 1 & 0 & 0 & 0 \\ 1 & 1 & 0 & 1 & 1 & 1 & 0 & 0 \\ 0 & 0 & 0 & 0 & 0 & 0 & 1 & 0 \\ 1 & 0 & 0 & 0 & 0 & 1 & 0 & 0 \\ 0 & 1 & 1 & 0 & 1 & 0 & 0 & 0 \\ 0 & 1 & 0 & 0 & 1 & 0 & 0 & 0 \\ 1 & 0 & 0 & 0 & 2 & 0 & 0 & 1 \\ 2 & 1 & 0 & 1 & 0 & 1 & 0 & 1 \end{pmatrix} \end{array}$$

with largest eigenvalue $\lambda = 2.9467\ldots$ and corresponding eigenvector which assigns weights

$$\text{weight}(d) = 0.23\ldots, \quad \text{weight}(w) = 1, (\text{up to scaling}).$$

Hence, we perform a valence 2-isotopy which removes the edge w, which has a larger weight than d. The image of the new edge, which we continue to label d, is given by $\mathfrak{g}(d)\mathfrak{g}(w) = \overline{b}\overline{w}wz$. We then remove w and $\overline{w}$ from the image of each edge of the graph map.

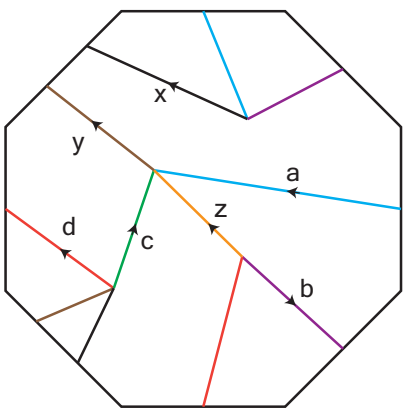

$$\begin{array}{rcl} \mathfrak{g} : G & \to & G \\ a & \mapsto & db\overline{a}\,\overline{z} \\ b & \mapsto & y\overline{x}\overline{b} \\ c & \mapsto & x \\ d & \mapsto & \overline{b}z \\ x & \mapsto & zy\overline{x}\overline{b}za \\ y & \mapsto & db \\ z & \mapsto & \overline{c} \end{array}$$

We claim that this graph map is efficient. We compute the gates at the vertices. At the vertex with edges $b, z, \overline{d}$ emanating from it, we iteratively apply $D\mathfrak{g}$ to each component of

$(b, z, \overline{d})$ until we find that an iterate repeats:

$$\begin{aligned}(b, z, \overline{d}) &\mapsto (y, \overline{c}, \overline{z}) \mapsto (d, \overline{x}, c) \mapsto (\overline{b}, \overline{a}, x) \mapsto (b, z, z) \mapsto \\ (y, \overline{c}, \overline{c}) &\mapsto (d, \overline{x}, \overline{x}) \mapsto (\overline{b}, \overline{a}, \overline{a}) \mapsto (b, z, z).\end{aligned}$$

We see that (b, z, z) repeats, hence the set of gates at the vertex is $\{\{b\}, \{z, \overline{d}\}\}$. Similarly, the sets of gates at the other vertices are $\{\{a, y\}, \{\overline{c}, \overline{z}\}\}, \{\{d, \overline{y}\}, \{\overline{x}, c\}\}, \{\{\overline{b}\}, \{\overline{a}, x\}\}$. We check that each edge-path in the image of $\mathfrak{g}$ enters and exits through distinct gates each time it enters a vertex, and therefore $\mathfrak{g}$ is efficient. The dilatation is $\lambda = 2.89005...$ Finally, adding infinitesimal edges as in Figure 3.26 gives an invariant train track for φ.

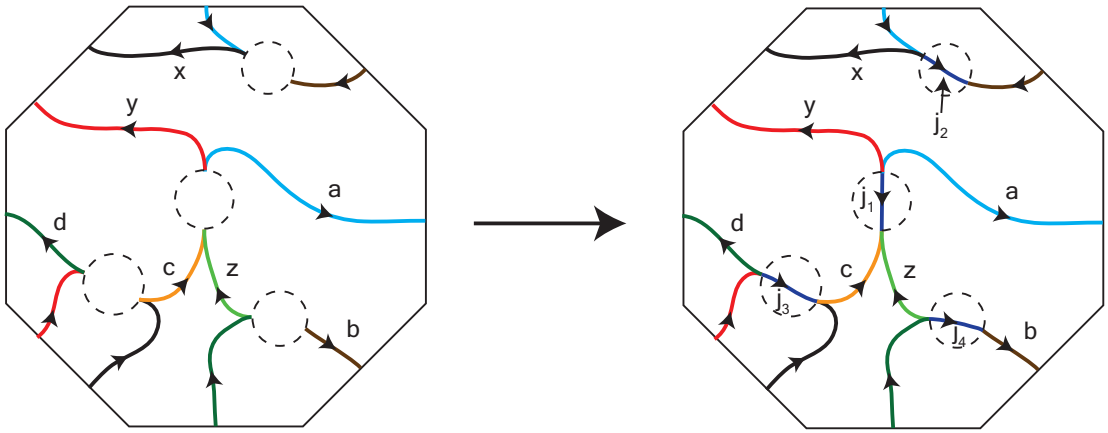

Figure 3.26: Insert infinitesimal edges. Since each vertex has two gates, they are joined by an infinitesimal edge. On the right we have an invariant train track for φ.

Chapter 4

Thurston's picture of surface diffeomorphisms

The main references for this chapter are [29], [18], [52], [40] and [1].

Definition 33. A *hyperbolic surface* S is a topological space with a *hyperbolic atlas*, which is a collection of pairs (U_α, ϕ_α), called *charts*, where $U_\alpha \subseteq S$ is open and $\phi_\alpha : U_\alpha \to \mathbb{H}^2$ is continuous, which satisfies the following:

(i) The charts cover S, that is, $\cup_\alpha U_\alpha = S$.

(ii) For each chart (U_α, ϕ_α), the image $\phi_\alpha(U_\alpha)$ is an open subset of $\mathbb{H}^2$, and the map ϕ_α is a homeomorphism onto its image.

(iii) If (U_α, ϕ_α) and (U_β, ϕ_β) are charts and $U_\alpha \cap U_\beta \neq \emptyset$ then

$$\phi_\beta \circ \phi_\alpha^{-1} : \phi_\alpha(U_\alpha \cap U_\beta) \to \phi_\beta(U_\alpha \cap U_\beta)$$

is a *local hyperbolic isometry*, that is, the restriction of $\phi_\beta \circ \phi_\alpha^{-1}$ to each path component of its domain is the restriction of a hyperbolic isometry to an open subset of $\mathbb{H}^2$.

Furthermore, S is *orientable* if each hyperbolic isometry in (iii) is orientation preserving.

A curve $\gamma \subseteq S$ is a *geodesic* if its image in each coordinate chart consists of geodesics. A geodesic on S is *complete* if it is not strictly contained in a geodesic of S.

Definition 34 (§10.1 of [17])**.** Let S be a surface with negative Euler characteristic. A *marked hyperbolic surface* with respect to S is a pair (f, M) where M is a complete finite-volume hyperbolic surface and $f : S \to M$ is a homeomorphism. The *Teichmüller space* of S is the set

$$\mathcal{T}(S) = \{(f, M) \mid (f, M) \text{ is a marked hyperbolic surface}\}/\sim$$

where $(f, M) \sim (f', M')$ if and only if $f' \circ f^{-1}$ is isotopic to an isometry.

Definition 35 (Appendix A of [40])**.** Let S be a surface with negative Euler characteristic with set of punctures P. We define an equivalence relation $\sim$ on the set of measured foliations on S, which is generated by the following relations:

(i) Isotopy rel P, that is, if $\mathcal{F}, \mathcal{F}'$ are measured foliations and $\varphi : S \to S$ is isotopic rel P to the identity map and $\varphi(\mathcal{F}) = \mathcal{F}'$ then $\mathcal{F} \sim \mathcal{F}'$.

(ii) Whitehead equivalence, that is, if L is a leaf of a measured foliation $\mathcal{F}$ joining two singularities, and at least one of the singularities is not a puncture, then $\mathcal{F} \sim \mathcal{F}'$ where $\mathcal{F}'$ is the measured foliation obtained by collapsing L to a point (Figure 4.1).

The *space of measured foliations* of S with respect to P is the set $\mathcal{MF}(S)$ of equivalence classes of measured foliations. If in addition to relations (i) and (ii) above we include,

(iii) if $\mathcal{F}$ is a measured foliation and $k \in \mathbb{R}_{>0}$ then $\mathcal{F} \sim k\mathcal{F}$,

we obtain the *space of projective measured foliations* $\mathcal{PMF}(S) = \mathcal{MF}(S)/\sim$.

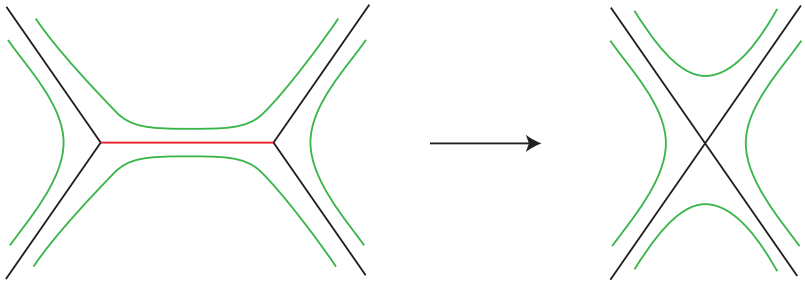

Figure 4.1: A Whitehead move collapsing the leaf shown in red. In general two $m, n \in \mathbb{Z}_{>0}$ prong singularities combine to form a $(n+m-2)$-prong singularity, shown is $n = m = 3$.

Let S be a closed surface with distinguished points P, which are considered to be punctures. Let $\mathcal{C}$ be the set of isotopy classes rel P of simple closed curves in $S \backslash P$ which do not bound a disk or a once punctured disk. Define

$$\begin{aligned} i : \mathcal{MF}(S) &\to \mathbb{R}^{\mathcal{C}} \\ (\mathcal{F}, \mu) &\mapsto f : \mathcal{C} \to \mathbb{R} \\ &\qquad\qquad [\alpha] \mapsto \inf\{\mu(\beta) \mid \beta \in [\alpha]\}, \end{aligned}$$

where $[\alpha]$ is the isotopy class rel P of α. Let $\pi : \mathbb{R}^{\mathcal{C}} \backslash \{0\} \to \mathrm{P}(\mathbb{R}^{\mathcal{C}})$ be the projection map, where $\mathrm{P}(\mathbb{R}^{\mathcal{C}})$ is the set of equivalence classes of functions $f : \mathcal{C} \to \mathbb{R}$, where two such functions f, f' are equivalent if $f = kf'$ for some $k \in \mathbb{R}_{>0}$. Then $\pi \circ i : \mathcal{MF}(S) \to \mathrm{P}(\mathbb{R}^{\mathcal{C}})$ is constant on elements which differ by multiplication by an element of $\mathbb{R}_{>0}$, and hence descends to a map $\pi \circ i : \mathcal{PMF}(S) \to \mathrm{P}(\mathbb{R}^{\mathcal{C}})$.

We define

$$\begin{aligned} i' : \mathcal{T}(S \backslash P) &\to \mathbb{R}^{\mathcal{C}} \\ (g, M) &\mapsto f : \mathcal{C} \to \mathbb{R} \end{aligned}$$

where $f([\alpha])$ is the length of the unique geodesic in M homotopic to $g(\alpha)$.

We give $\mathbb{R}^{\mathcal{C}}$ the product topology, and $\mathrm{P}(\mathbb{R}^{\mathcal{C}})$ the quotient topology.

Theorem 6 (Appendix A of [40])**.** Let g be the genus of S.

(i) $p \circ i(\mathcal{PMF}(S))$ is homeomorphic to a sphere of dimension $6g + 2|P| - 7$.

(ii) $p \circ i'(\mathcal{T}(S))$ is homeomorphic to an open ball of dimension $6, g + 2|P| - 6$.

(iii) The closure of $p \circ i'(\mathcal{T}(S))$ in $\mathrm{P}(\mathbb{R}^{\mathcal{C}})$ is

$$p \circ i'(\mathcal{T}(S)) \cup p \circ i(\mathcal{PMF}(S)).$$

(iv) Each of the maps $p \circ i'$ and $p \circ i : \mathcal{PMF}(S) \to \mathrm{P}(\mathbb{R}^{\mathcal{C}})$ is bijective onto its image in $\mathrm{P}(\mathbb{R}^{\mathcal{C}})$. We use these bijections to give $\mathcal{T}(S) \cup \mathcal{PMF}(S)$ a topology.

We denote by $\overline{\mathcal{T}}(S)$ the compactified Teichmuller space $\mathcal{T}(S) \cup \mathcal{PMF}(S)$, which is homeomorphic to a closed ball of dimension $6g + 2|P| - 6$.

See [18, Theorem 8.7] for a proof.

Define an action of $\mathrm{MCG}(S)$ on $\overline{\mathcal{T}}(S)$ as follows. Let $[\phi] \in \mathrm{MCG}(S)$, where the restriction $\phi : S \backslash P \to S \backslash P$ is a diffeomorphism.

- If $[\mathcal{F}] \in \mathcal{PMF}(S)$ then $\phi \cdot [\mathcal{F}] = [\phi(\mathcal{F})]$.
- If $(f, M) \in \mathcal{T}(S)$ then $\phi \cdot (f, M) = (f \circ \phi, M)$.

In fact, ϕ acts as a homeomorphism of the closed ball $\overline{\mathcal{T}}(S)$. By Brouwer's fixed point theorem, ϕ has a fixed point in $\overline{\mathcal{T}}(S)$. Before stating the main theorem for this section we introduce one last definition.

Definition 36 (Page 13 of [39])**.** A *leaf cycle* C of a measured foliation $\mathcal{F} \in \mathcal{MF}(S)$ is a union of finite leaf segments joining singularities of $\mathcal{F}$, such that either C is a simple closed curve in $S \backslash P$ or C is a simple curve where each endpoint is at a puncture of S. The measured foliation $\mathcal{F}$ is *arational* if there does not exist a leaf cycle of $\mathcal{F}$.

Theorem 7 (Appendix A of [40])**.** Let S be a surface with negative Euler characteristic. Let $\phi : S \to S$ be a homeomorphism. Then ϕ is isotopic to a homeomorphism $\phi' : S \to S$ such that at least one of the following two cases occurs:

(i) ϕ fixes an element of $\mathcal{T}(S)$. Then ϕ' has finite order.

(ii) ϕ fixes a point of the Thurston boundary $\mathcal{PMF}(S)$. Then there exists a measured foliation $\mathcal{F}$ and $\lambda \in \mathbb{R}_{>0}$ such that $\phi'(\mathcal{F}) = \lambda\mathcal{F}$. Furthermore, exactly one of the following three possibilities occurs:

  (a) $\mathcal{F}$ has a leaf cycle. Then ϕ' is reducible.

  (b) $\mathcal{F}$ is arational and $\lambda = 1$. Then ϕ' has finite order.

  (c) $\mathcal{F}$ is arational and $\lambda \neq 1$. Then ϕ' is pseudo-Anosov. In this case, ϕ has exactly two fixed points in $\overline{\mathcal{T}}(S)$ corresponding to the stable foliation and the unstable foliation.

For a proof of Theorem 7 see Exposé 9 of [18], or [52].

Chapter 5

Geodesic laminations

Most of this chapter is based on [12] and [11]. Other useful references include [32], [10], [45], [55], [37] and [7].

Convention 4. Throughout this section, all surfaces are assumed to be *complete hyperbolic finite-area* surfaces, and we consider all geodesics to be *complete*.

Definition 37. Let S be a hyperbolic surface. A *geodesic lamination* L (with compact support) is a non-empty compact subset of S which is a union of disjoint complete simple geodesics. A *leaf* of L is a geodesic contained in L. Denote by $\mathcal{L}(S)$ the set of geodesic laminations of S.

Remark 6. A geodesic lamination on a finite-area hyperbolic surface can be written as a union of simple geodesics in only one way, see Lemma 3.3 of [12].

Given a homeomorphism $\phi : S \to S$ and a geodesic lamination L on a hyperbolic surface S, the set $\phi(L)$ is generally not a geodesic lamination, but, roughly speaking, it can be "straightened" into a geodesic lamination $\phi_*(L)$, which we define precisely below.

Theorem 8. Let S be a surface and let $\varphi : S \to S$ be a homeomorphism. Let $p : \mathbb{H}^2 \to S$ be the universal cover, where $\widetilde{S}$ is identified with $\mathbb{H}^2$ via the developing map. Let $\widetilde{\varphi} : \mathbb{H}^2 \to \mathbb{H}^2$ be a lift of $\varphi \circ p : \mathbb{H}^2 \to S$ to the universal cover. Then $\widetilde{\varphi}$ extends to a homeomorphism

$$\overline{\varphi} : \overline{\mathbb{H}}^2 \to \overline{\mathbb{H}}^2,$$

where $\overline{\mathbb{H}}^2 = \mathbb{H}^2 \cup S^1_\infty$ is the hyperbolic plane with its boundary at infinity.

We will use the notation $\overline{\varphi}$ to denote the extension with respect to p (and a choice of lift $\widetilde{\varphi}$.)

The above theorem is known as Nielsen's extension theorem, see [12, Lemma 3.7] and [1] for a proof.

Definition 38. Let S be a surface and let $\phi : S \to S$ be a homeomorphism. Let $p : \mathbb{H}^2 \to S$ be the universal cover. Define

$$\varphi_* : \mathcal{L}(S) \to \mathcal{L}(S)$$

as follows. Let $L \in \mathcal{L}(S)$ be a geodesic lamination, and let $\widetilde{L}$ be a lift of L to $\mathbb{H}^2$. If ℓ is a leaf of $\widetilde{L}$ with endpoints $a, b \in S^1_\infty$, denote by γ_ℓ the geodesic in $\mathbb{H}^2$ with endpoints $\overline{\varphi}(a), \overline{\varphi}(b)$. Then

$$\varphi_*(L) = \bigcup_\ell p(\gamma_\ell),$$

where the union ranges over all leaves ℓ in $\widetilde{L}$. We call $p(\gamma_\ell)$ the *straightening* of $p(\ell)$.

Theorem 9 (Theorem 5.5 of [12])**.** Let S be a closed hyperbolic surface and let $h : S \to S$ be a homeomorphism which is not isotopic to a periodic or reducible homeomorphism. Then

(i) If $n \in \mathbb{Z}_{>0}$ and $\Phi : \mathbb{H}^2 \to \mathbb{H}^2$ is a lift of h^n, then Φ has finitely many fixed points on S^1_∞ and the fixed points are alternately contracting and expanding.

(ii) There exists a unique geodesic lamination Λ^+ on S such that:

  (a) $h_*(\Lambda^+) = \Lambda^+$.

  (b) If $n \in \mathbb{Z}_{>0}$ and $\Phi : \mathbb{H}^2 \to \mathbb{H}^2$ is a lift of h^n, then the lift $\widetilde{\Lambda}^+ \subseteq \mathbb{H}^2$ of Λ^+ contains the geodesics joining consecutive contracting fixed points of Φ on S^1_∞.

  (c) Every leaf of Λ^+ is dense in Λ^+.

Definition 39. The geodesic lamination Λ^+ defined in Theorem 9 is called the *stable lamination* of h. The *unstable lamination* of h is the stable lamination of h^{-1}.

Definition 40 (§1.7 of [45])**.** Let S be a complete hyperbolic surface. A *measured geodesic lamination* consists of a geodesic lamination L on S and a *transverse measure* on L, which is a function

$$\lambda : \mathcal{C} \to \mathbb{R}_{\geq 0}$$

where $\mathcal{C}$ is the set of simple (possibly closed) curves $\alpha : [0,1] \to S$, transverse to L with endpoints in $S - L$, such that the following holds:

(i) If $\alpha, \beta \in \mathcal{C}$ and $\text{image}(\alpha) = \text{image}(\beta)$ then $\lambda(\alpha) = \lambda(\beta)$.

(ii) If $\alpha, \beta \in \mathcal{C}$ and there is a homotopy F from α to β such that $F_t \in \mathcal{C}$ for $t \in [0,1]$, then

$$\lambda(\alpha) = \lambda(\beta).$$

(iii) Let $\alpha \in \mathcal{C}$ and $\alpha_i \in \mathcal{C}$ for i in I, a finite or countable index set. If $\text{image}(\alpha) = \cup_{i \in I} \text{image}(\alpha_i)$ and α_i and α_j intersect only at their endpoints for distinct $i, j \in I$, then

$$\lambda(\alpha) = \sum_{i \in I} \lambda(\alpha_i).$$

(iv) The support of λ is L, that is, if $\alpha \in \mathcal{C}$ then,

$$\lambda(\alpha) > 0 \quad \text{if and only if} \quad \alpha \cap L \neq \emptyset.$$

Definition 41. Let S be a hyperbolic surface. The *space of measured geodesic laminations* on S is the set $\mathcal{ML}(S)$ of measured geodesic laminations on S.

Define an equivalence relation $\sim$ on $\mathcal{ML}(S)$ by:

- $(L, \mu) \sim (L', \mu')$ if $L = L'$ and there exists $c \in \mathbb{R}_{>0}$ such that $\mu' = c\mu$.

The *space of projective measured laminations* on S is the set $\mathcal{PML}(S)$ of equivalence classes of measured geodesic laminations.

Definition 42. Let $\varphi : S \to S$ be a homeomorphism of a hyperbolic surface S. We assume, by an isotopy if necessary, that φ is a diffeomorphism. Define the *induced map* φ_* on $\mathcal{ML}(S)$ by

$$\begin{aligned} \varphi_* : \mathcal{ML}(S) &\to \mathcal{ML}(S) \\ (L, \mu) &\mapsto (\varphi_*(L), \mu'), \end{aligned}$$

where μ' is defined as follows. Let $\alpha : [0,1] \to S$ be a simple curve transverse to $\varphi_*(L)$ with endpoints in $S \backslash \varphi_*(L)$. Let $\beta : [0,1] \to S$ be a simple curve transverse to $\varphi(L)$, which has the same intersection pattern as α, that is, such that:

(i) $\alpha^{-1}(\varphi_*(L)) = \beta^{-1}(\varphi(L)) \subseteq [0,1]$, and

(ii) if $t \in [0,1]$ and $\beta(t)$ is in $\varphi(\ell)$ for some leaf ℓ of L, then $\alpha(t)$ is on the leaf of $\alpha_*(L)$ which is the straightening of $\varphi(\ell)$.

Define $\mu'(\alpha) = \mu(\varphi^{-1}(\beta))$.

Definition 43. Let L be a geodesic lamination on a surface S.

(i) A *complementary region* of L is a path connected component of $S \backslash L$.

(ii) L is *minimal* if each leaf ℓ is dense in L, that is, L is the closure of ℓ in S.

(iii) L is *full* if each complementary region is isometric to either

  (a) the interior of an ideal hyperbolic n-gon, where $n \geq 3$, or

  (b) the interior of a punctured ideal hyperbolic n-gon, where $n \geq 1$.

Theorem 10. Let S be an orientable hyperbolic surface of genus $g \geq 0$ with n punctures, and let $\phi : S \to S$ be a homeomorphism which is not isotopic to a reducible or periodic homeomorphism. Then there exist $\lambda \in \mathbb{R}_{>1}$ and measured geodesic laminations (Λ^+, μ_+) and (Λ^-, μ_-) such that:

$$\phi_*(\Lambda^+, \mu_+) = (\Lambda^+, \lambda\mu_+) \quad \text{and} \quad \phi_*(\Lambda^-, \mu_-) = (\Lambda^-, \lambda^{-1}\mu_-).$$

Moreover:

(i) The measured geodesics laminations are unique in $\mathcal{PML}(S)$, i.e. if $\lambda' \in \mathbb{R}_{>0}$ and (Λ, μ) is a measured geodesic lamination such that $\phi(\Lambda, \mu) = (\Lambda, \lambda'\mu)$ then one of the two cases occurs:

  - $\lambda' \geq 1$. Then $\lambda' = \lambda$ and $(\Lambda, \mu) = (\Lambda^+, c\mu_+)$ for some $c \in \mathbb{R}_{>0}$.
  - $\lambda' < 1$. Then $\lambda' = \frac{1}{\lambda}$ and $(\Lambda, \mu) = (\Lambda^-, c\mu_-)$ for some $c \in \mathbb{R}_{>0}$.

(ii) We call (Λ^+, μ_+) and (Λ^-, μ_-) the *stable* and *unstable* measured laminations, respectively, which are well-defined up to rescaling the measures. If S is a closed surface then Λ^+ and Λ^- are respectively the stable and unstable laminations of ϕ as defined in Theorem 9.

(iii) Each of the laminations $\Lambda^\pm$ is full and minimal.

For a proof in the case of closed surfaces see [11, Theorem 5.5], and [10, Theorem 1.47] for (iii). The general case follows from Theorem 7 and the following theorem.

Theorem 11. Let S be a hyperbolic surface. Then there is a bijection

$$\Phi : \mathcal{MF}(S) \to \mathcal{ML}(S),$$

such that:

If $\varphi : S \to S$ is a pseudo-Anosov homeomorphism with unstable and stable measured foliations $(\mathcal{F}^u, \mu^u)$ and $(\mathcal{F}^s, \mu^s)$ respectively, then

$$(\mathcal{L}^s, \lambda^s) = \Phi(\mathcal{F}^u, \mu^u) \quad \text{and} \quad (\mathcal{L}^u, \lambda^u) = \Phi(\mathcal{F}^s, \mu^s),$$

are the stable and unstable measured geodesic laminations of φ.

The bijection is given in [32, §11.8 and §11.9], [45, Construction 1.7.7, Extension 2.7.4 and Epilogue], [12, Lemma 6.2], and [10, Chapter 1].

Warning: Notice that the *unstable* measured foliation is sent to the *stable* lamination by the bijection. Intuitively, if we iterate a non-trivial simple closed curve on the surface by a pseudo-Anosov homeomorphism, then after many iterations, the simple closed curve roughly looks like the unstable measured foliation, and the stable lamination (at least if we straighten the curve to a hyperbolic geodesic representative.) Each leaf of the unstable foliation is stretched by a factor equal to the dilatation.

Very roughly, beginning with a foliation, the bijection in Theorem 11 is given by removing the leaves which have an endpoint at a singular point, straightening the remaining leaves of the foliation so that they are geodesics, then taking the closure to obtain a measured geodesic lamination. Vaguely, measured foliations and laminations "carry the same information."

Chapter 6

Triangulations and gluing equations

6.1 Triangulations

Definition 44. A *topological ideal tetrahedron* is a topological space homeomorphic to a 3-simplex with its vertices removed. The vertices of a topological ideal tetrahedron are called *ideal vertices*, although they are not strictly a part of the topological ideal tetrahedron.

Definition 45. Let T_1, T_2 be topological ideal tetrahedra. Let F_1, F_2 be distinct faces of T_1, T_2 respectively. Let $\{u_1, u_2, u_3\}$,$\{v_1, v_2, v_3\}$ be the ideal vertices of F_1 and F_2, respectively. A *face pairing* between F_1 and F_2 is a bijection between $\{u_1, u_2, u_3\}$ and $\{v_1, v_2, v_3\}$. If the bijection is given by

$$u_1 \leftrightarrow v_{\sigma(1)}, \quad u_2 \leftrightarrow v_{\sigma(2)}, \quad u_3 \leftrightarrow v_{\sigma(3)},$$

where $\sigma \in S_3$ is a permutation, then we write $(u_1, u_2, u_3) \leftrightarrow (v_{\sigma(1)}, v_{\sigma(2)}, v_{\sigma(3)})$.

Note that we allow the possibility that $T_1 = T_2$, but we require that the faces paired are distinct.

Definition 46. Let $\mathcal{T}$ be a finite collection of topological ideal tetrahedra. A (combinatorial) *ideal triangulation* is a pair $(\mathcal{T}, \mathcal{P})$ where $\mathcal{P}$ is a collection of face pairings between faces of tetrahedra in $\mathcal{T}$ such that:

- If $T \in \mathcal{T}$ and F is a face of T then there is exactly one face pairing in $\mathcal{P}$ which pairs F.

Definition 47. Let $(\mathcal{T}, \mathcal{P})$ be a combinatorial ideal triangulation, where $\mathcal{T} = \{T_1, \ldots, T_n\}$. We identify each T_i with an affine 3-simplex in $\mathbb{R}^3$, for $i = 1, \ldots, n$. The *topological realisation* of $\mathcal{P}$ is the topological space

$$M = \left(\coprod_{i=1}^{n} T_i \right) / \sim,$$

where, if two faces are combinatorially paired by $(u_1, u_2, u_3) \leftrightarrow (v_1, v_2, v_3)$ then the faces are glued via affine maps, i.e.

$$ru_1 + su_2 + tu_3 \quad \sim \quad rv_1 + sv_2 + tv_3, \qquad \text{for } r, s, t \in [0, 1) \text{ with } r + s + t = 1.$$

We also say that $(\mathcal{T}, \mathcal{P})$, or sometimes just $\mathcal{T}$ (with $\mathcal{P}$ being implicit), is a (topological) *ideal triangulation* of M.

If e is an edge of a tetrahedron in $\mathcal{T}$, then we denote by $[e]$ the *edge cycle* determined by e, which is the set of edges of tetrahedra in $\mathcal{T}$ which get identified in M.

6.1.1 Veering triangulations

The definitions in this subsection are based on those found in Section 1 of [27], however we require our veering triangulations to be taut as in [2, §4].

Definition 48. A *taut tetrahedron* is an ideal tetrahedron such that:

(i) A pair of opposite edges is assigned an angle of π, and all other edges are assigned an angle of 0.

(ii) Each face is assigned a *coorientation* which is an orientation such that the coorientations of adjacent faces agree if their common edge is assigned an angle of π, and disagree otherwise.

The coorientations can also be thought of as normal vectors to each face, where two normal vectors point into the tetrahedron and two point out of the tetrahedron.

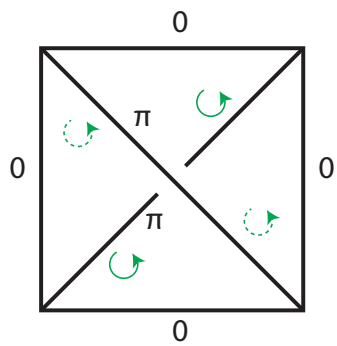

Figure 6.1: A taut tetrahedron. The coorientation normal vectors face out of the page.

Definition 49. A *taut ideal triangulation* is an ideal triangulation such that:

(i) Each tetrahedron is taut.

(ii) The face pairings respect the coorientations of the faces paired.

(iii) The sum of the angles assigned to the edges of an edge cycle is 2π.

Definition 50. A *veering tetrahedron* is an oriented taut tetrahedron such that the 0-angle edges are coloured either red or blue as in Figure 6.2. Note that the π-angle edges are neither required to be coloured nor to have a specific colour. We refer to the blue edges as *left veering* and the red edges as *right veering*.

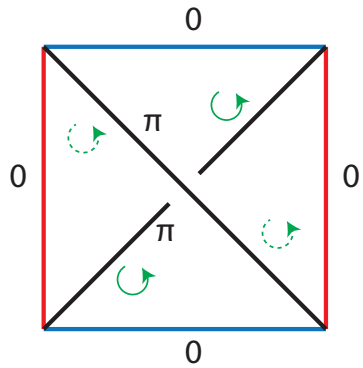

Figure 6.2: Canonical veering tetrahedron. All veering tetrahedra are combinatorially isomorphic to the one shown.

Definition 51. A *veering triangulation* is a taut triangulation such that each tetrahedron is veering, and all edges belonging to the same edge cycle are assigned the same colour.

Example 3. The triangulation shown in Figure 1.12 of Chapter 1 is a veering triangulation, with the colouring of edges shown.

6.1.2 Ideal tetrahedra

Definition 52. An *ideal hyperbolic tetrahedron*, or *ideal tetrahedron*, with *vertices* $V = \{v_1, v_2, v_3, v_4\} \subseteq \partial\overline{\mathbb{H}^3}$ is the set $T \subseteq \mathbb{H}^3$ which is the hyperbolic convex hull of the 6 geodesics joining pairs of vertices in V, that is, T is determined by the two conditions:

1. If g is a geodesic joining a pair of vertices in V then $g \subseteq T$.
2. If g is a geodesic segment joining two points in T then $g \subseteq T$.

Note that the vertices at infinity are "ideal points" and not points of an ideal tetrahedron. Unless stated otherwise we assume that an ideal hyperbolic tetrahedron is not flat or degenerate, that is, its vertices at infinity do not all lie on a circle or line.

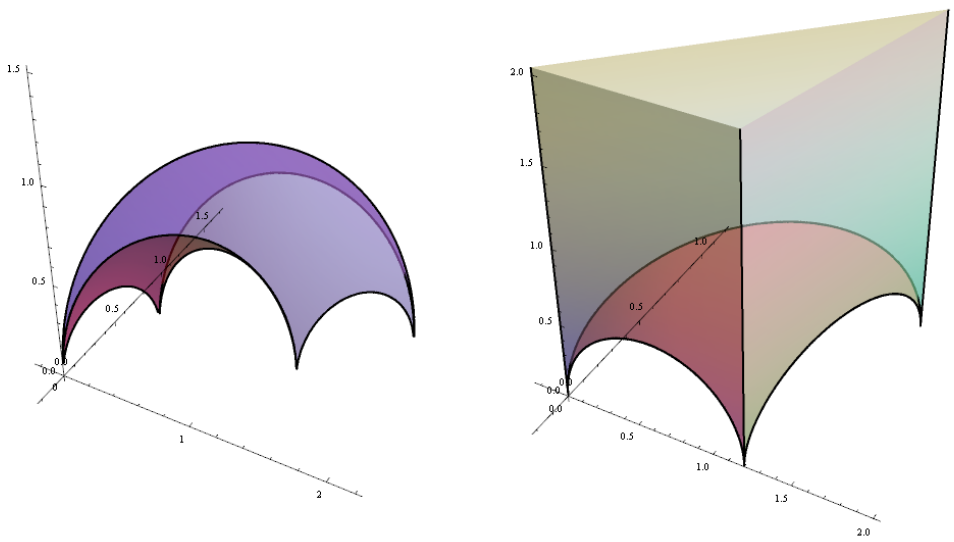

Figure 6.3: Ideal hyperbolic tetrahedra in the upper half space model of $\mathbb{H}^3$. The tetrahedron on the right has a vertex at ∞.

Definition 53. An *orientation* on an ideal tetrahedron with vertices $\{v_1, v_2, v_3, v_4\}$ is a choice of ordering of the vertices, written as $[v_{i_1}, v_{i_2}, v_{i_3}, v_{i_4}]$, where two orientations are considered equivalent if they differ by an even permutation, that is, if $\sigma \in S_4$ is an even permutation then $[v_{i_1}, v_{i_2}, v_{i_3}, v_{i_4}]$ and $[v_{\sigma(i_1)}, v_{\sigma(i_2)}, v_{\sigma(i_3)}, v_{\sigma(i_4)}]$ are equivalent orientations.

Notation 3. We write $[v_1, v_2, v_3, v_4]$ for the oriented ideal tetrahedron with vertices $\{v_1, v_2, v_3, v_4\}$ and orientation $[v_1, v_2, v_3, v_4]$.

Definition 54. Let $z_1, z_2, z_3 \in \widehat{\mathbb{C}}^4$ be distinct points, where $\widehat{\mathbb{C}} = \mathbb{R}^2 \cup \{\infty\}$. The cross ratio defines a Möbius transformation

$$\begin{aligned} \mathrm{CR}[z_1, z_2, z_3, \cdot] : \widehat{\mathbb{C}} &\to \widehat{\mathbb{C}} = \mathbb{R}^2 \cup \{\infty\} \\ z &\mapsto \mathrm{CR}[z_1, z_2, z_3, z] = \frac{(z - z_1)(z_3 - z_2)}{(z - z_2)(z_3 - z_1)}. \end{aligned}$$

This Möbius transformation can also be thought of as the orientation preserving isometry of $\mathbb{H}^3$ which sends z_1, z_2, z_3 to $0, \infty, 1$ respectively.

We would like to say that an oriented tetrahedron $T = [v_1, v_2, v_3, v_4]$ is *positively* oriented if there is an orientation-preserving isometry of $\mathbb{H}^3$ which sends T to an ideal tetrahedron $[0, \infty, 1, z]$ where $\mathrm{Im}(z) > 0$. More precisely, let $\phi = \mathrm{CR}[v_1, v_2, v_3, z] \in \mathrm{Isom}^+(\mathbb{H}^3)$. Then $\phi(T) = [\phi(v_1), \phi(v_2), \phi(v_3), \phi(v_4)] = [0, \infty, 1, \phi(v_4)]$ which is positively oriented exactly when

$$\phi(v_4) = \mathrm{CR}[v_1, v_2, v_3, v_4]$$

has positive imaginary part.

Definition 55. Let $T = [v_1, v_2, v_3, v_4]$ and let $z = \mathrm{CR}[v_1, v_2, v_3, v_4] \in \mathbb{C}$. Then T is said to be:

(i) *positively oriented* if $\mathrm{Im}(z) > 0$,

(ii) *negatively oriented* if $\mathrm{Im}(z) < 0$,

(iii) *flat* if $z \in \mathbb{R} \backslash \{0, 1\}$, and

(iv) *degenerate* if $z \in \{0, 1, \infty\}$.

Definition 56. Let T be a positively oriented ideal tetrahedron, and let e be an edge of T joining vertices u and v. The *edge parameter* of e is the complex number $z(e) = \mathrm{CR}[u, v, x, y]$, where $[u, v, x, y]$ is a positive orientation for T.

Proposition 4. Let $T = [v_1, v_2, v_3, v_4]$ be an ideal hyperbolic tetrahedron and let $\phi \in \mathrm{Isom}^+(\mathbb{H}^3)$. Then,

$$\mathrm{CR}[v_1, v_2, v_3, v_4] = \mathrm{CR}[\phi(v_1), \phi(v_2), \phi(v_3), \phi(v_4)],$$

that is, the cross ratio is invariant under orientation preserving isometry.

The proof is left as a straightforward calculation.

The above proposition implies that *edge parameter* is invariant under orientation preserving isometry. Hence, given a tetrahedron T and an edge e, we can use an isometry to put it in standard form $[0, \infty, 1, z]$, where the edge e is sent to the edge 0∞. Then

$$z(e) = \mathrm{CR}[0, \infty, 1, z] = \frac{(z - 0)(1 - \infty)}{(z - \infty)(1 - 0)} = z.$$

We can compute the edge invariants associated with the other edges of the tetrahedron in terms of z, these are shown in Figure 6.4. For example, to compute the edge invariant of the edge e' joining 0 and z, notice that $[0, \infty, 1, z]$ is the same orientation as $[z, 0, 1, \infty]$. Hence,

$$z(e') = \mathrm{CR}[z, 0, 1, \infty] = \frac{(\infty - z)(1 - 0)}{(\infty - 0)(1 - z)} = \frac{1}{1 - z}.$$

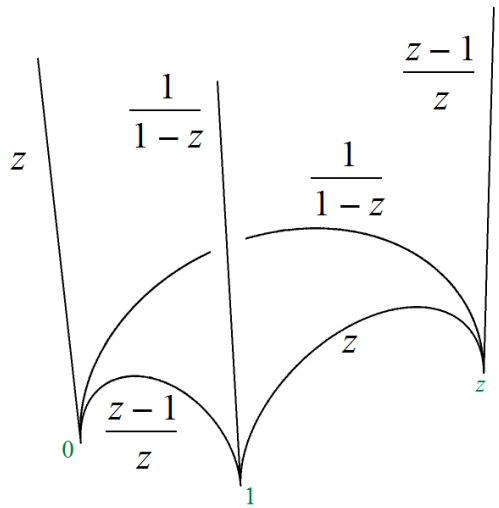

Figure 6.4: Edge invariants of an ideal hyperbolic tetrahedron are related as shown.

6.2 Gluing equations

References for this section include Chapter 4 of [51] and Chapter 10 of [46].

Let $n \in \mathbb{Z}_{>0}$ and let $\mathcal{T} = \{T_1, T_2, \ldots, T_n\}$ be a collection of distinct, disjoint ideal hyperbolic tetrahedra such that no two tetrahedra have a common ideal vertex. Let $\mathcal{P}$ be a combinatorial triangulation of $\mathcal{T}$.

For each pair of faces which are paired by some $\Phi \in \mathcal{P}$, the face pairing Φ gives a bijection between their ideal vertices at infinity and hence determines a unique isometry $\varphi \in \mathrm{Isom}^+(\mathbb{H}^3)$ which agrees with Φ on the ideal vertices. Define the topological space

$$M = \left(\coprod_{i=1}^{n} T_i \right) / \sim,$$

where, if two faces F_i and F_j are combinatorially paired and $\varphi \in \mathrm{Isom}^+(\mathbb{H}^3)$ realises the pairing of ideal vertices then

$$x \sim \varphi(x), \qquad \text{for } x \in F_i.$$

Warning: M is not necessarily homeomorphic to the topological realisation of $\mathcal{P}$. Depending on the face pairing isometries, distinct points on an edge of a tetrahedron of $\mathcal{T}$ may be identified in the quotient M, whereas this does not happen in the topological realisation of $\mathcal{P}$. In fact, it is exactly this behaviour which we shall want to rule out below.

A hyperbolic atlas for M.

We would like to use the ideal hyperbolic tetrahedra to find a hyperbolic atlas on M. In order to do so, we will need to impose conditions on the edge parameters known as the gluing equations. We will then say that M is the hyperbolic manifold obtained by gluing the hyperbolic ideal tetrahedra. For a more careful and detailed treatment, see Section 10.1 of [46].

We construct a chart around each point of M. Let $[\,\cdot\,] : \cup_i T_i \to M$ be the quotient map and let $[x] \in M$, where x is a point of a tetrahedron T in $\mathcal{T}$. There are 3 cases to consider:

(i) **The point x is in the interior of the tetrahedron T.** Then there exists $r > 0$ and a hyperbolic open ball $B_r(x)$ completely contained in T. A chart around $[x] \in M$ is given by the identity map $\psi : [B_r(x)] \to \mathbb{H}^3$ where $\psi([z]) = z$.

(ii) **The point x is in the interior of a face F.** Then the face F is paired with a face F' of a tetrahedron T' by an isometry $f \in \mathrm{Isom}^+(\mathbb{H}^3)$. Let $x' = f(x)$. Then there is a radius $r > 0$ such that the union of two half open balls $f(B_r(x) \cap T)$ and $B_r(x') \cap T'$ form the open ball $B_r(x')$.

A chart around x is given by

$$\psi : [B_r(x) \cap T] \cup [B_r(x') \cap T'] \to \mathbb{H}^3,$$

where

- $\psi([z]) = z$ for $z \in B_r(x') \cap T'$, and
- $\psi([z]) = f(z)$ for $z \in B_r(x) \cap T$.

(iii) **The point x is on an edge e_1 of T_1.** Let F_1 and F_1' be the faces of T_1 adjacent to $x_1 := x$. Then F_1' is paired to some face F_2 of a tetrahedron T_2, by an isometry ϕ_1 such that $\phi_1(F_1') = F_2$. Let $x_2 = \phi_1(x_1)$. The point x_2 is common to two faces F_2 and F_2' of T_2.

We can continue developing tetrahedra around the edge e_1 in this manner, to get tetrahedron T_3 with faces F_3 and F_3', an isometry ϕ_2 taking F_2' to F_3, and a point $x_3 = \phi_2(x_2)$, and so on.

Then F_k' is paired with F_1 for some minimal $k \in \mathbb{Z}_{>0}$. Let $e_1, e_2, \ldots, e_k$ be the edges of $T_1, T_2, \ldots, T_k$ which get identified with e_1 in M. Let $r > 0$ be a sufficiently small radius, and for $i = 1, 2, \ldots, k$, let $B_i = B_r(x_i) \cap T_i$ be slices of an open ball of radius r. We require that these slices glue together consistently via the face pairing isometries to form a hyperbolic ball of radius r. A necessary condition is the following:

Angle condition: The sum of the dihedral angles at the edges $e_1, e_2, \ldots, e_k$ add up to 2π, that is,

$$\mathrm{Arg}\ z(e_1) + \mathrm{Arg}\ z(e_2) + \cdots + \mathrm{Arg}\ z(e_k) = 2\pi,$$

where $0 < \mathrm{Arg}(z_i) < \pi$, and $z(e_i)$ is the edge parameter of e_i in T_i, for $i = 1, 2, \ldots, k$.

Assume the angle condition holds. When we develop tetrahedra around the edge e_1, slices of open balls will fit together forming a partial hyperbolic open ball as shown in Figure 6.5, until finally all that is left is to glue F_k' to F_1, in which case one of two scenarios occurs.

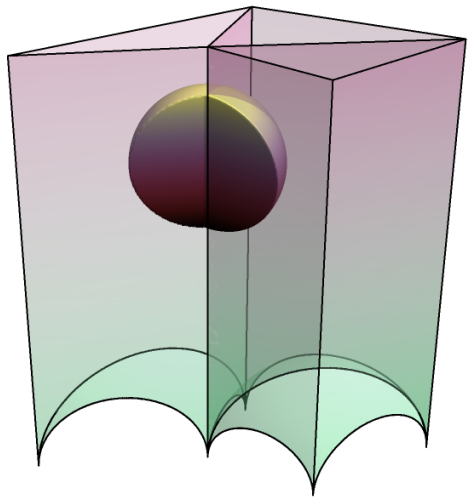

Figure 6.5: Partial developing of tetrahedra around an edge.

Firstly, if F'_k coincides exactly with F_1 then the slices of open balls piece together consistently to form an open ball $B_r(x)$ and we obtain a chart around $[x]$ in a similar manner as in case (ii). The condition for this to occur is given by:

Gluing condition:

$$z(e_1) \cdot z(e_2) \cdots z(e_k) = 1.$$

On the other hand, if F'_k does not coincide with F_1 then the isometry sending F'_k to F_1 results in a shearing, or hyperbolic translation along the edge e_1. In particular, x_k is not sent to x_1 and the equivalence class $[x]$ contains infinitely many points. The slices do not glue together to form an open ball.

Proposition 5 (Theorem 10.5.3 of [46])**.** Let $n \in \mathbb{Z}_{>0}$ and let $\mathcal{T}$ be a collection of distinct, disjoint ideal hyperbolic tetrahedra such that no two tetrahedra have a common ideal vertex and let $\mathcal{P}$ consist of face pairings of $\mathcal{T}$. Assume that the following condition is satisfied. If edges $e_1, e_2, \ldots, e_k$ form an edge cycle then the *gluing equation* is satisfied at this edge cycle, that is,

$$z(e_1)z(e_2) \cdots z(e_k) = 1,$$

where

$$\text{Arg } z(e_1) + \text{Arg } z(e_2) + \cdots + \text{Arg } z(e_k) = 2\pi,$$

and $0 < \text{Arg}(z_i) < \pi$, for $i = 1, 2, \ldots, k$. Then the charts constructed above define a (possibly incomplete) hyperbolic 3-manifold M. We call M the hyperbolic 3-manifold obtained by gluing the ideal tetrahedra $\mathcal{T}$.

Example 4. We calculate the gluing equations for the triangulation in Figure 6.6. Note that this is also the triangulation from Chapter 1, Figure 1.12.

The gluing of the two tetrahedra are shown below, where the face pairings are uniquely determined by the edge identification shown.

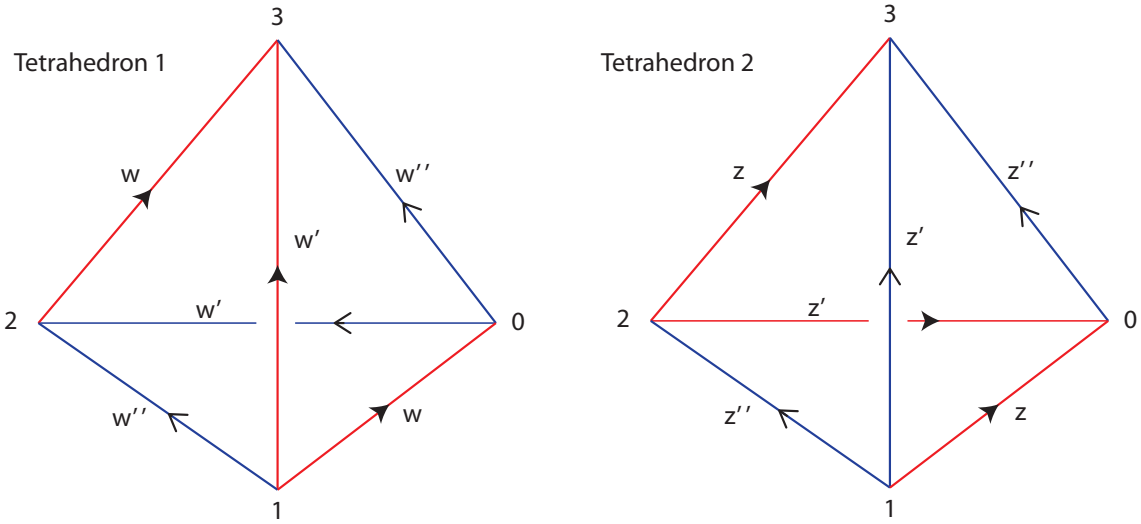

Figure 6.6: The edges of the tetrahedra are labelled with edge parameters where $z' = 1/(1-z)$ and $z'' = (z-1)/z$, and similarly for w' and w''.

We see that there are two distinct edge cycles, coloured in red and blue respectively. The gluing equation at the red edges is:

$$w(w')w \cdot zz'z = 1, \quad 2\mathrm{Arg}(w) + \mathrm{Arg}(w') + 2\mathrm{Arg}(z) + \mathrm{Arg}(z') = 2\pi,$$

and at the blue edges:

$$w''w'w'' \cdot z''z'z'' = 1, \quad 2\mathrm{Arg}(w') + \mathrm{Arg}(w'') + 2\mathrm{Arg}(z'') + \mathrm{Arg}(z') = 2\pi.$$

6.3 Completeness and Dehn filling equations

This section is based on Section 2 of [42]. Other references include Chapter 4 of [51] and Chapter 10 of [46]. The running example in this section is a continuation of Example 4.

Let $\mathcal{T}$ be an ideal triangulation of a one-cusped hyperbolic 3-manifold M which is the interior of a compact manifold with torus boundary.

In each ideal tetrahedron in $\mathcal{T}$ we may consider small triangles which cut off a small tetrahedron neighbourhood of each ideal vertex. These triangles glue together via the face pairings of $\mathcal{T}$ to form a torus T in M called the *link* of the cusp of M, see Figure 6.7.

More precisely, recall that each ideal tetrahedron is a 3-simplex with its vertices removed, so we may choose the vertices of each triangle in the link to be at a (Euclidean) distance from the tetrahedron vertex which is a third of the Euclidean length of the tetrahedron edge it lies on, see Figure 6.7. The triangle is then the convex hull of the vertices. In the topological realisation of $\mathcal{T}$, the faces are glued via affine maps, which induces identifications of the edges of triangles in the link.

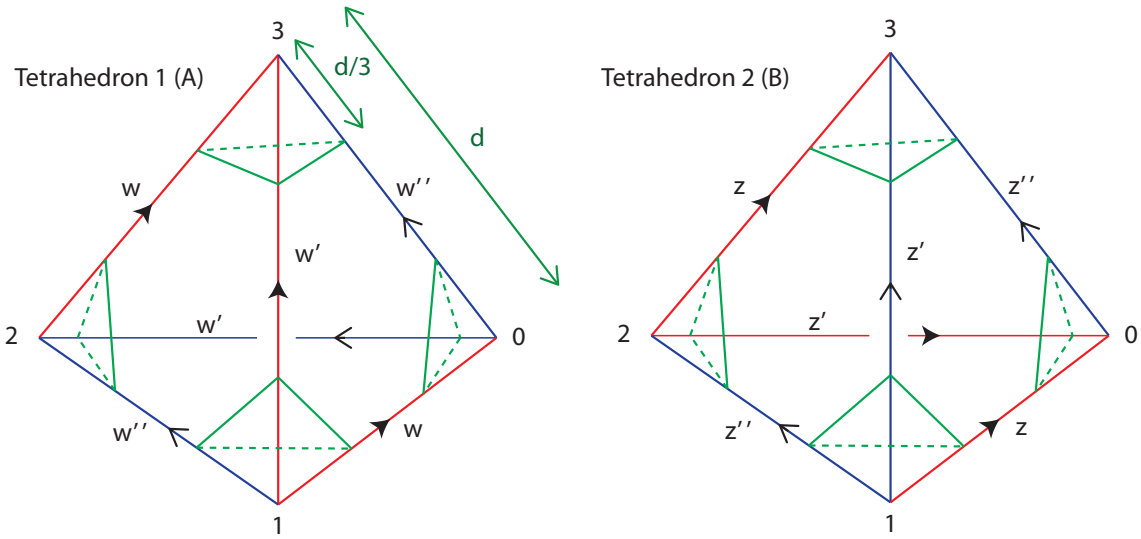

Figure 6.7: The edges of the triangles which glue to form the link are shown in green. The triangles are shown as viewed from the ideal vertices and are oriented by a normal vector facing out of the page towards the reader. The edges of the tetrahedra are labelled with edge parameters where $z' = 1/(1-z)$ and $z'' = (z-1)/z$, and similarly for w' and w''. d is the Euclidean length of the edge indicated.

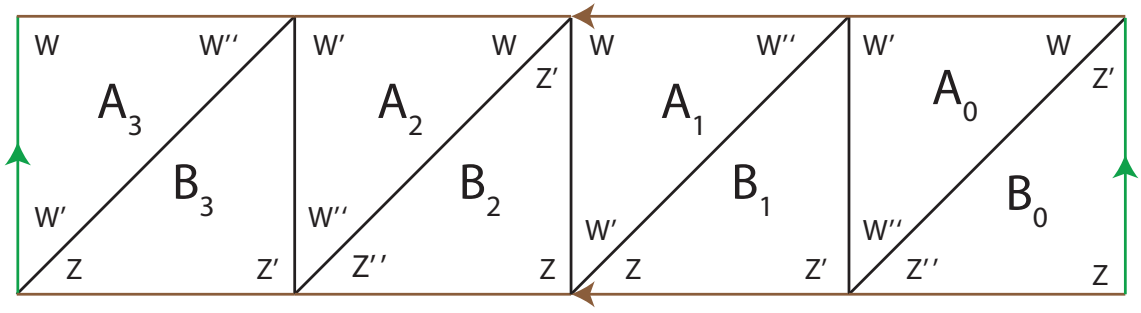

Figure 6.8: Obtained by gluing the triangles which form the torus link. Opposite sides of the rectangle are identified. The diagram is as viewed from the ideal vertices.

The ideal triangulation induces a triangulation of the link T, e.g. see Figure 6.8. To each vertex of each triangle we associate an edge parameter as in Figure 6.8. Let $p \in T$ be a point at a vertex of a triangle in the induced triangulation, which we consider to be a base point.

Definition 57. Let $n \in \mathbb{Z}_{>0}$ and $e_1, e_2, \ldots, e_n$ be a sequence of (not necessarily distinct) oriented edges of triangles in T which concatenate to form a closed path γ based at p, that is,

(i) p is the initial vertex of e_1 and the terminal vertex of e_n, and

(ii) the terminal vertex of e_i equals the initial vertex of e_{i+1} for $1 \leq i < n$.

Then we call γ a (closed) *simplicial path* in T, based at p. We denote the length of the simplicial path by $|\gamma| = n$.

Definition 58. Let $\gamma \in \pi_1(T, p)$ be a simplicial path. Define $\mu(\gamma) \in \mathbb{C}$ to be $(-1)^{|\gamma|}$ times the product of the edge parameters for the triangle vertices touching γ on the right, see Figure 6.9.

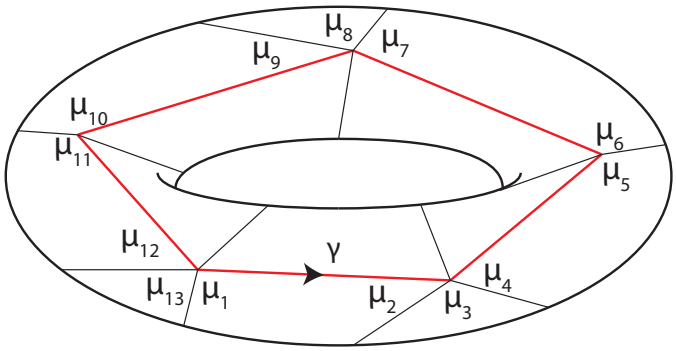

Figure 6.9: $\mu(\gamma) = (-1)^5 \cdot \mu_1\mu_2 \cdots \mu_{13}$

Definition 59. Let m and ℓ be simplicial paths which are generators for $\pi_1(T, p)$. The *completeness equations* with respect to m and ℓ are

$$\mu(m) = 1 \quad \text{and} \quad \mu(\ell) = 1.$$

Observe that these are polynomial equations in the edge parameters.

Theorem 12. Let N be the hyperbolic 3-manifold given by gluing positively-oriented hyperbolic ideal tetrahedra of the triangulation $\mathcal{T}$, with edge parameters satisfying the gluing equations. Let m and ℓ be simplicial paths which are generators for $\pi_1(T, p)$.

Then N is complete if and only if the completeness equations with respect to m and ℓ are satisfied.

See Section 2 of [42], or [46, §10.5].

Remark 7. For simplicity we have chosen to state Theorem 12 for one-cusped hyperbolic manifolds. However, this generalises to the case where M has multiple cusps, by requiring that the torus link at each cusp satisfies the completeness equations.

Definition 60. An ideal triangulation is *geometric* if there exists a solution to the gluing and completeness equations such that each edge parameter has positive imaginary part. Otherwise, we say that the ideal triangulation is *non-geometric*.

Example 5. We calculate the completeness equations, continuing Example 4. The link T is triangulated as shown below, with simplicial paths m and ℓ as indicated.

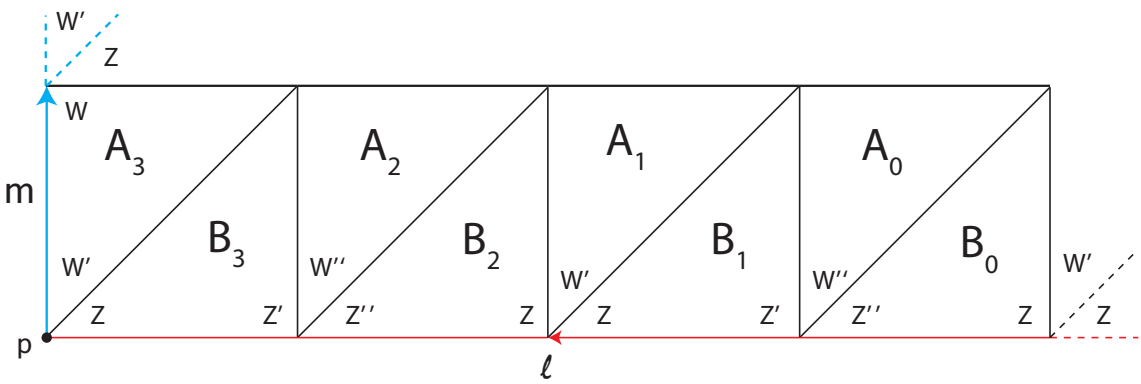

Figure 6.10: Torus link with a longitude ℓ shown in red.

The equation $\mu(\ell) = 1$ becomes

$$(z'w''z'')(zw'z)(z'w''z'')(zw'z) \quad = \quad 1,$$

which simplifies to $z^2 = w^2$. Since we are looking for solutions with $\mathrm{Im}(z), \mathrm{Im}(w) > 0$, we must have $z = w$.

Similarly, the equation $\mu(m) = 1$ becomes $-ww'z = 1$ or $-w \cdot \frac{1}{1-w} \cdot z = 1$. Since $z = w$, we obtain $w^2 - w + 1 = 0$. Hence the only positively-oriented solution is

$$z = w = \frac{1}{2}(1 + i\sqrt{3}).$$

We check that this solution satisfies the gluing equations given in Example 4, and thus the hyperbolic tetrahedra with these edge parameters glue to give a complete hyperbolic 3-manifold.

Hyperbolic Dehn surgery equations

We fix a branch of the logarithm as follows:

$$\begin{aligned} \log : \mathbb{C}\backslash\{0\} &\to \mathbb{C} \\ z &\mapsto \log(z) = \log|z| + i\,\mathrm{Arg}(z), \end{aligned}$$

where $-\pi < \mathrm{Arg}(z) \leq \pi$.

Definition 61. Let $\gamma \in \pi_1(T, p)$ be a simplicial path. Let $\mu_1, \mu_2, \ldots, \mu_k$, where $k \in \mathbb{Z}_{>0}$, be the edge parameters for the triangle vertices touching γ on the right, as in Figure 6.9. Define

$$\widetilde{H}(\gamma) = -i\pi|\gamma| + \sum_{i=1}^{k} \log(\mu_i).$$

Definition 62. A *meridian* and *longitude* pair for T is a choice of $m, \ell \in \pi_1(T, p)$, where m is called the meridian and ℓ is called the longitude, such that m, ℓ generate $\pi_1(T, p) \cong \mathbb{Z}^2$.

Note that for a complete solution, $\widetilde{H}(m) = \widetilde{H}(\ell) = 0$.

Definition 63 (§10.5 of [46])**.** Fix a meridian m and longitude ℓ for the link T, each of which is a simplicial path which does not have any "local loops," that is, its lift to the universal cover of T is a simple curve. Let $\vec{z}$ be a solution to the gluing equations with every tetrahedron positively-oriented.

- The *Dehn surgery invariant* with respect to (m, ℓ) is the pair $(a, b) \in \mathbb{R}^2 \cup \{\infty\}$ such that

$$a\widetilde{H}(\mu) + b\widetilde{H}(\ell) = 2\pi i, \tag{6.1}$$

  or, if the edge parameters satisfy the completeness equations then the Dehn surgery invariant is ∞.

- If $(a, b) \in \mathbb{R}^2$ is specified then (6.1) defines an equation in the edge parameters called the (a, b)-*Dehn surgery equation* of T.

Definition 64 (Chapter 4, [15])**.**

- Let M be a hyperbolic 3-manifold which is the interior of a compact manifold $\overline{M}$ with torus boundary T.
- Let $p \in T$ be a base point and let m and ℓ be generators for $\pi_1(T, p)$.
- Let T' be the standard solid torus with meridian m' and longitude ℓ' based at $p' \in T'$.
- Let $(a, b) \in \mathbb{Z}^2$ such that $\gcd(a, b) = 1$.

- Let $\varphi : \partial T' \to T$ be a homeomorphism such that

$$\begin{array}{rcl} \varphi_* : \pi_1(\partial T', p') & \to & \pi_1(T, p) \\ m' & \mapsto & m^a \ell^b. \end{array}$$

The topological manifold obtained by (a, b)-*Dehn filling* on M is

$$M_{(a,b)} = \left(\overline{M} \sqcup T'\right) / \sim,$$

where the equivalence relation is generated by

$$x' \sim \varphi(x') \qquad \text{for } x' \in \partial T'.$$

We also say that $M_{(a,b)}$ is obtained by Dehn filling *along the curve* $m^a \ell^b$ of M.

Remark: The resulting Dehn filled manifold depends only on the Dehn filling coefficients (a, b) and choice of meridian m and longitude ℓ, and not on the choice of homeomorphism φ.

Theorem 13 (Theorem 10.5.9 of [46])**.** Let M be an incomplete one-cusped hyperbolic 3-manifold obtained by gluing positively oriented ideal hyperbolic tetrahedra, such that M is the interior of a compact manifold $\overline{M}$ with torus boundary T. We identify T with the link of the cusp of M. Let m and ℓ be a meridian and longitude for T. Let (a, b) be the Dehn surgery invariant of M with respect to m and ℓ, and assume that a and b are relatively prime integers.

Then the metric completion of M is homeomorphic to the topological manifold $M_{(a,b)}$ obtained by (a, b)-Dehn filling of M with respect to m and ℓ.

Chapter 7

Agol's construction

In this chapter we give an exposition of the veering triangulations introduced by Agol in [2].

7.1 Periodic splitting sequences of train tracks

In this section we will be particularly interested in *trivalent* train tracks, that is, train tracks for which every switch has degree 3. If τ is a trivalent train track and e is an edge of τ then it has two ends. An end of e is *large* if it comes into a switch s on the side of the tangent space at s opposite the side with two incident branches. The branch e is *large* if both of its ends are large.

Definition 65. Let (τ, μ) be a measured train track on a surface S, and let e be a large branch with neighbouring edges labelled as in the left of Figure 7.1.

A *split* at e is a move producing the train track (τ', μ') which is obtained from (τ, μ) by splitting e and inserting a new edge e' in one of two possible ways depending on the weights of the neighbouring edges, see Figure 7.1.

We use the notation $(\tau, \mu) \rightharpoonup_e (\tau', \mu')$ to denote that (τ', μ') is obtained from (τ, μ) by splitting e.

Note:

1. The weights of all other edges are kept the same.
2. The train track (τ', μ') is only well-defined up to isotopy.
3. We only define a split for $\max(a, d) \neq \max(b, c)$.

Definition 66. Let (τ, μ) be a measured train track on a surface S. A *maximal split* of (τ, μ) is a move which produces the train track (τ', μ') obtained by splitting the edges of τ that have the highest weight. This is denoted by $(\tau, \mu) \rightharpoonup (\tau', \mu')$.

If

$$(\tau_0, \mu_0) \rightharpoonup (\tau_1, \mu_1) \rightharpoonup \cdots \rightharpoonup (\tau_n, \mu_n)$$

is a sequence of $n \in \mathbb{Z}_{>0}$ maximal splits then we write $(\tau_0, \mu_0) \rightharpoonup^n (\tau_n, \mu_n)$.

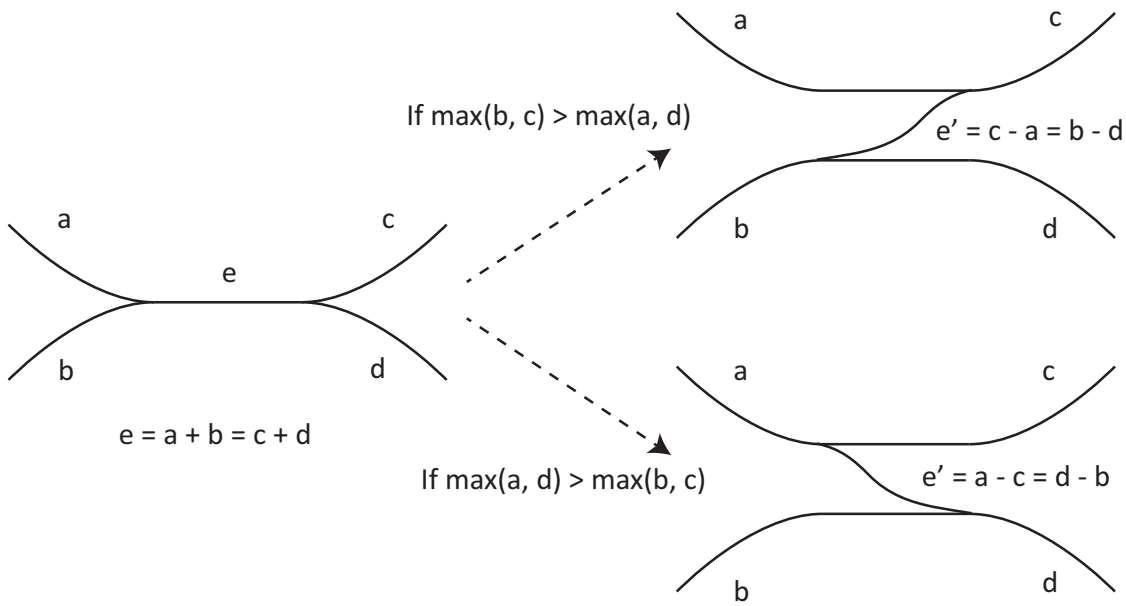

Figure 7.1: The two possibilities for a split of the large branch e. We use the label of an edge to represent its weight.

Definition 67. Let $(\tau, \mu), (\tau', \mu')$ be measured train tracks on a (possibly punctured) surface S. The two train tracks are *equal*, written

$$(\tau, \mu) = (\tau', \mu'),$$

if there is a diffeomorphism of S isotopic to the identity $\phi : S \to S$, such that $\phi(\tau) = \tau'$ and $\phi(\mu) = \mu'$, where if e is an edge of τ' then $\phi(\mu)(e) := \mu(\phi^{-1}(e))$.

Definition 68. Let S be a punctured surface with its punctures removed. Let $(\mathcal{L}, \lambda)$ be a measured geodesic lamination on S, and let (τ, μ) be a measured train track on S. The measured lamination $\mathcal{L}$ is *suited to* τ if the following conditions are satisfied:

(i) There exists a differentiable map $f : S \to S$ homotopic to the identity such that $f(\mathcal{L}) = \tau$.

(ii) f is non-singular on the tangent space to leaves of $\mathcal{L}$, that is, if $v \neq 0$ is a vector tangent to a leaf of $\mathcal{L}$ then $df(v)$ is a non-zero tangent vector to τ.

(iii) The map f respects the transverse measures, that is, if p is a point in the interior of an edge e of τ then $\lambda(f^{-1}(p)) = \mu(e)$.

Theorem 14 (Theorem 3.5 of [2])**.** Let $\varphi : S \to S$ be a pseudo-Anosov homeomorphism with dilatation λ and stable measured geodesic lamination $(\mathcal{L}^s, \delta)$. If $(\mathcal{L}^s, \delta)$ is suited to the measured train track (τ, μ) then there exist $n, m \in \mathbb{Z}_{>0}$ such that

$$(\tau, \mu) \rightharpoonup^n (\tau_n, \mu_n) \rightharpoonup^m (\tau_{n+m}, \mu_{n+m}),$$

and $\tau_{n+m} = \varphi(\tau_n)$ and $\mu_{n+m} = \lambda^{-1}\varphi(\mu_n)$, where if e is an edge of τ_{n+m} then $\varphi(\mu_n)(e) := \mu_n(\varphi^{-1}(e))$.

We call the sequence

$$(\tau_n, \mu_n) \rightharpoonup \cdots \rightharpoonup (\tau_{n+m}, \mu_{n+m}) \rightharpoonup \cdots,$$

of train tracks in Theorem 14 a *periodic splitting sequence*, with respect to φ, as it is periodic modulo the action of the monodromy and scaling.

Proposition 6. Let $\varphi : S \to S$ be a pseudo-Anosov homeomorphism with stable measured geodesic lamination $(\mathcal{L}^s, \lambda)$. Let (τ, μ) be the invariant train track with respect to φ, which is given by the Bestvina-Handel algorithm. Then $(\mathcal{L}^s, \lambda)$ is suited to (τ, μ).

Proof. In the proof of [45, Construction 1.7.7], it is shown that from the region $\mathcal{R}$ constructed from τ in Section 3.3.8, one can obtain the stable geodesic lamination which is suited to τ, proving Proposition 6. □

Although train tracks given by the Bestvina-Handel algorithm are not always trivalent, one can produce a trivalent train track from a non-trivalent train track as discussed in Step 4c of Chapter 8. Hence, we see that the Bestvina-Handel invariant train track can be used as a starting point for Theorem 14.

7.2 Agol's triangulations

We outline how the periodic splitting sequence of train tracks from Theorem 14 can be used to construct a veering, layered ideal triangulation, following Section 4 of [2].

Let $\varphi : S \to S$ be a pseudo-Anosov homeomorphism with dilatation $\lambda \in \mathbb{R}_{>1}$ and let

$$(\tau_0, \mu_0) \rightharpoonup (\tau_1, \mu_1) \rightharpoonup \cdots \rightharpoonup (\tau_m, \mu_m), \quad m \in \mathbb{Z}_{>0}$$

be a periodic splitting sequence of train tracks, i.e. such that $\tau_m = \varphi(\tau_0)$ and $\mu_m = \lambda^{-1}\varphi(\mu_0)$, as in Theorem 14. Let $S^\circ \subseteq S$ denote the surface obtained by removing the singular points of the stable measured foliation of φ and let $\varphi^\circ : S^\circ \to S^\circ$ denote the restriction.

Let $i \in \{0, 1, 2, \ldots, m\}$. Then each connected component of $S^\circ \backslash \tau_i$ is homeomorphic to a punctured disk. There is an ideal triangulation T_i of S° which is dual to τ_i. For each edge of τ_i, we obtain an ideal arc connecting punctures of neighbouring regions. These ideal arcs decompose S° into ideal triangles of T_i. Each switch of τ_i is interior to a unique ideal triangle.

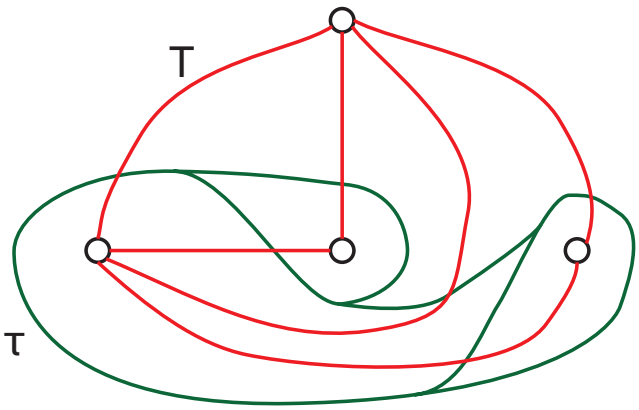

Figure 7.2: A train track on the surface $\mathbb{R}^2 \cup \{\infty\}$ with 4 punctures, and its dual ideal triangulation, shown in red.

When a large branch of τ_i splits, the effect on the dual ideal triangulation is that a diagonal exchange occurs, i.e. an ideal arc is removed and the 'other' diagonal ideal arc is inserted, see Figure 7.3.

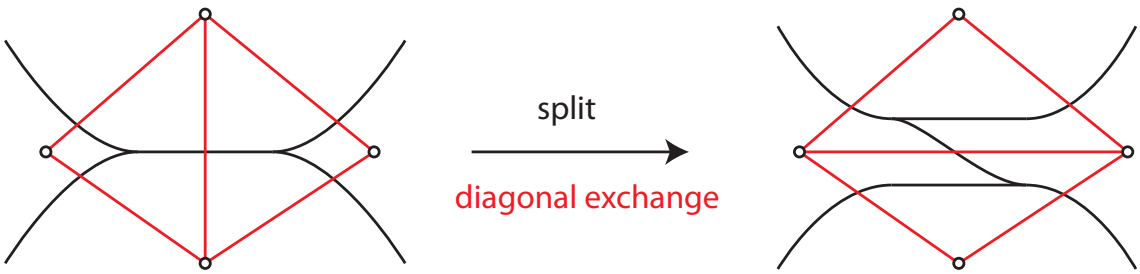

Figure 7.3

The back faces of a taut tetrahedron are attached to the two ideal triangles of T_i which are removed by the diagonal exchange, and the front faces are thought of as attached to the two ideal triangles of T_{i+1}.

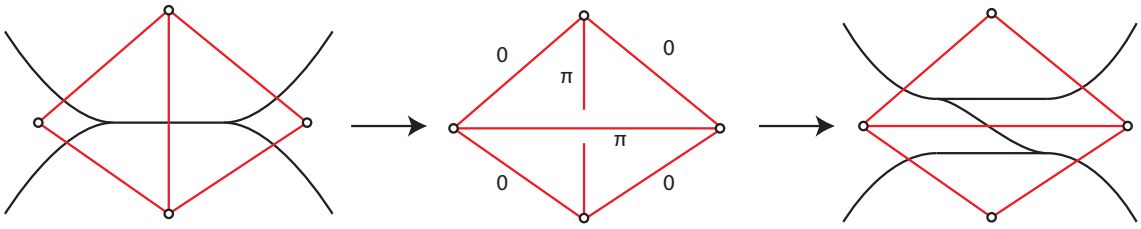

Figure 7.4: The faces of the taut tetrahedron attached are oriented by a normal facing out of the page, towards the reader. The taut tetrahedron interpolates between the triangulations of the surface.

The maximal split $\tau_i \rightharpoonup \tau_{i+1}$ is a split of possibly more than one large branch of τ_i. We attach a tetrahedron for each split, and the tetrahedra attached can be thought of as interpolating between the triangulations T_i and T_{i+1}. Combinatorially, attaching a tetrahedron Δ gives a face pairing between the back faces of Δ and the top of a taut tetrahedron below it (provided that there is one.) Finally, since $\varphi(T_0) = T_m$, the bottom faces of tetrahedra attached to triangles of T_0 are paired with the top faces of tetrahedra attached to T_m via the monodromy.

This procedure produces a taut triangulation $\mathcal{T}$ with topological realisation homeomorphic to the mapping torus M_{φ°, which we refer to it as *Agol's triangulation* of M_{φ°.

Agol's triangulation is a taut *layered* triangulation with respect to φ°, that is, it is obtained by starting with a triangulation T of the surface S° and performing a sequence of diagonal exchanges which interpolate between the triangulations T and $\varphi(T)$ of S°, where a taut tetrahedron is attached each time a diagonal exchange occurs, and then gluing T to $\varphi(T)$.

Agol proves that triangulations obtained from this process are veering and moreover that they are canonical in the sense of the following proposition.

Proposition 7 (Proposition 4.2 of [2])**.** Let $\varphi^\circ : S^\circ \to S^\circ$ be a pseudo-Anosov homeomorphism which is punctured along the singular points of the stable foliation of φ°. Let $\mathcal{T}$ be a combinatorial taut ideal triangulation of the mapping torus M_{φ°, which is layered with respect to φ°. Then $\mathcal{T}$ is combinatorially isomorphic to Agol's triangulation of M_{φ° if and only if it is veering.

Furthermore, Agol mentions that the Floyd-Hatcher triangulations of the once-punctured torus bundles, which we discussed in Chapter 1, are veering taut layered triangulations, so, by the above proposition, they are Agol's triangulations of once-punctured torus bundles. These are the triangulations we looked at in Section 1.7, and we have coloured the edges in Figure 1.12 to illustrate the veering structure for the example we calculated.

7.3 Example — Once-punctured torus

We construct Agol's triangulation for the example in Section 3.4; see there for a description of the pseudo-Anosov homeomorphism $f : T \to T$ of the once-punctured torus T. We start with the invariant measured train track τ' shown in Figure 7.5. In brief, we will convert τ' into a trivalent train track. We then split the train track until we obtain the periodic splitting sequence, and construct the ideal triangulation of the mapping torus M_f.

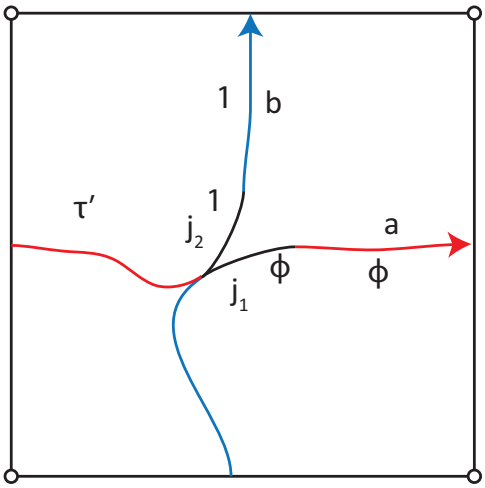

Figure 7.5: Invariant train track τ', where $\phi = \frac{1}{2}(1 + \sqrt{5})$ is the golden ratio.

We modify τ' to obtain a trivalent train track τ. We combine the branches j_1 and a into a single branch, which we also label a. Similarly we combine j_2 and b, labelling the new edge by b. The resulting train track has a single 4-valent switch, which we comb to obtain the trivalent train track τ, with new branch c, shown in Figure 7.6. See Step 4c of Chapter 8 for more detail on combing.

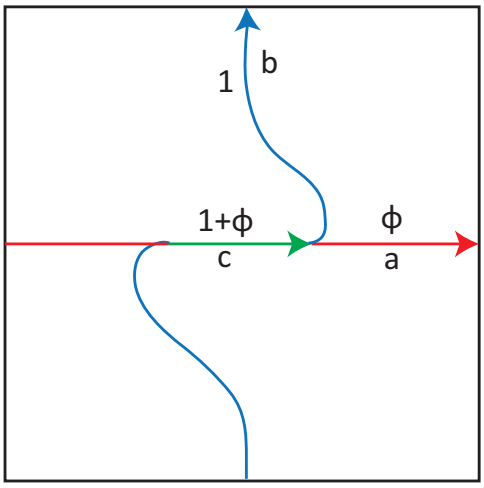

Figure 7.6: Trivalent weighted train track τ.

The resulting train track map $\mathfrak{g}$ on τ is given by

$$\begin{aligned} \mathfrak{g} : \tau &\to \tau \\ a &\mapsto acbca \\ b &\mapsto bca \\ c &\mapsto c \end{aligned}$$

Let $\tau_0 = \tau$, as this will be our initial train track. We compute the image of τ_0 after applying f by using the graph map to draw the image of each edge. (Compare with Figure 7.7.)

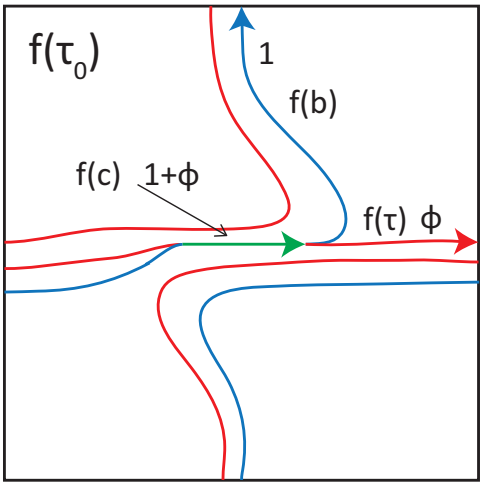

Figure 7.7: $f(\tau_0)$ up to isotopy.

In Figure 7.8, we illustrate three maximal splits starting with τ_0.

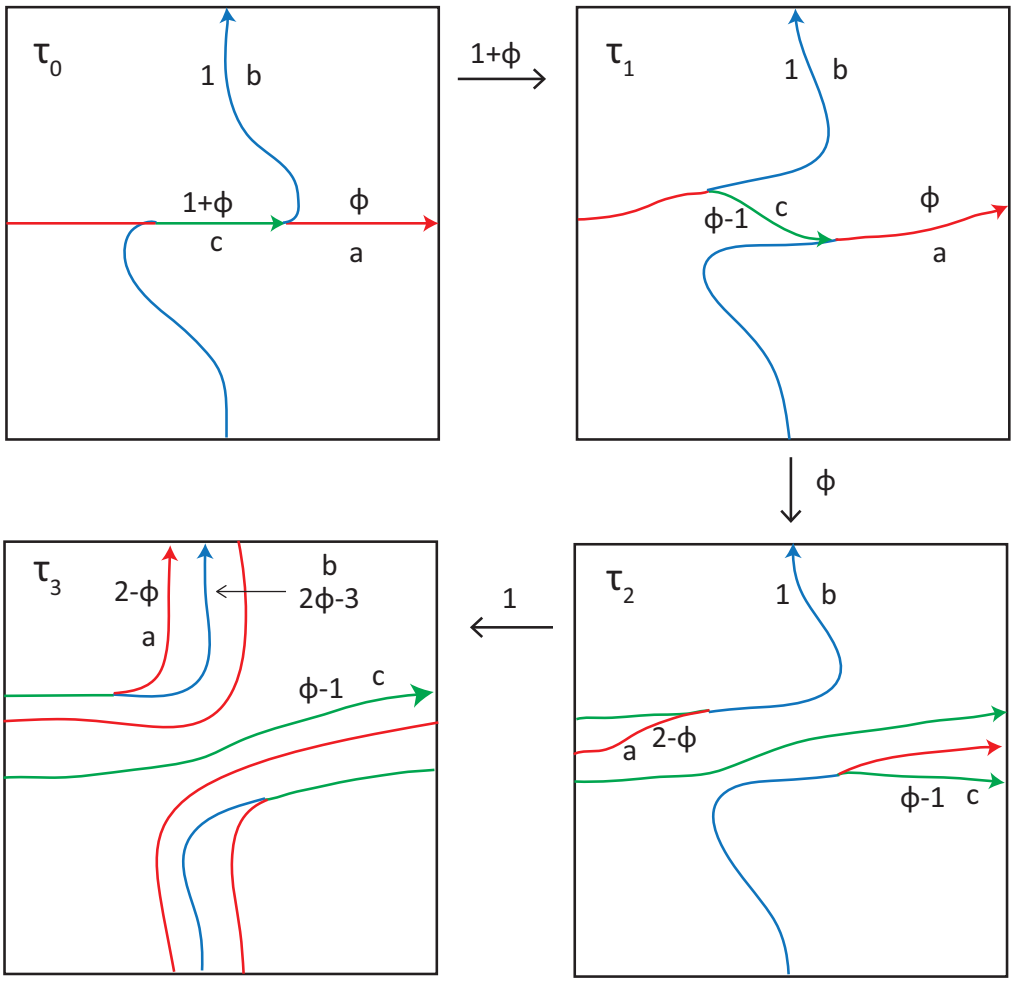

Figure 7.8: Splitting sequence. We have indicated the weight of the branch undergoing a split.

We claim that $f(\tau_1)$ and τ_3 are isotopic in such a way that after scaling the weights of τ_3 by the dilatation $\lambda = 1 + \varphi$, the branches of the train tracks which are identified have equal weights. We compute $f(\tau_1)$ by splitting $f(\tau_0)$ (Figure 7.7), this is shown in Figure 7.9. We have $f(a) = c$, $f(b) = a$ and $f(c) = b$. The weights are preserved after scaling, e.g. $\lambda\mu_3(a) = \lambda(2 - \varphi) = 1$.

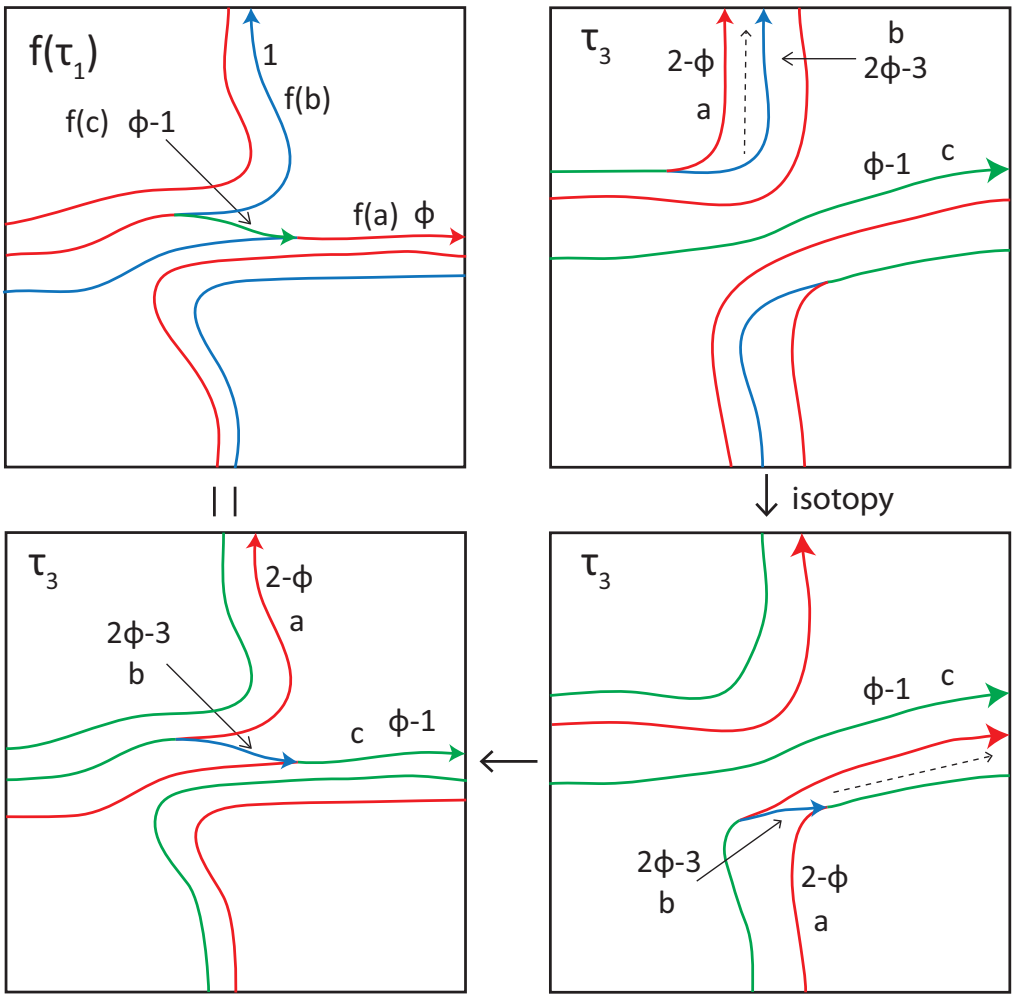

Figure 7.9: Isotoping τ_3 shows that $f(\tau_1) = \tau_3$.

We use the periodic splitting sequence to construct Agol's triangulation, see Figure 7.10. We note that this is the same triangulation that we computed in Figure 1.12 of Section 1.7. We draw the triangulation of the punctured torus T dual to each train track in the periodic splitting sequence, to obtain "layers" of triangulations of T. Between every two layers a tetrahedron is inserted which interpolates between the layers. Layers 0 and 2 are then glued by the monodromy.

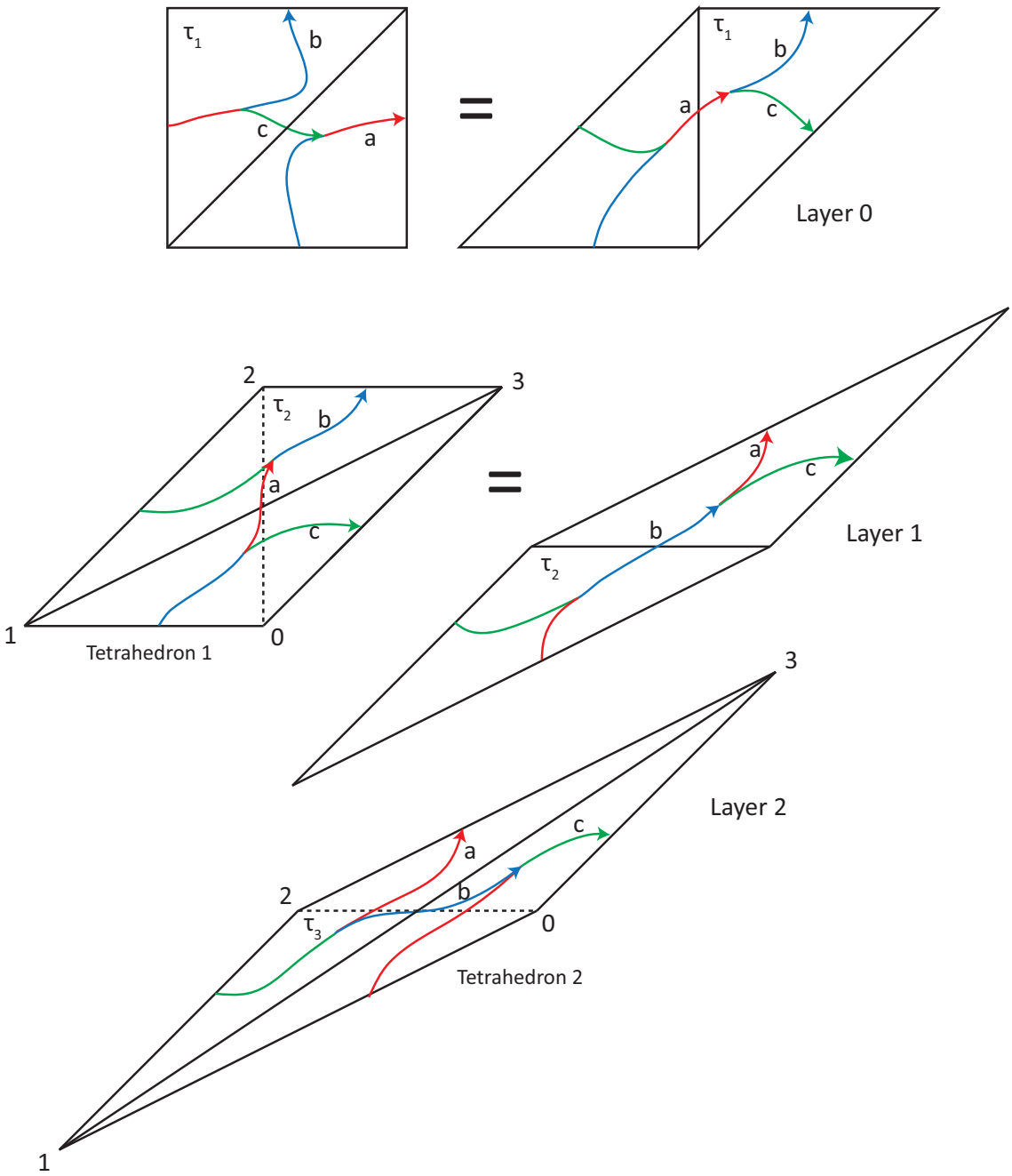

Figure 7.10: Triangulations of the punctured torus, dual to the train tracks of the splitting sequence. For aesthetic reasons we rearrange the triangles in layers 0 and 1 so that the diagonal of the parallelogram crosses the large branch of a train track.

Let T_1 and T_2 be tetrahedron 1 and 2, respectively. Since the triangles of the front (back) face of T_1 (T_2) correspond to triangles of layer 1, we obtain face pairings between the front of T_1 and back face of T_2. In order to completely specify all the tetrahedron face pairings it is necessary to pair the triangles of tetrahedron 1 attached to layer 0, to the triangles of tetrahedron 2 attached to layer 2.

The edges of triangles in layer 0 are in one to one correspondence with oriented branches of τ_1 which emanate from the unique vertex of τ_1 interior to the triangle. Since we know that $f(\tau_1) = \tau_3$, and we found earlier that this equality gives $f(a) = c$, $f(b) = a$ and $f(c) = b$, we use this information to determine the remaining face pairings. Hence, we have that (102) of T_1 is paired with (103) of T_2, and (032) of T_1 is paired with (132) of T_2.

Table 7.1: Tetrahedron face pairings

Tetrahedron 1	Tetrahedron 2
(103)	(203)
(321)	(021)
(102)	(103)
(032)	(132)

Chapter 8

Implementation

In this chapter we first discuss a computer program we implemented to construct examples of veering triangulations coming from Agol's construction, then give an algorithm for conjugacy testing in the mapping class group of a punctured surface.

8.1 Outline of steps

We outline the steps taken to produce examples of Agol's triangulations for pseudo-Anosov homeomorphisms of a once-punctured genus two surface S. We remark that we have also produced examples of Agol's triangulations for pseudo-Anosov homeomorphisms of a once-punctured genus three surface, and pseudo-Anosov homeomorphisms of a punctured disk.

Step 1

Let $n \in \mathbb{Z}_{>0}$, and create a list of all words of length at most n in the alphabet

$$\mathcal{A} = \{-5, -4, -3, -2, -1, 1, 2, 3, 4, 5\}.$$

Each letter $i \in \mathcal{A}$ represents a Dehn twist in the curve C_i shown in Figure 8.1, where a positive number indicates a left twist, and a negative number indicates a right twist. For example, -1 represents the Dehn twist in C_1 such that, intuitively, as we approach C_1 from either side, we move towards the right (where the surface is oriented by the outward normal.) A word $a_1 a_2 ... a_k$ represents the element of $\mathrm{MCG}(S)$ given by the twist a_1 followed by the twist a_2 and so on, up to a_k. The Dehn twists in the curves $C_1, \ldots, C_5$ generate the mapping class group $\mathrm{MCG}(S)$, and are known as the Humphries generators; see [17, §4.4.4] and [28].

In practice, we actually generated a somewhat smaller list containing at least one representative of each mapping class element up to conjugacy and inversion, which can be expressed as a word of length at most $n = 7$. Note that conjugation and inversion result in combinatorially isomorphic veering triangulations.

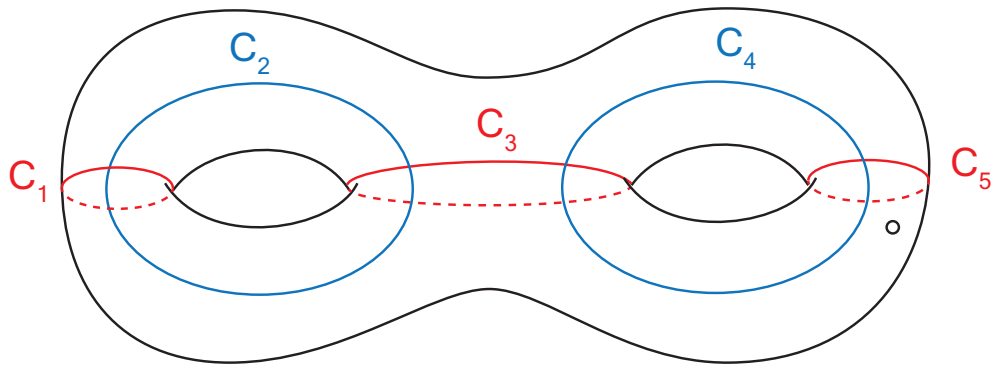

Figure 8.1: Humphries generators for MCG(S).

Step 2

For each mapping class element $\varphi : S \to S$ in our list we compute a graph map $\mathfrak{g} : G \to G$ representing φ, where $G \subseteq S$ is the graph shown below, which is homotopy equivalent to S.

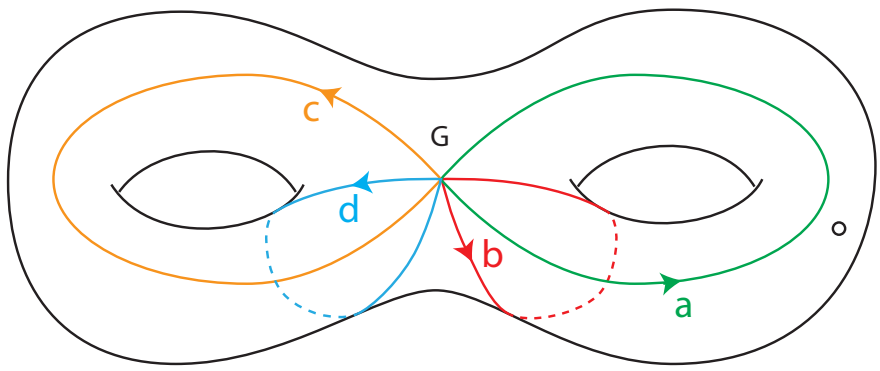

Step 3

Each graph map produced is input into the computer program Trains [25], written by Toby Hall, which is a software implementation of the Bestvina-Handel algorithm for punctured surfaces. The computer program Trains will determine whether or not the homeomorphism represented by the graph map is isotopic to a pseudo-Anosov homeomorphism, and in the case that it is, it will produce an invariant train track suited to the stable geodesic lamination, as in the Bestvina-Handel algorithm. Other information is also given, such as the train track map and dilatation $\lambda \in \mathbb{R}_{>1}$.

Step 4

For each train track produced by Trains we construct Agol's triangulation. More specifically, let $\varphi : S \to S$ be a pseudo-Anosov homeomorphism, let τ be an invariant train track, as produced by Trains, and let $\lambda > 1$ be the dilatation of φ. We do the following.

(a) Use the train track map given by Trains to compute the weights of branches of τ to a specified (arbitrary) precision.

(b) Agol's construction begins with a trivalent train track suited to $\mathcal{L}^s$, however those produced by the Bestvina-Handel algorithm are generally not trivalent. We modify τ

by applying a 'combing' procedure at each switch of τ with degree greater than 3 to produce a measured train track, which we continue to denote by τ, which is suited to $\mathcal{L}^s$.

More precisely, let v be a switch of τ with degree greater than 3. Let e_1, e_2 be consecutive edges incident to v, and let $U \subseteq S$ be a closed disk such that $v \in \mathrm{Int}(U)$ (see Figure 8.2.) Identify the arcs $e_1 \cap U$ and $e_2 \cap U$ to produce a train track, obtained from τ by *combing*. By repeatedly combing we can obtain a trivalent train track, which we will continue to denote by τ. By Proposition 8, $\mathcal{L}$ is suited to τ. (Further discussion of combing can be found on Page 40 of §1.4 of [45].)

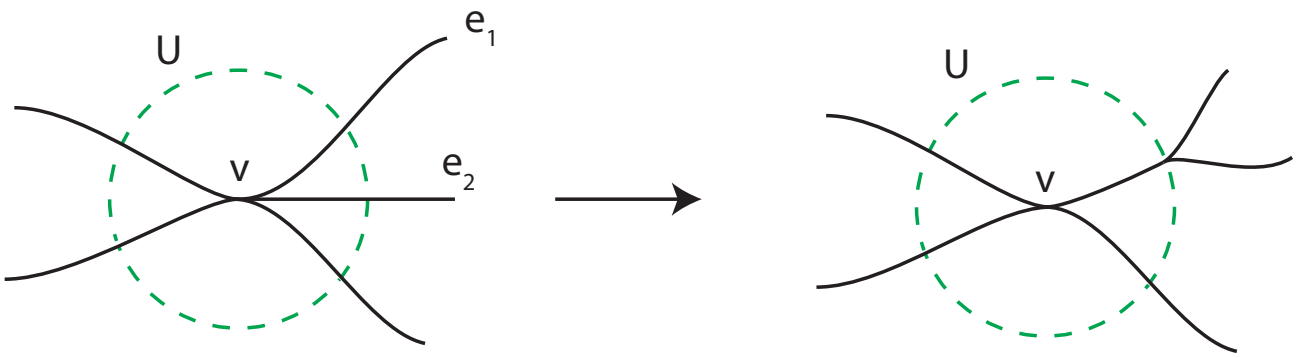

Figure 8.2: Combing a train track

Proposition 8. Let $\mathcal{L}$ be a lamination suited to a train track $\tau' \subseteq S$. Let τ'' be obtained from τ' by combing $e_1, e_2 \in \mathcal{E}_{dir}(\tau')$ with respect to the closed disk $U \subseteq S$. Then $\mathcal{L}$ is suited to τ''.

Proof. By definition since $\mathcal{L}$ is suited to τ' there exists a differentiable map $f : S \to S$ homotopic to the identity such that $f(\mathcal{L}) = \tau'$ and f is non-singular on the tangent space to leaves of $\mathcal{L}$. Let $h : S \to S$ be a differentiable map homotopic to the identity which, intuitively, folds together $e_1 \cap U$ and $e_2 \cap U$. Then $h \circ f : S \to S$ is a differentiable map homotopic to the identity such that $h \circ f(\mathcal{L}) = \tau''$ and is non-singular on the tangent space to leaves of $\mathcal{L}$. $\square$

(c) Perform maximal splits beginning with the train track τ, producing a sequence of measured train tracks

$$(\tau, \mu) \rightharpoonup (\tau_1, \mu_1) \rightharpoonup \cdots \rightharpoonup (\tau_n, \mu_n) \rightharpoonup \cdots \rightharpoonup (\tau_{n+m}, \mu_{n+m}) \rightharpoonup \cdots, \quad n, m \in \mathbb{Z}_{>0}.$$

Ideally, we would stop performing maximal splits as soon as we find that the sequence becomes periodic, that is, $(\varphi(\tau_n), \lambda^{-1}\varphi(\mu_n)) = (\tau_{n+m}, \mu_{n+m})$ for some $n, m \in \mathbb{Z}_{>0}$, where $\lambda > 1$ is the dilatation of φ. However, we do not keep track of the embedding of train tracks in the surface S so we can not compare train tracks up to isotopy in S. Despite this, we can determine if two measured train tracks $(\tau', \mu'), (\tau'', \mu'')$ are *combinatorially equivalent*, that is, there is a bijection between their vertices and oriented edges which:

(i) respects incidence, i.e. the combinatorial graph structure of the train tracks,

(ii) respects the clockwise cyclic order of oriented edges around a switch,

(iii) respects the weights of branches, and

(iv) preserves complementary regions, that is, if p is a puncture of S, then the clockwise sequence of edges which form the boundary of the complementary region of

τ containing p are mapped by the bijection to the clockwise sequence of edges which form the boundary of the complementary region of τ' containing p.

See [39, §3.15] for further discussion on combinatorial equivalence. We write $(\tau', \mu') \sim (\tau'', \mu'')$ to denote combinatorial equivalence.

We stop performing maximal splits as soon as we find that $(\tau_{n+m}, \mu_{n+m}) \sim (\tau_n, \lambda^{-1}\mu_n)$ for some $n, m \in \mathbb{Z}_{>0}$. Observe that $(\varphi(\tau_n), \lambda^{-1}\varphi(\mu_n)) \sim (\tau_n, \lambda^{-1}\mu_n)$ and therefore $(\tau_{n+m}, \mu_{n+m}) \sim (\varphi(\tau_n), \lambda^{-1}\varphi(\mu_n))$.

(d) We construct the layered triangulation as in Section 7.2. Recall that we add punctures to S at the singular points of the transverse measured foliations of φ to obtain a surface S° so that each complementary region (in S°) of a train track in our splitting sequence is homeomorphic to a punctured disk. For a given train track there is a dual ideal triangulation of the surface S° so that edges of triangles are in bijection with branches of the train track. A maximal split $\tau_i \rightharpoonup \tau_{i+1}$ corresponds to a sequence of diagonal exchanges, and for each diagonal exchange an ideal tetrahedron is attached.

Finally, we need to specify how the triangulation T_n of S° dual to τ_n glues to the triangulation T_{n+m} of S° dual to τ_{n+m}, which is required in order to completely determine the tetrahedron face pairings. A combinatorial equivalence between τ_n and τ_{n+m} (with weights appropriately scaled) gives a bijection between the edges of τ_n and τ_{n+m}, which induces a gluing of the ideal triangles in T_n to those in T_{n+m}, as required.

However, there may be more than one combinatorial equivalence between the train tracks τ_n and τ_{n+m} (roughly, this is due to symmetries in the train tracks.) We enumerate all ways in which the train tracks are combinatorially equivalent. Each equivalence determines a gluing of T_n to T_{n+m} for which we construct a triangulation. The following proposition shows that one of these combinatorial equivalences produces Agol's triangulation.

Proposition 9. There exists a combinatorial equivalence between $(\tau_n, \lambda^{-1}\mu_n)$ and (τ_{n+m}, μ_{n+m}) for which the above procedure constructs Agol's triangulation.

Proof. By Theorem 14, there exists $k, c \in \mathbb{Z}_{>0}$ such that

$$(\tau_{(n+k)+c}, \mu_{(n+k)+c}) = (\varphi(\tau_{n+k}), \lambda^{-1}\varphi(\mu_{n+k})),$$

where c is the period of the periodic splitting sequence.

Claim: $c = m$**.**

Since $(\tau_n, \lambda^{-1}\mu_n)$ and (τ_{n+m}, μ_{n+m}) are combinatorially equivalent, by further splitting we see that the sum of the weights of $\lambda^{-1}\varphi(\mu_{n+k})$ and $\mu_{(n+k)+m}$ are equal. The sum of the weights strictly decreases each time a maximal split occurs, so we must have $c = m$, proving the claim.

By further splitting of the train tracks if necessary, we may assume that k is a multiple of m, i.e. $k = pm$ for some $p \in \mathbb{Z}_{\geq 0}$. Since τ_n and τ_{n+m} are combinatorially equivalent and fill S, there is a diffeomorphism $h : S \to S$ such that $h(\tau_n, \mu_n) = (\tau_{n+m}, \lambda\mu_{n+m})$ (e.g. see [39, Proposition 3.15.1] and Proposition 10 in Section 8.2 below.) For convenience, we may assume, by an isotopy if necessary, that φ is a diffeomorphism. Then $(\tau_{n+pm}, \mu_{(n+pm)}) = (h^p(\tau_n), \lambda^{-p}h^p(\mu_n))$. The periodic splitting sequences

$$(\tau_{n+pm}, \mu_{n+pm}) \rightharpoonup \cdots \rightharpoonup (\tau_{(n+pm)+m}, \mu_{(n+pm)+m}) = (\varphi(\tau_{n+pm}), \lambda^{-1}\varphi(\tau_{n+pm})) \quad (8.1)$$

and

$$(\tau_n, \mu_n) \rightharpoonup \cdots \rightharpoonup (\tau_{n+m}, \mu_{n+m})$$

are equivalent up to reembedding of train tracks in the surface and rescaling of weights. More precisely, the diffeomorphism h^{-p} conjugates between the two sequences, after rescaling of weights. Thus, there is a combinatorial equivalence between $(\tau_n, \lambda^{-1}\mu_n)$ and (τ_{n+m}, μ_{n+m}) which produces the same triangulation as is produced by the periodic splitting sequence (8.1) with combinatorial equivalence induced by the equality $\varphi(\tau_{n+pm}) = \tau_{(n+pm)+m}$. □

For each triangulation $\mathcal{T}$:

(i) Input the triangulation $\mathcal{T}$ into SnapPy to obtain a manifold $M_{\mathcal{T}}$. For each additional cusp of $M_{\mathcal{T}}$, i.e. a cusp of $M_{\mathcal{T}}$ which does not arise from the puncture of S, use SnapPy to perform a Dehn filling along a loop which bounds a puncture in the fiber S°. Denote the Dehn filled manifold by $M^*_{\mathcal{T}}$. If $\mathcal{T}$ is Agol's triangulation for the monodromy φ°, then $M^*_{\mathcal{T}}$ is isometric to M_φ. The Dehn fillings can be thought of as filling in the curves which were drilled out of M_φ when we removed the singular points of the foliations.

(ii) Use SnapPy to check whether $M^*_{\mathcal{T}}$ is isometric to M_φ, and if not, discard the triangulation $\mathcal{T}$. In order to check for isometry, we use the computer program *Twister* [3] which, given a sequence of Dehn twists representing φ, constructs a triangulation of M_φ.

If there is a unique triangulation not discarded by the above procedure, then it is Agol's triangulation for M_{φ°. In all the examples we have computed, there was a unique triangulation not discarded.

Step 5

We have now obtained a list of mapping classes and their associated veering triangulations. We used a program of Henry Segerman to check these triangulations are veering. Mapping classes which are related by conjugation and inversion produce combinatorially isomorphic veering triangulations. In order to organise our data we would like to obtain one representative from each mapping class up to conjugation and inversion.

If we label a left Dehn twist in the curves $C_1, \ldots, C_5$ by $\sigma_1, \sigma_2, \ldots, \sigma_5$ then the generators $\sigma_1, \ldots, \sigma_5$ satisfy the braid relations on 6 strands (see Proposition 3.11 of [17].) We use the software *Braiding* [31] to obtain one representative of each mapping class up to inversion and conjugation in the braid group, from our list of Dehn twists. We remark that since the mapping class group satisfies additional relations, this procedure produces a slightly longer list than we would ideally hope for. In the next section we explain how we were able to obtain one representative of each conjugacy class up to conjugation and inversion.

8.2 Conjugacy testing

Given a pseudo-Anosov homeomorphism $\phi, \phi' : S \to S$ of a punctured surface S, in this section we give an algorithm to effectively decide whether or not ϕ and ϕ' are conjugate in $\mathrm{MCG}(S)$. We have implemented this algorithm as part of our computer program.

Definition 69. Let S be a punctured surface. Let $\phi, \phi' : S \to S$ be pseudo-Anosov homeomorphisms with periodic splitting sequences

$$(\tau_0, \mu_0) \rightharpoonup^m (\tau_m, \mu_m) = \phi(\tau_0, \mu_0) \rightharpoonup \cdots$$

and

$$(\tau'_0, \mu'_0) \rightharpoonup^n (\tau'_n, \mu'_n) = \phi'(\tau'_0, \mu'_0) \rightharpoonup \cdots$$

respectively, where $n, m \in \mathbb{Z}_{>0}$, as in Theorem 14. We denote the periodic splitting sequences of ϕ, ϕ' by $\mathcal{S}, \mathcal{S}'$ respectively.

We say that $\mathcal{S}$ and $\mathcal{S}'$ are *combinatorially isomorphic* if there exists a diffeomorphism which projectively conjugates between them, that is, $n = m$ and there exists $h : S \to S$, $p, q \in \mathbb{Z}_{\geq 0}$ and $c \in \mathbb{R}_{>0}$ such that:

(i) $\phi' = h \circ \phi \circ h^{-1}$, and

(ii) $h(\tau_{p+i}, \mu_{p+i}) = (\tau'_{q+i}, c\mu'_{q+i})$, for $i \in \mathbb{Z}_{\geq 0}$.

Lemma 3 (Corollary 3.4 of [2])**.** Let $\mathcal{L}$ be a measured geodesic lamination suited to train tracks $(\tau, \mu), (\tau', \mu')$. Then (τ, μ) and (τ', μ') eventually split to a common train track, that is, there exists (τ'', μ'') and $n, m \in \mathbb{Z}_{\geq 0}$ such that $(\tau, \mu) \rightharpoonup^n (\tau'', \mu'')$ and $(\tau', \mu') \rightharpoonup^m (\tau'', \mu'')$.

Theorem 15. Let $\phi, \phi' : S \to S$ be pseudo-Anosov homeomorphisms with periodic splitting sequences $\mathcal{S}$ and $\mathcal{S}'$ respectively, as in Theorem 14. Then ϕ and ϕ' are conjugate in $\mathrm{MCG}(S)$ if and only if $\mathcal{S}$ and $\mathcal{S}'$ are combinatorially isomorphic.

Proof. Assume that ϕ and ϕ' are conjugate, and let $h \in \mathrm{MCG}(S)$ such that $\phi' = h \circ \varphi \circ h^{-1}$. Let the periodic splitting sequences $\mathcal{S}$ and $\mathcal{S}'$ be given by

$$(\tau_0, \mu_0) \rightharpoonup^m (\tau_m, \mu_m) = \phi(\tau_0, \mu_0) \rightharpoonup \cdots$$

and

$$(\tau'_0, \mu'_0) \rightharpoonup^n (\tau'_n, \mu'_n) = \phi'(\tau'_0, \mu'_0) \rightharpoonup \cdots$$

respectively, where $n, m \in \mathbb{Z}_{>0}$.

Let $\mathcal{L}, \mathcal{L}'$ be the stable measured laminations of ϕ, ϕ' which are suited to $(\tau_0, \mu_0), (\tau'_0, \mu'_0)$ respectively. Then $(\tau'', \mu'') = h(\tau_0, \mu_0)$ is an invariant train track for ϕ' and there exists a stable measured lamination $\mathcal{L}''$ suited to (τ'', μ'') (which is essentially given by straightening the leaves of $h(\mathcal{L})$.) By uniqueness of stable laminations in $\mathcal{PML}(S)$ (see Theorem 10), there exists $c \in \mathbb{R}_{>0}$ such that $\mathcal{L}' = c\,\mathcal{L}''$, where $c\,\mathcal{L}''$ denotes the measured geodesic lamination equal to $\mathcal{L}''$ as a lamination but with transverse measure scaled by c. Then $\mathcal{L}'$ is suited to $(\tau'', c\mu'')$ and (τ'_0, μ'_0). Therefore by Lemma 3, we know that $(\tau'', c\mu'') = h(\tau_0, c\mu_0)$ and (τ'_0, μ'_0) have a common split, that is, there exists $p, q \in \mathbb{Z}_{\geq 0}$ such that $h(\tau_p, c\mu''_p) = (\tau'_q, \mu'_q)$, which implies

$$h(\tau_{p+i}, c\mu''_{p+i}) = (\tau'_{q+i}, \mu'_{q+i}) \text{ for } i \in \mathbb{Z}_{\geq 0}.$$

Thus, $\mathcal{S}$ and $\mathcal{S}'$ are combinatorially isomorphic.

We now prove the other direction. Assume that $\mathcal{S}$ and $\mathcal{S}'$ are combinatorially isomorphic. Then by definition there exists a diffeomorphism $h \in \mathrm{MCG}(S)$ such that $\phi' = h \circ \phi \circ h^{-1}$, as required. □

We remark that Theorem 15 seems similar to [39, Theorem 10.3.2] of Lee Mosher.

Proposition 10. Let $(\tau, \mu), (\tau', \mu')$ be measured train tracks on a punctured surface S which fill the surface, that is, all the complementary regions of each of the train tracks are homeomorphic to a disk or once-punctured disk. Then (τ, μ) and (τ', μ') are combinatorially equivalent if and only if there exists a diffeomorphism $\phi : S \to S$ such that $\phi(\tau, \mu) = (\tau', \mu')$.

See [39, Proposition 3.15.1].

8.2.1 Algorithm for determining conjugacy in MCG(S)

Proposition 10 allows us to determine combinatorially whether or not two periodic splitting sequences are combinatorially isomorphic, which when combined with Theorem 15 gives an effective algorithm for testing for conjugacy of pseudo-Anosov mapping classes in the mapping class group.

Let $\phi, \phi' : S \to S$ be pseudo-Anosov homeomorphisms with periodic splitting sequences

$$(\tau_0, \mu_0) \rightharpoonup^m (\tau_m, \mu_m) = \phi(\tau_0, \mu_0) \rightharpoonup \cdots$$

and

$$(\tau'_0, \mu'_0) \rightharpoonup^n (\tau'_n, \mu'_n) = \phi'(\tau'_0, \mu'_0) \rightharpoonup \cdots$$

respectively, where $n, m \in \mathbb{Z}_{>0}$, as in Theorem 14. We determine whether or not ϕ and ϕ' are conjugate in MCG(S) using the following procedure.

(i) If $n \neq m$ then ϕ and ϕ' are not conjugate in MCG(S).

(ii) Otherwise, we enumerate all combinatorial equivalences (up to rescaling of measures) between (τ_i, μ_i) and (τ'_j, μ'_j), for $0 \leq i < m = n$ and $0 \leq j < n$, then check whether any combinatorial equivalence conjugates between ϕ and ϕ' (in fact one only needs to check this for $i = 0$ and $0 \leq j < n$.)

More precisely, let Φ be a combinatorial equivalence between (τ_i, μ_i) and $(\tau'_j, c\mu'_j)$, where $c \in \mathbb{R}_{>0}$, $0 \leq i < n$ and $0 \leq j < n$. Then Φ gives a bijection between the edges of the train tracks which we denote by

$$\Phi_0 : \mathcal{E}_{dir}(\tau_i) \to \mathcal{E}_{dir}(\tau'_j),$$

where the notation $\mathcal{E}_{dir}(\tau_i)$ means the set of directed edges of τ_i. Furthermore, by splitting the train tracks (τ_i, μ_i) and (τ_j, μ_j) simultaneously, keeping track of the bijection between the edges induced by Φ_0, we obtain a combinatorial equivalence

$$\Phi_n : \mathcal{E}_{dir}(\tau_{i+n}) \to \mathcal{E}_{dir}(\tau'_{j+n}).$$

(Φ_0 and Φ_n should be thought of as representing the diffeomorphism induced by Φ given by Proposition 10, in terms of different underlying train tracks.) The homeomorphisms ϕ and ϕ' induce combinatorial equivalences

$$\phi_* : \mathcal{E}_{dir}(\tau_i) \to \mathcal{E}_{dir}(\tau'_{i+n}) \text{ and } \phi'_* : \mathcal{E}_{dir}(\tau'_j) \to \mathcal{E}_{dir}(\tau'_{j+n}),$$

respectively.

(a) If $\phi'_* \circ \Phi_0 = \Phi_n \circ \phi_*$ then we conclude that ϕ and ϕ' are conjugate in MCG(S).

(b) Otherwise, if for no combinatorial equivalence does (a) hold, then ϕ and ϕ' are not conjugate in MCG(S).

Chapter 9

Results

By performing the steps outlined in Chapter 8, we constructed triangulation files of veering triangulations coming from Agol's construction, which can readily be input into SnapPy. We have included the beginning of longer lists of data which we have collected, given as tables in Appendix A. A number of triangulations which SnapPy reports are non-geometric were found, and in the case that we start with a pseudo-Anosov homeomorphism of a once-punctured genus 2 surface, a table of such examples is given in Appendix A. We remark that we have also found veering triangulations which SnapPy reports are non-geometric starting with homeomorphisms of the once-punctured genus 3 surface, as well as the 4-punctured disk

Many of the veering triangulations produced are relatively large, and could be simplified by SnapPy to much smaller triangulations, see Figure 9.1. Heuristically, triangulations of a fixed hyperbolic manifold with a relatively small number of tetrahedra have a better chance of being geometric, and SnapPy makes an effort to simplify triangulations of link complements that it produces [38, Chapter 10].

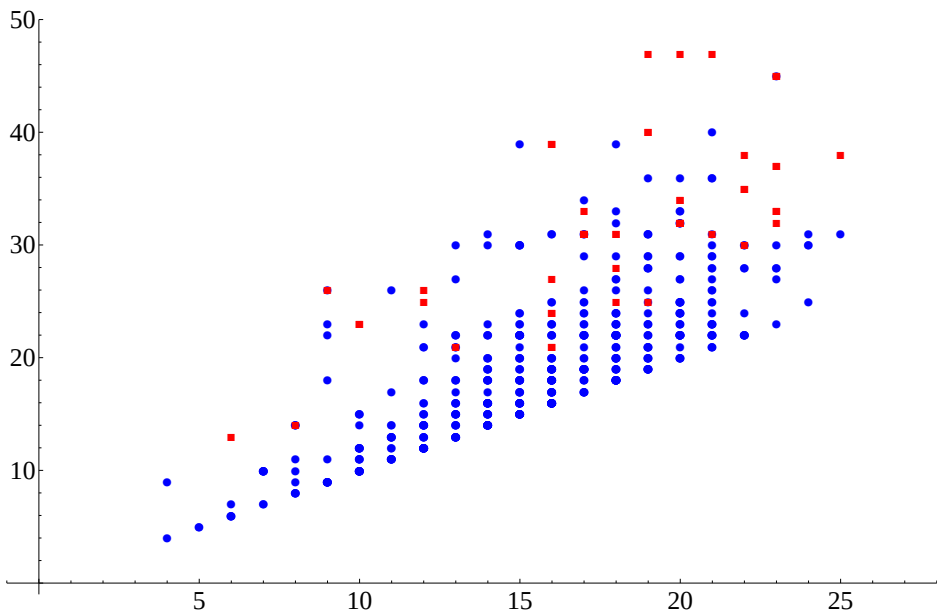

Figure 9.1: Vertical axis: number of tetrahedra in Agol's triangulation. Horizontal axis: number of tetrahedra after Agol's triangulation is simplified by SnapPy. Red points indicate veering triangulations which SnapPy reports are non-geometric.

9.1 A non-geometric example

The example with the fewest number of tetrahedra that we have found, which SnapPy reports is non-geometric, is a 13 tetrahedron triangulation $\mathcal{T}$ coming from the pseudo-Anosov homeomorphism $\varphi : S \to S$ of the once-punctured genus 2 surface given by the Dehn twist word $5, 4, 5, 5, 5, 2, 3$ with notation as discussed in Step 1 of Chapter 8. In Section 3.5 we computed an invariant train track τ for φ as given by the Bestvina-Handel algorithm, see Figure 9.2.

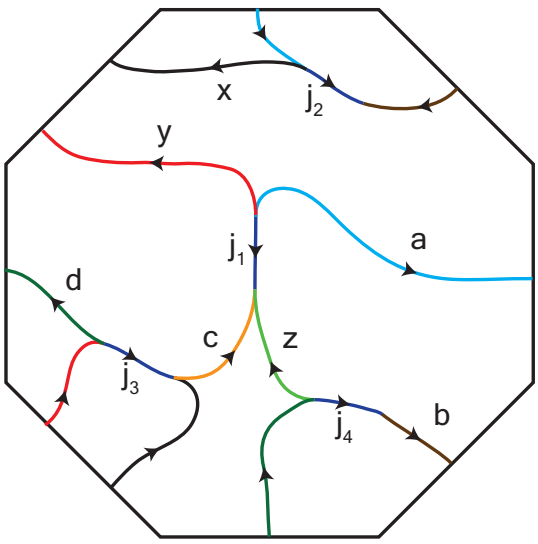

Approximate weights of branches:

$$\begin{array}{c} j_1 \\ j_2 \\ j_3 \\ j_4 \\ a \\ b \\ c \\ d \\ x \\ y \\ z \end{array} \begin{pmatrix} 1.34601 \\ 1.46574 \\ 1.30459 \\ 1.46574 \\ 0.50717 \\ 1.46574 \\ 0.34601 \\ 0.46574 \\ 0.95857 \\ 0.83885 \\ 1.00000 \end{pmatrix}.$$

Figure 9.2: Invariant train track τ obtained by performing the Bestvina-Handel algorithm.

The train track map is $\mathfrak{g} : \tau \to \tau$:

$$\begin{array}{lcl} a & \mapsto & d\ j_4\ b\ \overline{j_2}\ \overline{a}\ j_1\ \overline{z} \\ b & \mapsto & y\ j_3\ \overline{x}\ j_2\ \overline{b} \\ c & \mapsto & x \\ d & \mapsto & \overline{b}\ \overline{j_4}\ z \end{array} \qquad \begin{array}{lcl} x & \mapsto & z\ \overline{j_1}\ y\ j_3\ \overline{x}\ j_2\ \overline{b}\ \overline{j_4}\ z\ \overline{j_1}\ a \\ y & \mapsto & d\ j_4\ b \\ z & \mapsto & \overline{c} \end{array} \qquad \begin{array}{lcl} j_1 & \mapsto & j_3 \\ j_2 & \mapsto & j_4 \\ j_3 & \mapsto & \overline{j_2} \\ j_4 & \mapsto & \overline{j_1} \end{array}$$

The dilatation of φ is $\lambda = 2.89005..$, which is the largest real root of $x^4 - 2x^3 - 2x^2 - 2x + 1$. From the invariant train track we see that the invariant measured foliations have a 6-prong singular point at the puncture, and that there are no other singular points. The mapping torus M_φ is 1-cusped and has hyperbolic volume 4.85117... It is identified as manifold s479 in the SnapPy census of manifolds, which has a geometric triangulation of M_φ by 6 ideal tetrahedra. Agol's triangulation of M_φ is given in the SnapPy file format in Appendix B, and the triangulation of the link of the cusp of M_φ is shown in Figure 9.3.

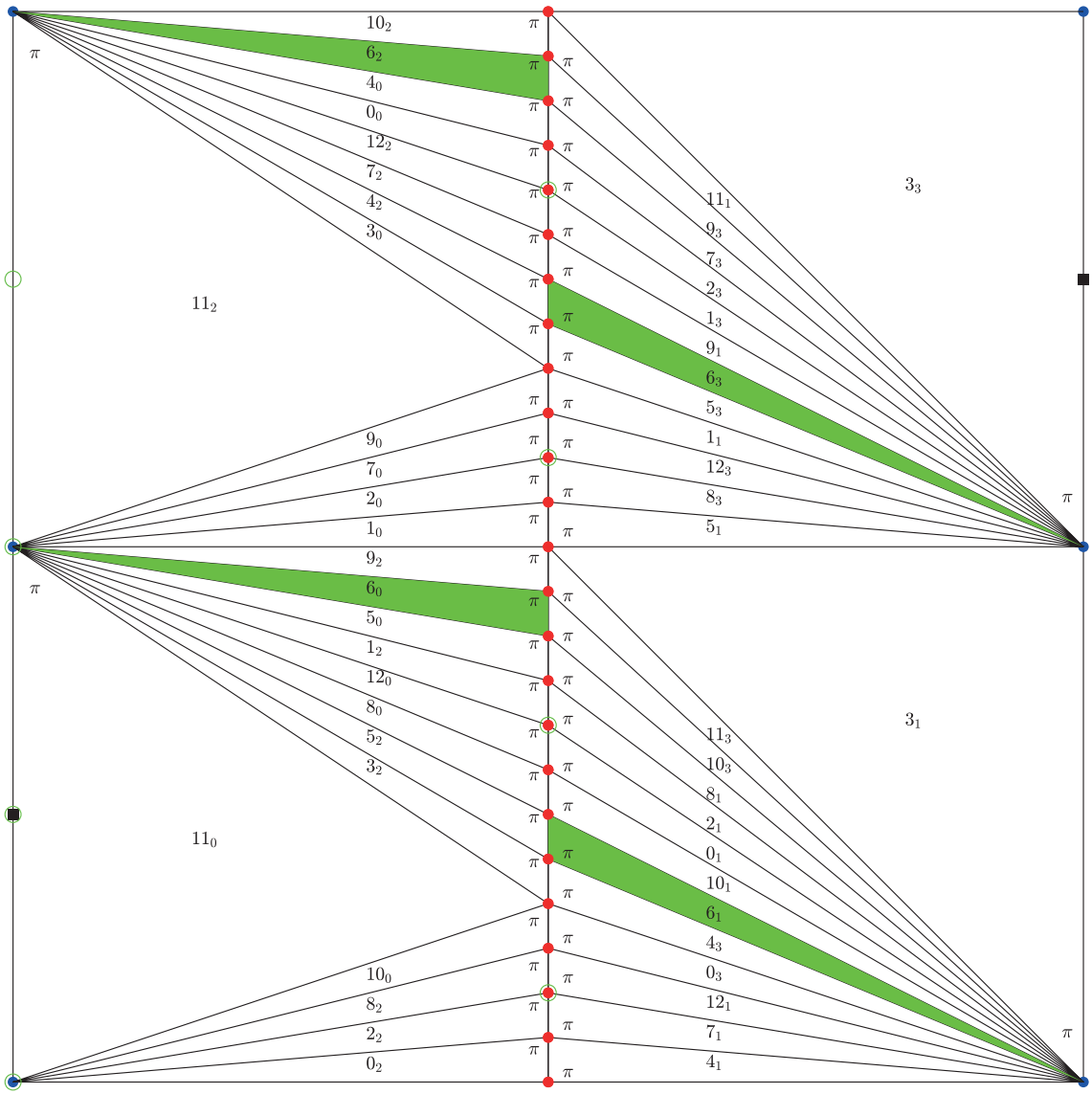

Figure 9.3: Induced triangulation of boundary torus of the triangulation $\mathcal{T}$, produced by Henry Segerman. SnapPy finds a solution to the gluing and completeness equations where the shaded triangles correspond to the tetrahedron reported to be negatively oriented. The notation 6_3 means tetrahedron 6, face 3.

Generally, we can not immediately rule out the possibility that SnapPy finds a non-geometric solution although a geometric solution exists. We now outline how we rigorously verified that the triangulation $\mathcal{T}$ is non-geometric.

Definition 70. Let $\mathcal{T}$ be an ideal triangulation, with tetrahedron edge parameters given by a vector $\vec{z}$. The *algebraic volume* $\mathrm{vol}(\vec{z})$ of $\vec{z}$ is the sum of the signed volumes of hyperbolic tetrahedra with shapes given by $\vec{z}$, i.e. where a negatively oriented tetrahedron contributes negative its volume to the sum. If it is clear which edge parameters we are referring to, we shall write $\mathrm{vol}(\mathcal{T})$ for $\mathrm{vol}(\vec{z})$.

Theorem 16. Let $\mathcal{T}$ be an ideal triangulation of a hyperbolic 3-manifold M. Then there exists at most one solution $\vec{z}$ to the gluing and completeness equations for $\mathcal{T}$ such that

$$\mathrm{vol}(\vec{z}) = \mathrm{vol}(M),$$

where $\mathrm{vol}(M)$ is the hyperbolic volume of M.

This is a corollary of [19, Remark 4.1.20] and [19, Theorem 5.4.1] (in particular the corollary given in the last dot point of Page 6.)

Corollary 1. Let $\vec{z}$ be a solution to the gluing and completeness equations for an ideal triangulation $\mathcal{T}$ of a hyperbolic 3-manifold M such that

1. $\mathrm{vol}(\vec{z}) = \mathrm{vol}(M)$, and
2. $\vec{z}$ is non-geometric, i.e. at least one of the edge parameters has non-positive imaginary part.

Then $\mathcal{T}$ is non-geometric, that is, there is no solution to the gluing and completeness equations with all tetrahedra positively-oriented.

Proof. Assume that $\vec{z'}$ is a geometric solution to the gluing and completeness equations, then $\mathrm{vol}(\vec{z'}) = \mathrm{vol}(M)$. Hence, by Theorem 16 we have $\vec{z} = \vec{z'}$, contradicting that $\vec{z}$ is non-geometric. □

By Corollary 1, in order to show that $\mathcal{T}$ is non-geometric it suffices to find a non-geometric solution to the gluing and completeness equations which has algebraic volume equal to the volume of M. We find an exact non-geometric solution to the gluing and completeness equations using the computer program Snap [22], then verify that it has algebraic volume equal to the volume of M.

If $\vec{z}$ consists of the edge parameters to a solution of the gluing and completeness equations then the numbers z_i are in fact algebraic numbers. The computer program Snap attempts to find such a solution, expressing each edge parameter z_i as a polynomial in a number field $\mathbb{Q}(\tau)$, where τ is an algebraic number. In order to specify τ exactly, Snap provides the minimal polynomial $m(x)$ of τ as well as calculates τ to sufficiently many decimal places to uniquely specify it as the root of $m(x)$ closest to the decimal approximation. See [13] for more information about Snap.

Definition 71. [48, §3.1] Let $\mathcal{T}$ be a triangulation. A *Pachner 2-3 move* is a move at a common face of two tetrahedra in $\mathcal{T}$ which produces the triangulation $\mathcal{T}'$, obtained by removing the face and inserting a dual edge, see Figure 9.4. If the tetrahedra in $\mathcal{T}$ are assigned edge parameters, then the three new tetrahedra in $\mathcal{T}'$ are assigned edge parameters as shown in Figure 9.4. A *Pachner 3-2 move* is the reverse of a Pachner 2-3 move, that is, an edge with three surrounding tetrahedra is replaced by a dual face.

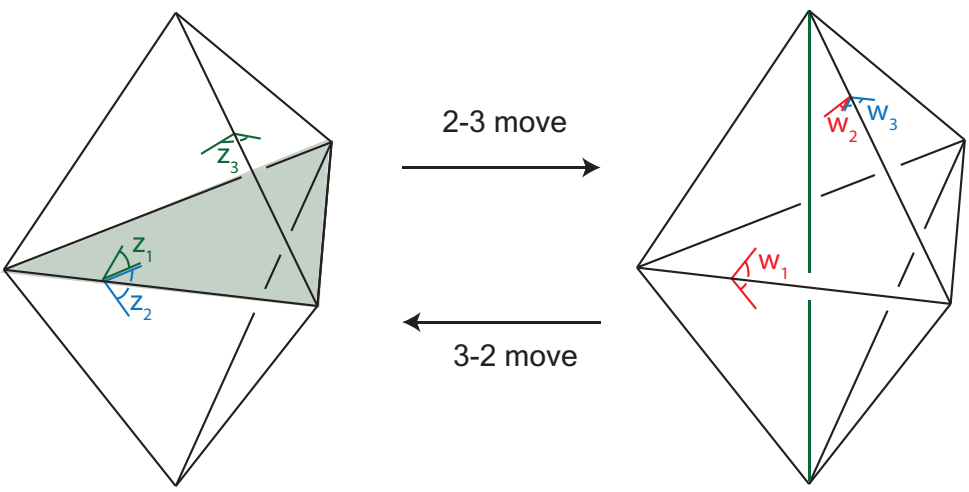

Figure 9.4: Pachner 2-3 and 3-2 moves. On the left two tetrahedra have a common face and on the right three tetrahedra have a common edge, shown in green. The edge parameters are related by: $z_3 = w_2 w_3$ and $w_1 = z_1 z_2$, and similar relations at the other edges allow us to determine the shapes of each tetrahedron.

Theorem 17. Let M be a hyperbolic 3-manifold and let $\mathcal{T}$ be an ideal triangulation of M. Let $\vec{z}$ be a solution to the gluing and completeness equations for $\mathcal{T}$, where we allow negatively oriented and flat tetrahedra, i.e. $z_i \in \mathbb{C}\backslash\{0,1\}$ for each edge parameter z_i. Let $\mathcal{T}'$ be the ideal triangulation obtained from $\mathcal{T}$ by a 2-3 or 3-2 Pachner move, and let $\vec{z'}$ be the corresponding edge parameters. If the edge parameters $\vec{z'}$ are non-degenerate tetrahedra, i.e. no edge parameter is equal to $0, 1$ or ∞, then the algebraic volumes of $\vec{z}$ and $\vec{z'}$ are equal.

This theorem is a consequence of the "five-term relation," an identity of the dilogarithm function, see paragraph 2 in the proof of Proposition 10.1 in [41] for further discussion.

Proposition 11. Let $\varphi : S \to S$ be the the pseudo-Anosov homeomorphism of the once-punctured genus 2 surface given by the Dehn twist word $5, 4, 5, 5, 5, 2, 3$ with notation as discussed in Step 1 of Chapter 8. Let $\mathcal{T}$ be Agol's triangulation of the mapping torus M_φ. Then $\mathcal{T}$ is non-geometric.

We outline the steps we took to verify Proposition 11. We found a sequence

$$\mathcal{T} \xrightarrow{2-3} \mathcal{T}_1 \xrightarrow{3-2} \mathcal{T}_2 \xrightarrow{3-2} \mathcal{T}_3 \xrightarrow{3-2} \mathcal{T}_4,$$

of Pachner 2-3 and 3-2 moves starting with an exact non-geometric solution to Agol's triangulation $\mathcal{T}$, as given by Snap. We verified that the edge parameters of $\mathcal{T}_4$ are all positively-oriented, so that $\mathcal{T}_4$ is geometric and thus $\mathrm{vol}(\mathcal{T}_4)$ equals the hyperbolic volume of M_φ. Furthermore, for $i = 1, 2, 3$, we checked that none of the tetrahedron shapes of $\mathcal{T}_i$ are degenerate. Hence, by Theorem 17, $\mathrm{vol}(\mathcal{T}) = \mathrm{vol}(\mathcal{T}_4)$. Therefore $\mathrm{vol}(\mathcal{T})$ equals the hyperbolic volume of M_φ. Thus, by Corollary 1 Agol's triangulation $\mathcal{T}$ is non-geometric, as required.

Remark 8. We expect that all the other examples in Tables A.3 and A.4 of Appendix A are also non-geometric. But we have not shown this rigorously in the other cases.

9.2 Further work

Although we have found that veering triangulations are not always geometric, we may ask:

Question: Given a veering triangulation coming from Agol's construction, can we find positively-oriented hyperbolic ideal tetrahedra shapes for a (possibly incomplete) hyperbolic structure?

This is equivalent to finding a solution to the gluing equations where every edge parameter has positive imaginary part. Such a solution corresponds to a point in Dehn surgery space. Figure 9.5, produced by Henry Segerman, is obtained by using SnapPy to numerically solve the gluing and (p, q)-Dehn surgery equations and colouring each point (p, q). A point is coloured green when a solution with all tetrahedra positively oriented is found, and blue when SnapPy finds a solution where at least one tetrahedron is negatively oriented. We see that even in this non-geometric example SnapPy finds positively-oriented hyperbolic ideal tetrahedra shapes for incomplete structures of the bundle.

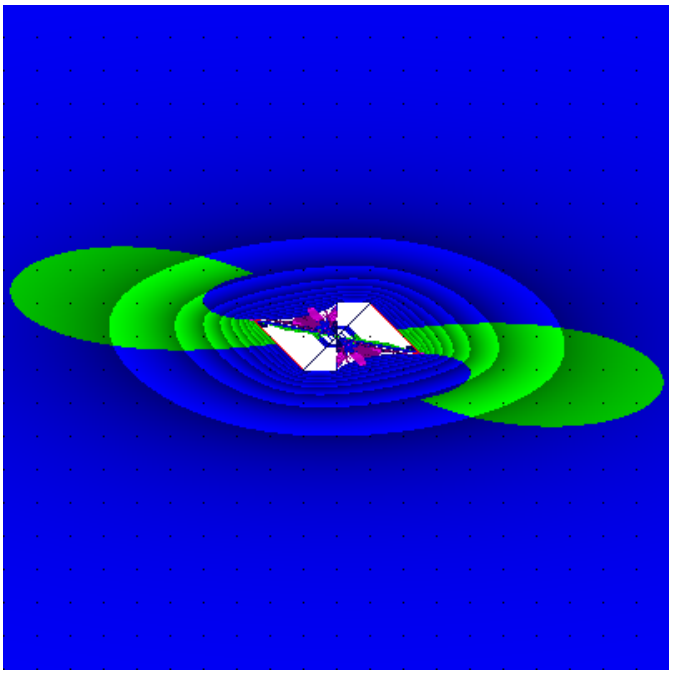

Figure 9.5: Dehn surgery space for 13 tetrahedron non-geometric example.

In the conclusion of [2], Agol explains how, given a pseudo-Anosov homeomorphism φ, the veering triangulation associated with φ together with an encoding of the homology class of the fiber, is a complete conjugacy invariant for φ in the mapping class group. He further outlines how one can canonically encode the homology class of the fiber. It would be interesting to extend our computer program to implement this.

Appendix A

Tables

Let $\varphi : S \to S$ be a pseudo-Anosov homeomorphism of a once-punctured genus two surface, and let $M = M_{\varphi^\circ}$, where φ° is the restriction of φ to the surface with all singular points of the invariant foliations removed.

Table: Column key for the following tables.

Dehn twist word	Dehn twists representing φ, as explained in Step 1 of Chapter 8.
Isom. class	Hyperbolic isometry class of M.
Growth rate	Dilatation of φ.
Volume	Hyperbolic volume of M. An asterisk following the volume indicates that SnapPy reports that Agol's veering triangulation of M is non-geometric.
#Sing.	Number of singular points in invariant foliation of φ.
#Cusps	Number of cusps of M.
#Tet.	Number of tetrahedra in Agol's triangulation.
Prongs.	Number of prongs at each singular point. The first value in the list is the number of prongs at the puncture of S.
Sing. perm	Permutation of singular points with respect to the order listed in the column *Prongs.*, where e.g. $1, 2, 0$ represents the permutation $0 \to 1$, $1 \to 2$, $2 \to 0$.
Sing. to cusp	Cusp number of respective singular point, i.e. indicating which singular points are identified as a single cusp of M. For example, 0, 0, 1 would indicate that singular points 0 and 1 form one cusp, and singular point 2 forms another cusp of M.
Tri. Class	Combinatorial isomorphism class of Agol's triangulation.

Tables A.1 and A.2 include 54 mapping classes, which is the beginning of a longer list of data we have available, where there are 602 mapping classes in total.

Table A.1: Start of list of examples for once-punctured genus 2 surface.

Dehn twist word	Isom. class	Growth rate	Volume	#Sing.	#Cusps	#Tet.	Prongs	Sing. perm	Sing. to cusp	Tri. class
$5,4,5,5,3,2$	8	1.72208	3.17729	1	1	4	6	0	0	8
$5,4,3,2,3,3,1$	195	1.8832	4.05977	2	2	9	$4,4$	0, 1	$0,1$	195
$5,4,4,3,2$	3	2.08102	4.46466	1	1	5	6	0	0	3
$5,4,5,3,3,2,3$	131	2.29663	4.46466	1	1	7	6	0	0	131
$5,4,5,5,-2,3,-1$	128	1.8832	4.7495	2	2	5	$1,7$	0, 1	$0,1$	128
$5,4,5,5,5,3,2$	125	2.89005	4.85117*	1	1	13	6	0	0	125
$5,-4,3,4,2,3$	62	2.36921	5.0449	1	1	6	6	0	0	62
$5,4,5,3,-2,-1$	11	1.72208	5.33349	4	3	6	$1,3,4,4$	0, 1, 3, 2	$0,1,2,2$	11
$5,-4,-3,-2$	1	2.15372	5.33349	3	2	6	$2,4,4$	0, 2, 1	$0,1,1$	1
$5,-4,-3,-4,-2$	1	2.29663	5.33349	2	2	6	$2,6$	0, 1	$0,1$	1
$4,3,2,2,1,-2,-2$	456	2.61803	5.33349	1	1	7	6	0	0	456
$5,4,3,1,2,2$	31	2.29663	6.02305	2	2	10	$4,4$	0, 1	$0,1$	31
$5,-4,-3,-4,-2,-1$	72	1.9165	6.35459	6	3	10	$1,3,3,3,3,3$	0, 1, 5, 2, 3, 4	$0,1,2,2,2,2$	72
$5,3,4,4,3,2$	83	2.89005	6.35459	1	1	7	6	0	0	83
$5,-4,-5,-5,-3,2,2$	9	3.09066	6.35459	3	2	10	$2,4,4$	0, 2, 1	$0,1,1$	9
$5,4,5,3,-2,-2$	9	3.25426	6.35459	2	2	10	$2,6$	0, 1	$0,1$	9
$5,-4,-5,-5,1,-2,-3$	262	1.96355	6.36674	6	2	9	$1,3,3,3,3,3$	0, 5, 1, 2, 3, 4	$0,1,1,1,1,1$	262
$5,-4,5,-2,3,4,-1$	43	1.68491	6.55174	6	3	10	$1,3,3,3,3,3$	0, 5, 3, 2, 1, 4	$0,1,2,2,1,1$	43
$5,4,-2,-3,-1,-2$	43	1.97482	6.55174	4	3	10	$1,3,3,5$	0, 2, 1, 3	$0,1,1,2$	43
$5,-4,5,5,-3,-2$	46	4.05624	6.75519	3	2	14	$2,4,4$	0, 2, 1	$0,1,1$	46
$5,-4,5,5,-3,-2,-3$	46	4.21208	6.75519	2	2	14	$2,6$	0, 1	$0,1$	46
$5,4,-5,4,3,2,1$	150	2.61803	6.92738	2	2	11	$4,4$	0, 1	$0,1$	150
$5,4,3,-2,-2,-2,-2$	201	5.03756	6.95235	3	2	18	$2,4,4$	0, 2, 1	$0,1,1$	201
$5,4,5,3,2,2,1$	134	2.61803	7.16394	2	2	9	$4,4$	0, 1	$0,1$	134
$4,2,3,3,4,1$	122	4.13016	7.16394*	1	1	14	6	0	0	122
$5,4,3,4,-2,-1,-1$	186	1.97482	7.32772	5	4	8	$1,4,3,3,3$	0, 1, 2, 4, 3	$0,1,2,3,3$	186
$5,4,3,3,2,1$	27	2.61803	7.32772	2	2	10	$4,4$	0, 1	$0,1$	27

Table A.2: Continuation of Table A.1

Dehn twist word	Isom. class	Growth rate	Volume	#Sing.	#Cusps	#Tet.	Prongs	Sing. perm	Sing. to cusp	Tri. class
$5, 4, -5, 4, 3, 2, 2$	149	3.34697	7.41416	1	1	8	6	0	0	149
$5, 4, 4, 4, 3, 2$	17	4.30933	7.50977	1	1	14	6	0	0	17
$5, 4, 5, 3, -2, 1$	10	3.50607	7.56148	2	2	9	$2, 6$	0, 1	$0, 1$	10
$5, 4, 5, 2, 3, -4, 3$	142	4.13016	7.60355	1	1	11	6	0	0	142
$5, 4, 5, 2, 3, 3, 4$	143	3.73205	7.77234	1	1	8	6	0	0	143
$5, 4, 3, -2, -1, -2$	30	1.96355	7.8679	5	3	9	$1, 3, 4, 3, 3$	0, 4, 2, 1, 3	$0, 1, 2, 1, 1$	30
$5, -2, 3, 4, -5, 4, -1$	30	2.08102	7.8679	4	3	9	$1, 5, 3, 3$	0, 1, 3, 2	$0, 1, 2, 2$	30
$5, 2, -3, 4, 2, 3, 3$	422	5.27451	7.94511	1	1	15	6	0	0	422
$5, 3, -4, 2, 1$	5	3.44148	7.97974	3	2	10	$2, 4, 4$	0, 2, 1	$0, 1, 1$	5
$5, -2, -3, 4, 4, -3, -1$	438	2.08102	8.00023	4	3	9	$1, 3, 4, 4$	0, 1, 3, 2	$0, 1, 2, 2$	438
$5, 3, -2, -3, -4, -4, -3$	98	2.61803	8.00023	3	2	9	$2, 4, 4$	0, 2, 1	$0, 1, 1$	98
$5, -3, -4, -4, -2, -2$	98	2.89005	8.00023	2	2	9	$2, 6$	0, 1	$0, 1$	98
$5, 4, 3, -1, 2, -1$	32	2.98307	8.00577	6	2	17	$1, 3, 3, 3, 3, 3$	0, 5, 1, 2, 3, 4	$0, 1, 1, 1, 1, 1$	32
$5, -4, -3, -4, -2, 1$	71	2.96557	8.11953	2	2	8	$2, 6$	0, 1	$0, 1$	71
$5, -4, 5, -3, -2, -3, -1$	257	2.94699	8.1957	6	3	22	$1, 3, 3, 3, 3, 3$	0, 1, 5, 2, 3, 4	$0, 1, 2, 2, 2, 2$	257
$5, 4, 3, 1, 1, 2, 2$	210	4.21208	8.24198*	2	2	26	$4, 4$	0, 1	$0, 1$	210
$5, 2, 2, 3, 3, 4, 2$	427	6.11129	8.25157*	1	1	23	6	0	0	427
$4, 2, 3, 3, 3, 3, 1$	477	6.37425	8.25986	1	1	23	6	0	0	477
$5, 4, 5, 3, -2, 1, 1$	136	4.61158	8.41069	2	2	12	$2, 6$	0, 1	$0, 1$	136
$5, 4, 3, 1, 2, 2, 2$	209	4.41948	8.5032	2	2	26	$4, 4$	0, 1	$0, 1$	209
$5, -4, -5, -4, 2, -3, -4$	264	2.61803	8.51918	3	2	10	$2, 4, 4$	0, 2, 1	$0, 1, 1$	264
$5, 4, 3, 2, -1, -1, -1$	198	3.99112	8.58353*	6	2	25	$1, 3, 3, 3, 3, 3$	0, 5, 1, 2, 3, 4	$0, 1, 1, 1, 1, 1$	198
$5, 3, 4, 5, 2, 2, 3$	362	4.61158	8.61242	1	1	10	6	0	0	362
$5, 3, 4, 5, 2, 3, 3$	361	4.96069	8.71643	1	1	11	6	0	0	361
$5, 4, 5, 3, 3, 2, 1$	132	3.25426	8.77866	2	2	12	$4, 4$	0, 1	$0, 1$	132
$5, 4, 3, -4, 3, 2, 1$	187	3.13	8.8656	2	2	11	$4, 4$	0, 1	$0, 1$	187
$5, -3, -3, 4, -2, -1$	100	1.8832	8.92932	6	3	11	$1, 3, 3, 3, 3, 3$	0, 5, 3, 2, 1, 4	$0, 1, 2, 2, 1, 1$	100

Table A.3: Triangulations that SnapPy reports are non-geometric.

Dehn twist word	Isom. class	Growth rate	Volume	#Sing.	#Cusps	#Tet.	Prongs	Sing. perm	Sing. to cusp	Tri. class
$5,4,5,5,5,2,3$	125	2.89005	4.85117	1	1	13	6	0	0	125
$4,2,3,3,4,1$	122	4.13016	7.16394	1	1	14	6	0	0	122
$5,4,3,1,1,2,2$	210	4.21208	8.24198	2	2	26	$4,4$	0, 1	$0,1$	210
$5,2,2,3,3,4,2$	427	6.11129	8.25157	1	1	23	6	0	0	427
$5,4,3,2,-1,-1,-1$	198	3.99112	8.58353	6	2	25	$1,3,3,3,3,3$	0, 5, 1, 2, 3, 4	$0,1,1,1,1,1$	198
$4,3,1,2,2,2,1$	460	7.22040	9.14624	1	1	23	6	0	0	460
$5,3,4,2,2,3,1$	368	5.52042	10.77524	2	2	26	$4,4$	0, 1	$0,1$	368
$5,-4,-5,3,-4,-2,3$	265	9.16582	11.40320	1	1	21	6	0	0	265
$5,4,3,2,-1,2,-1$	197	4.43066	12.86506	6	2	27	$1,3,3,3,3,3$	0, 5, 1, 2, 3, 4	$0,1,1,1,1,1$	197
$5,-3,-3,2,-3,4,-3$	401	12.40010	13.37217	3	2	39	$4,3,3$	0, 2, 1	$0,1,1$	401
$5,-3,4,-3,2,-3,-3$	401	12.40010	13.37217	3	2	39	$4,3,3$	0, 2, 1	$0,1,1$	401
$5,4,-2,3,-2,3,1$	199	7.99808	13.78589	3	2	21	$2,4,4$	0, 2, 1	$0,1,1$	199
$5,4,3,-2,3,-2,1$	199	7.99808	13.78589	3	2	21	$2,4,4$	0, 2, 1	$0,1,1$	199
$5,-3,4,4,2,-3$	93	6.97984	14.17690	3	2	24	$4,3,3$	0, 2, 1	$0,1,1$	93
$5,2,3,3,-4,-4,2$	93	7.87298	14.17690	2	2	24	$4,4$	0, 1	$0,1$	93
$5,4,-3,-3,2,2,-3$	217	14.48078	14.86313	3	2	31	$4,3,3$	0, 2, 1	$0,1,1$	217
$5,-3,2,2,-3,-3,4$	217	14.48078	14.86313	3	2	31	$4,3,3$	0, 2, 1	$0,1,1$	217
$5,-3,-3,4,4,2,-3$	410	9.89898	14.88705	3	2	33	$4,3,3$	0, 2, 1	$0,1,1$	410
$4,3,-2,3,-2,1$	114	8.19987	15.05432	3	2	31	$4,3,3$	0, 2, 1	$0,1,1$	114
$5,4,2,-3,4,5,-3$	114	9.89898	15.05432	2	2	31	$4,4$	0, 1	$0,1$	114
$5,-3,4,-3,4,5,2$	114	9.89898	15.05432	2	2	31	$4,4$	0, 1	$0,1$	114
$4,-3,2,-3,2,1$	114	8.19987	15.05432	3	2	31	$4,3,3$	0, 2, 1	$0,1,1$	114
$5,3,3,3,-4,-4,2$	390	8.30401	15.60969	3	2	25	$4,3,3$	0, 2, 1	$0,1,1$	390
$4,3,-2,-2,3,-2,1$	344	12.21889	15.73326	3	2	47	$4,3,3$	0, 2, 1	$0,1,1$	344
$5,-4,2,3,-4,-4,3$	344	12.21889	15.73326	3	2	47	$4,3,3$	0, 2, 1	$0,1,1$	344

Table A.4: Triangulations that SnapPy reports are non-geometric. (Continuation of Table A.3)

Dehn twist word	Isom. class	Growth rate	Volume	#Sing.	#Cusps	#Tet.	Prongs	Sing. perm	Sing. to cusp	Tri. class
$4,3,3,2,3,-1,2$	451	4.19530	16.38405	5	3	28	$2,3,3,3,3$	0, 3, 4, 1, 2	$0,1,2,1,2$	451
$5,-4,3,-4,5,2,3$	300	11.31474	16.62155	3	2	32	$4,3,3$	0, 2, 1	$0,1,1$	300
$5,3,-4,2,3,-4,5$	300	11.31474	16.62155	3	2	32	$4,3,3$	0, 2, 1	$0,1,1$	300
$5,-4,-4,2,3,-4,3$	292	12.99411	16.80174	3	2	40	$4,3,3$	0, 2, 1	$0,1,1$	292
$5,-4,3,-4,-4,2,3$	292	12.99411	16.80174	3	2	40	$4,3,3$	0, 2, 1	$0,1,1$	292
$5,-3,-1,2,-3,4,-3$	220	10.12331	17.14005	4	3	34	$3,3,3,3$	0, 1, 3, 2	$0,1,2,2$	220
$5,4,-3,2,-3,-3,-1$	220	10.12331	17.14005	4	3	34	$3,3,3,3$	0, 1, 3, 2	$0,1,2,2$	220
$5,4,4,-3,4,2,-3$	175	10.59023	17.31324	3	2	32	$4,3,3$	0, 2, 1	$0,1,1$	175
$5,4,-3,4,4,-3,2$	175	10.59023	17.31324	3	2	32	$4,3,3$	0, 2, 1	$0,1,1$	175
$5,-4,3,-4,2,3,-4$	307	14.19162	17.64673	3	2	47	$4,3,3$	0, 2, 1	$0,1,1$	307
$5,-3,-3,2,-3,4,1$	414	8.90988	17.69647	5	3	32	$2,3,3,3,3$	0, 2, 1, 4, 3	$0,1,1,2,2$	414
$5,4,4,3,3,2,-1$	169	5.10315	17.96735	6	3	25	$1,3,3,3,3,3$	0, 4, 5, 2, 1, 3	$0,1,2,2,1,2$	169
$5,4,4,4,4,3,-2$	160	5.52042	18.05663	5	2	31	$2,3,3,3,3$	0, 3, 1, 4, 2	$0,1,1,1,1$	160
$5,4,2,-3,1,2,-3$	231	7.84775	18.92441	5	3	33	$2,3,3,3,3$	0, 2, 1, 4, 3	$0,1,1,2,2$	231
$5,1,2,-3,2,-3,4$	231	7.84775	18.92441	5	3	33	$2,3,3,3,3$	0, 2, 1, 4, 3	$0,1,1,2,2$	231
$5,4,-3,4,-3,2,-1$	213	8.73741	19.05808	4	3	35	$3,3,3,3$	0, 1, 3, 2	$0,1,2,2$	213
$5,4,-3,4,-1,2,-3$	213	8.73741	19.05808	4	3	35	$3,3,3,3$	0, 1, 3, 2	$0,1,2,2$	213
$4,-2,-3,-3,-1,-2,-2$	481	5.96799	19.15756	5	2	38	$2,3,3,3,3$	0, 3, 1, 4, 2	$0,1,1,1,1$	481
$5,-4,-1,2,2,-3,-3$	360	7.20200	19.51039	4	3	30	$3,3,3,3$	0, 1, 3, 2	$0,1,2,2$	360
$5,-4,-3,-3,-4,5,-2$	330	6.53277	20.27426	5	3	38	$2,3,3,3,3$	0, 2, 1, 4, 3	$0,1,1,2,2$	330
$5,-4,3,-4,-1,2,3$	304	8.51867	20.38781	4	3	37	$3,3,3,3$	0, 1, 3, 2	$0,1,2,2$	304
$5,-4,3,-4,3,2,-1$	304	8.51867	20.38781	4	3	37	$3,3,3,3$	0, 1, 3, 2	$0,1,2,2$	304
$5,-4,-4,-3,-3,-4,-2$	170	8.02836	20.54293	5	3	45	$2,3,3,3,3$	0, 2, 1, 4, 3	$0,1,1,2,2$	170
$5,4,4,3,-2,3,3$	170	8.02836	20.54293	5	3	45	$2,3,3,3,3$	0, 3, 4, 1, 2	$0,1,2,1,2$	170

Appendix B

A non-geometric triangulation

Shown below is the contents of a SnapPy triangulation file of the triangulation discussed in Section 9.1. It can be copied and saved to a text file, then loaded into SnapPy.

```
% Triangulation
Traintrack_Triangulation
not_attempted 0.0
unknown_orientability
CS_unknown
1 0
torus 0.0 0.0
13
   10   4   12   2
 3120 0213 2031 3120
0 0 0 0
  0  0  0  0  0  0  0  0  0  0  0  0  0  0  0  0
  0  0  0  0  0  0  0  0  0  0  0  0  0  0  0  0
  0  0  0  0  0  0  0  0  0  0  0  0  0  0  0  0
  0  0  0  0  0  0  0  0  0  0  0  0  0  0  0  0
0.0 0.0
12 2 9 5
 1302 0213 2031 1302
0 0 0 0
  0  0  0  0  0  0  0  0  0  0  0  0  0  0  0  0
  0  0  0  0  0  0  0  0  0  0  0  0  0  0  0  0
  0  0  0  0  0  0  0  0  0  0  0  0  0  0  0  0
  0  0  0  0  0  0  0  0  0  0  0  0  0  0  0  0
0.0 0.0
0 7 1 8
 3120 0213 0213 3120
0 0 0 0
  0  0  0  0  0  0  0  0  0  0  0  0  0  0  0  0
  0  0  0  0  0  0  0  0  0  0  0  0  0  0  0  0
  0  0  0  0  0  0  0  0  0  0  0  0  0  0  0  0
  0  0  0  0  0  0  0  0  0  0  0  0  0  0  0  0
0.0 0.0
  11 4 11 5
 3201 2031 2310 3120
0 0 0 0
  0  0  0  0  0  0  0  0  0  0  0  0  0  0  0  0
  0  0  0  0  0  0  0  0  0  0  0  0  0  0  0  0
  0  0  0  0  0  0  0  0  0  0  0  0  0  0  0  0
  0  0  0  0  0  0  0  0  0  0  0  0  0  0  0  0
```

```
0.0 0.0
3 6 0 7
 1302 2031 0213 3120
0 0 0 0
  0  0  0  0  0  0  0  0  0  0  0  0  0  0  0  0
  0  0  0  0  0  0  0  0  0  0  0  0  0  0  0  0
  0  0  0  0  0  0  0  0  0  0  0  0  0  0  0  0
  0  0  0  0  0  0  0  0  0  0  0  0  0  0  0  0
0.0 0.0
3 6 1 8
 3120 0213 2031 1302
0 0 0 0
  0  0  0  0  0  0  0  0  0  0  0  0  0  0  0  0
  0  0  0  0  0  0  0  0  0  0  0  0  0  0  0  0
  0  0  0  0  0  0  0  0  0  0  0  0  0  0  0  0
  0  0  0  0  0  0  0  0  0  0  0  0  0  0  0  0
0.0 0.0
4 9 5 10
 1302 2031 0213 3120
0 0 0 0
  0  0  0  0  0  0  0  0  0  0  0  0  0  0  0  0
  0  0  0  0  0  0  0  0  0  0  0  0  0  0  0  0
  0  0  0  0  0  0  0  0  0  0  0  0  0  0  0  0
  0  0  0  0  0  0  0  0  0  0  0  0  0  0  0  0
0.0 0.0
4 9 2 12
 3120 0213 0213 3120
0 0 0 0
  0  0  0  0  0  0  0  0  0  0  0  0  0  0  0  0
  0  0  0  0  0  0  0  0  0  0  0  0  0  0  0  0
  0  0  0  0  0  0  0  0  0  0  0  0  0  0  0  0
  0  0  0  0  0  0  0  0  0  0  0  0  0  0  0  0
0.0 0.0
2 12 5 10
 3120 0213 2031 1302
0 0 0 0
  0  0  0  0  0  0  0  0  0  0  0  0  0  0  0  0
  0  0  0  0  0  0  0  0  0  0  0  0  0  0  0  0
  0  0  0  0  0  0  0  0  0  0  0  0  0  0  0  0
  0  0  0  0  0  0  0  0  0  0  0  0  0  0  0  0
0.0 0.0
6 11 7 1
 1302 2031 0213 1302
0 0 0 0
  0  0  0  0  0  0  0  0  0  0  0  0  0  0  0  0
  0  0  0  0  0  0  0  0  0  0  0  0  0  0  0  0
  0  0  0  0  0  0  0  0  0  0  0  0  0  0  0  0
  0  0  0  0  0  0  0  0  0  0  0  0  0  0  0  0
0.0 0.0
6 11 8 0
 3120 0213 2031 3120
0 0 0 0
  0  0  0  0  0  0  0  0  0  0  0  0  0  0  0  0
  0  0  0  0  0  0  0  0  0  0  0  0  0  0  0  0
  0  0  0  0  0  0  0  0  0  0  0  0  0  0  0  0
  0  0  0  0  0  0  0  0  0  0  0  0  0  0  0  0
0.0 0.0
9 3 10 3
```

```
 1302 3201 0213 2310
0 0 0 0
  0  0  0  0  0  0  0  0  0  0  0  0  0  0  0  0
  0  0  0  0  0  0  0  0  0  0  0  0  0  0  0  0
  0  0  0  0  0  0  0  0  0  0  0  0  0  0  0  0
  0  0  0  0  0  0  0  0  0  0  0  0  0  0  0  0
0.0 0.0
7 1 8 0
 3120 2031 0213 1302
0 0 0 0
  0  0  0  0  0  0  0  0  0  0  0  0  0  0  0  0
  0  0  0  0  0  0  0  0  0  0  0  0  0  0  0  0
  0  0  0  0  0  0  0  0  0  0  0  0  0  0  0  0
  0  0  0  0  0  0  0  0  0  0  0  0  0  0  0  0
0.0 0.0
```

Bibliography

[1] William Abikoff. *The real analytic theory of Teichmüller space*, volume 820 of *Lecture Notes in Mathematics*. Springer, Berlin, 1980.

[2] Ian Agol. Ideal triangulations of pseudo-Anosov mapping tori. In *Topology and geometry in dimension three*, volume 560 of *Contemp. Math.*, pages 1–17. Amer. Math. Soc., Providence, RI, 2011.

[3] Mark Bell, Tracy Hall, and Saul Schleimer. *Twister* [computer software]. http://surfacebundles.wordpress.com/ (Accessed 1 October 2012), 2012. Included with SnapPy version 1.5.

[4] Lipman Bers. An extremal problem for quasiconformal mappings and a theorem by Thurston. *Acta Math.*, 141(1-2):73–98, 1978.

[5] M. Bestvina and M. Handel. Train-tracks for surface homeomorphisms. *Topology*, 34(1):109–140, 1995.

[6] Mladen Bestvina and Michael Handel. Train tracks and automorphisms of free groups. *Ann. of Math. (2)*, 135(1):1–51, 1992.

[7] Francis Bonahon. Geodesic laminations on surfaces. In *Laminations and foliations in dynamics, geometry and topology (Stony Brook, NY, 1998)*, volume 269 of *Contemp. Math.*, pages 1–37. Amer. Math. Soc., Providence, RI, 2001.

[8] Francis Bonahon. *Low-dimensional geometry*, volume 49 of *Student Mathematical Library*. American Mathematical Society, Providence, RI, 2009. From Euclidean surfaces to hyperbolic knots, IAS/Park City Mathematical Subseries.

[9] Peter Brinkmann. Pseudo-Anosov automorphisms of free groups. MSc thesis, The University of Tennessee, Knoxville, 1995.

[10] Danny Calegari. *Foliations and the geometry of 3-manifolds*. Oxford Mathematical Monographs. Oxford University Press, Oxford, 2007.

[11] A. Casson and S. Bleiler. Automorphisms of surfaces after Nielsen and Thurston. Handwritten notes, University of Texas at Austin, Volume 1 Fall 1982, Volume 2 Spring 1983.

[12] Andrew J. Casson and Steven A. Bleiler. *Automorphisms of surfaces after Nielsen and Thurston*, volume 9 of *London Mathematical Society Student Texts*. Cambridge University Press, Cambridge, 1988.

[13] David Coulson, Oliver A. Goodman, Craig D. Hodgson, and Walter D. Neumann. Computing arithmetic invariants of 3-manifolds. *Experiment. Math.*, 9(1):127–152, 2000.

[14] Marc Culler and Nathan Dunfield. *SnapPy* (version 1.5) [computer software]. http://www.math.uic.edu/t3m/SnapPy/ (Accessed 3 October 2012), 2012. Uses the SnapPea kernel written by Jeff Weeks.

[15] R. J. Daverman and R. B. Sher, editors. *Handbook of geometric topology*. North-Holland, Amsterdam, 2002.

[16] D. B. A. Epstein and R. C. Penner. Euclidean decompositions of noncompact hyperbolic manifolds. *J. Differential Geom.*, 27(1):67–80, 1988.

[17] Benson Farb and Dan Margalit. *A primer on mapping class groups*, volume 49 of *Princeton Mathematical Series*. Princeton University Press, Princeton, NJ, 2012.

[18] A. Fathi, F. Laudenbach, V. Poénaru, and et al. *Thurston's Work on Surfaces*. Princeton University Press, 2012. translated from the French original by Djun Kim and Dan Margalit.

[19] Stefano Francaviglia. Hyperbolicity equations for cusped 3-manifolds and volume-rigidity of representations. Ph.D. thesis, Scuola Normale Superiore, 2004.

[20] George K. Francis. *A topological picturebook*. Springer-Verlag, New York, 1987.

[21] F. R. Gantmacher. *The theory of matrices. Vols. 2*. Translated by K. A. Hirsch. Chelsea Publishing Co., New York, 2000.

[22] Oliver Goodman. *Snap* (version 1.5) [computer software]. http://www.ms.unimelb.edu.au/~snap/ (Accessed 3 October 2012), 2012. Uses the SnapPea kernel written by Jeff Weeks.

[23] François Guéritaud. On canonical triangulations of once-punctured torus bundles and two-bridge link complements. *Geom. Topol.*, 10:1239–1284, 2006. With an appendix by David Futer.

[24] François Guéritaud and David Futer. *Explicit angle structures for veering triangulations*. arXiv:1012.5134v1 [math.GT], 2010.

[25] Toby Hall. *Trains* (version 4.32, 2009) [computer software]. http://www.liv.ac.uk/~tobyhall/T_Hall.html (Accessed 3 October 2012). An implementation of the Bestvina-Handel algorithm.

[26] Eriko Hironaka and Eiko Kin. A family of pseudo-Anosov braids with small dilatation. *Algebr. Geom. Topol.*, 6:699–738 (electronic), 2006.

[27] Craig D. Hodgson, J. Hyam Rubinstein, Henry Segerman, and Stephan Tillmann. Veering triangulations admit strict angle structures. *Geom. Topol.*, 15(4):2073–2089, 2011.

[28] Stephen P. Humphries. Generators for the mapping class group. In *Topology of low-dimensional manifolds (Proc. Second Sussex Conf., Chelwood Gate, 1977)*, volume 722 of *Lecture Notes in Math.*, pages 44–47. Springer, Berlin, 1979.

[29] Y. Imayoshi and M. Taniguchi. *An introduction to Teichmüller spaces*. Springer-Verlag, Tokyo, 1992. Translated and revised from the Japanese by the authors.

[30] Weeks Jeffrey. *SnapPea* [computer software]. http://www.geometrygames.org/SnapPea/ (Accessed 1 October 2012).

[31] González-Meneses Juan. *Braiding* (version 1.0) [computer software]. http://personal.us.es/meneses/index2.swf (Accessed 1 October 2012), 2004. for computations in Artin braid groups.

[32] Michael Kapovich. *Hyperbolic manifolds and discrete groups*, volume 183 of *Progress in Mathematics*. Birkhäuser Boston Inc., Boston, MA, 2001.

[33] Marc Lackenby. The canonical decomposition of once-punctured torus bundles. *Comment. Math. Helv.*, 78(2):363–384, 2003.

[34] John M. Lee. *Introduction to topological manifolds*, volume 202 of *Graduate Texts in Mathematics*. Springer-Verlag, New York, 2000.

[35] Jérôme E. Los. Pseudo-Anosov maps and invariant train tracks in the disc: a finite algorithm. *Proc. London Math. Soc. (3)*, 66(2):400–430, 1993.

[36] Feng Luo, Saul Schleimer, and Stephan Tillmann. Geodesic ideal triangulations exist virtually. *Proc. Amer. Math. Soc.*, 136(7):2625–2630, 2008.

[37] Daniel Mathews. Basic ideas about laminations. Unpublished manuscript, 2007.

[38] William Menasco and Morwen Thistlethwaite, editors. *Handbook of knot theory*. Elsevier B. V., Amsterdam, 2005.

[39] Lee Mosher. Train track expansions of measured foliations. preprint, December, 2003.

[40] Lee Mosher. Pseudo-Anosovs on punctured surfaces. Ph.D. thesis, Princeton University, 1983.

[41] Walter D. Neumann and Jun Yang. Bloch invariants of hyperbolic 3-manifolds. *Duke Math. J.*, 96(1):29–59, 1999.

[42] Walter D. Neumann and Don Zagier. Volumes of hyperbolic three-manifolds. *Topology*, 24(3):307–332, 1985.

[43] Jakob Nielsen. *Jakob Nielsen: collected mathematical papers. Vol. 1*. Contemporary Mathematicians. Birkhäuser Boston Inc., Boston, MA, 1986. Edited and with a preface by Vagn Lundsgaard Hansen.

[44] Jean-Pierre Otal. *The hyperbolization theorem for fibered 3-manifolds*, volume 7 of *SMF/AMS Texts and Monographs*. American Mathematical Society, Providence, RI, 2001. Translated from the 1996 French original by Leslie D. Kay.

[45] R. C. Penner and J. L. Harer. *Combinatorics of train tracks*, volume 125 of *Annals of Mathematics Studies*. Princeton University Press, Princeton, NJ, 1992.

[46] John G. Ratcliffe. *Foundations of hyperbolic manifolds*, volume 149 of *Graduate Texts in Mathematics*. Springer, New York, second edition, 2006.

[47] Dale Rolfsen. *Knots and links*, volume 7 of *Mathematics Lecture Series*. Publish or Perish Inc., Houston, TX, 1990. Corrected reprint of the 1976 original.

[48] Henry Segerman. *A generalisation of the deformation variety*. arXiv:0904.1893v3 [math.GT], 2012.

[49] Caroline Series. The geometry of Markoff numbers. *Math. Intelligencer*, 7(3):20–29, 1985.

[50] Caroline Series. The modular surface and continued fractions. *J. London Math. Soc. (2)*, 31(1):69–80, 1985.

[51] W. P. Thurston. The geometry and topology of 3-manifolds. Mimeographed notes, Princeton University Mathematics Department, 1979.

[52] William P. Thurston. On the geometry and dynamics of diffeomorphisms of surfaces. *Bull. Amer. Math. Soc. (N.S.)*, 19(2):417–431, 1988.

[53] William P. Thurston. *Three-dimensional geometry and topology. Vol. 1*, volume 35 of *Princeton Mathematical Series*. Princeton University Press, Princeton, NJ, 1997. Edited by Silvio Levy.

[54] Masaaki Wada, Yasushi Yamashita, and Han Yoshida. An inequality for polyhedra and ideal triangulations of cusped hyperbolic 3-manifolds. *Proc. Amer. Math. Soc.*, 124(12):3905–3911, 1996.

[55] Howard Weiss. The geometry of measured geodesic laminations and measured train tracks. *Ergodic Theory Dynam. Systems*, 9(3):587–604, 1989.